University of Kentucky
UKnowledge

Theses and Dissertations--Physiology | Physiology

2012

THE CARDIAC L-TYPE CALCIUM CHANNEL DISTAL CARBOXYL-TERMINUS AUTO-INHIBITION IS REGULATED BY CALCIUM

Shawn M. Crump
University of Kentucky, crump@uky.edu

Right click to open a feedback form in a new tab to let us know how this document benefits you.

Recommended Citation
Crump, Shawn M., "THE CARDIAC L-TYPE CALCIUM CHANNEL DISTAL CARBOXYL- TERMINUS AUTO-INHIBITION IS REGULATED BY CALCIUM" (2012). *Theses and Dissertations--Physiology*. 5.
https://uknowledge.uky.edu/physiology_etds/5

This Doctoral Dissertation is brought to you for free and open access by the Physiology at UKnowledge. It has been accepted for inclusion in Theses and Dissertations--Physiology by an authorized administrator of UKnowledge. For more information, please contact UKnowledge@lsv.uky.edu.

STUDENT AGREEMENT:

I represent that my thesis or dissertation and abstract are my original work. Proper attribution has been given to all outside sources. I understand that I am solely responsible for obtaining any needed copyright permissions. I have obtained and attached hereto needed written permission statements(s) from the owner(s) of each third-party copyrighted matter to be included in my work, allowing electronic distribution (if such use is not permitted by the fair use doctrine).

I hereby grant to The University of Kentucky and its agents the non-exclusive license to archive and make accessible my work in whole or in part in all forms of media, now or hereafter known. I agree that the document mentioned above may be made available immediately for worldwide access unless a preapproved embargo applies.

I retain all other ownership rights to the copyright of my work. I also retain the right to use in future works (such as articles or books) all or part of my work. I understand that I am free to register the copyright to my work.

REVIEW, APPROVAL AND ACCEPTANCE

The document mentioned above has been reviewed and accepted by the student's advisor, on behalf of the advisory committee, and by the Director of Graduate Studies (DGS), on behalf of the program; we verify that this is the final, approved version of the student's dissertation including all changes required by the advisory committee. The undersigned agree to abide by the statements above.

Shawn M. Crump, Student

Dr. Jonathan Satin, Major Professor

Dr. Bret N. Smith, Director of Graduate Studies

THE CARDIAC L-TYPE CALCIUM CHANNEL DISTAL CARBOXYL- TERMINUS AUTO-INHIBITION IS REGULATED BY CALCIUM

DISSERTATION

A dissertation submitted in partial fulfillment of the

requirements for the degree of Doctor of Philosophy in the

College of Medicine at the University of Kentucky

By

Shawn M. Crump

Lexington, KY

Director: Dr. Jonathan Satin, Professor of Physiology

Lexington, Kentucky

Copyright © Shawn M. Crump 2012

ABSTRACT OF DISSERTATION

THE CARDIAC L-TYPE CALCIUM CHANNEL DISTAL CARBOXYL- TERMINUS AUTO-INHIBITION IS REGULATED BY CALCIUM

The L-type calcium channel (LTCC) provides trigger Ca^{2+} for sarcoplasmic reticulum Ca^{2+}-release and LTCC function is influenced by interacting proteins including the LTCC Distal Carboxyl-terminus (DCT) and calmodulin. DCT is proteolytically cleaved, and re-associates with the LTCC complex to regulate calcium channel function. DCT reduces LTCC barium current ($I_{Ba,L}$) in reconstituted channel complexes, yet the contribution of DCT to $I_{Ca,L}$ in cardiomyocyte systems is unexplored. This study tests the hypothesis that DCT attenuates cardiomyocyte $I_{Ca,L}$. We measured LTCC current and Ca^{2+} transients with DCT co-expressed in murine cardiomyocytes. We also heterologously co-expressed DCT and $Ca_V1.2$ constructs with truncations corresponding to the predicted proteolytic cleavage site, $Ca_V1.2\ \Delta\ 1801$, and a shorter deletion corresponding to well-studied construct, $Ca_V1.2\ \Delta\ 1733$. DCT inhibited $I_{Ba,L}$ in cardiomyocytes, and in HEK 293 cells expressing $Ca_V1.2\ \Delta\ 1801$ and $Ca_V1.2\ \Delta\ 1733$. Ca^{2+}-CaM relieved DCT block in cardiomyocytes and HEK cells. The selective block of $I_{Ba,L}$ combined with Ca^{2+}-CaM effects suggested that DCT-mediated blockade may be relieved under conditions of elevated Ca^{2+}. We therefore tested the hypothesis that DCT block is dynamic, increasing under relatively low Ca^{2+}, and show that DCT reduced diastolic Ca^{2+} at low stimulation frequencies but spared high frequency Ca^{2+}-entry. DCT reduction of diastolic Ca^{2+} and relief of block at high pacing frequencies, and under conditions of supraphysiological bath Ca^{2+} suggests that a physiological function of DCT is to increase the dynamic range of Ca^{2+} transients in response to elevated pacing frequencies. Our data motivates the new hypothesis that DCT is a native reverse use-dependent inhibitor of LTCC current.

KEYWORDS: L-type Calcium Channel, Distal Carboxyl-Terminus, Calcium Channel Auto-Inhibition, Cardiomyocyte, Reverse Use Dependent Inhibition.

THE CARDIAC L-TYPE CALCIUM CHANNEL DISTAL CARBOXYL- TERMINUS AUTO-INHIBITION IS REGULATED BY CALCIUM

By

Shawn M. Crump

Jonathan Satin

Director of Dissertation

Bret N. Smith

Director of Graduate Studies

11/30/2013

This dissertation is dedicated to my family, Jo Anne and John Crump.

ACKNOLWEDGEMENTS

The following dissertation benefited from the support of key individuals. First, my Dissertation Chair, Jonathan Satin, set the standard for scholarly work to which I hope to continue. He provided insights and comments that improved the dissertation. Next, I wish to thank the Dissertation Committee, including the outside examiner, respectively: Timothy McClintock, Brian Delisle, Douglas Andres, James Geddes, and Olivier Thibault. Each committee member provided challenges that shaped my body of work, thinking, and approach to research that elevated the finished dissertation.

I would like to thank my wife, Jo Anne, for her logical approach to science and writing that I always value more than she will ever know. Jo Anne, John, Mom, Mike, and Imogene Thomas (grandmother) provided the kind of support that only family could provide.

TABLE OF CONTENTS

ACKNOWLEDGMENTS iii

TABLE OF CONTENTS iv

LIST OF TABLES vii

LIST OF FIGURES viii

Chapter 1: Background 1

1.1 Introduction 1

1.2 The L-type Calcium channel 1

1.3 $Ca_V1.2$ is a voltage gated calcium channel 4

1.4 L-type Calcium channel modulation by kinases 9

1.5 L-type calcium channel distal carboxyl-terminus 11

1.6 Regulation of $Ca_V1.2$ by DCT 11

1.7 L-type Calcium channel cardiomyocyte cytosolic Ca^{2+} homeostasis 13

1.8 Summary 14

1.9 Dissertation Overview 16

1.9.1 Regulation of $Ca_V1.2$ function by DCT and CaM (in Chapter 3) 19

1.9.2 $Ca_V1.2$-DCT as a reverse use dependent inhibitor (in Chapter 4) 20

Chapter 2: Materials and methods 29

2.1 HEK cell culture 29

2.2 E18 primary cell isolation 29

2.3 Adult ventricular myocyte isolation 32

2.4 Plasmids 33

2.5 Lipofectamine transfection 33

2.6 Ca^{2+} imaging 33

2.7 Electrophysiology 34

Chapter 3: Regulation of CaV1.2 function by DCT and CaM 41

3.1 Introduction 41

3.2 Results 41

3.2.1 DCT inhibits IBa,L, but not ICa,L in HEKs. 41

3.2.2 DCT has no effect on LTCC current kinetics 43

3.2.3 Role of Ca^{2+}-CaM in CaM-DCT current restoration. 43

3.2.4 Role of Ca^{2+} in Time to peak current. 44

3.2.5 DCT co-expression requires a double Boltzmann equation 44

3.3 Discussion 45

Chapter 4: Regulation of $Ca_V1.2$ function by DCT and CaM in Cardiomyocytes 62

4.1 Introduction 62

4.2 Results 62

4.2.1 DCT inhibits IBa,L, but not ICa,L in ventricular cardiomyocytes. 62

4.2.2 DCT has no effect on LTCC current kinetics in cardiomyocytes 63

4.2.3 Role of Ca^{2+}-CaM in CaM-DCT current restoration in cardiomyocytes.. 64

4.2.4 Role of DCT on Voltage-dependent inactivation 64

4.2.5 DCT does not change the channel number at the surface 65

4.2.6 DCT-RNAi reduces LTCC current in cardiomyocytes 65

4.2.7 DCT-RNAi reduces LTCC Ca^{2+} transients in cardiomyocytes 66

4.2.8 Long term Ca^{2+} channel block in cardiomyocytes 66

4.2.9 DCT increases the dynamic range of Ca^{2+} transients by lowering diastolic Ca^{2+}. 69

4.3 Discussion 70

Chapter 5. Dissertation Summary 98

5.1 Major Findings 98

5.1.1 DCT block Ba current, not Ca^{2+} current in HEKs 98

5.1.2 DCT Ba current, not Ca^{2+} current in cardiomyocytes. 100

5.2 Future Directions 102

5.2.1 DCT Ser1928 modifies Ca^{2+} transient response to Isoproteranol 102

5.2.2 DCT over-expression is required for ISO response in cardiomyocytes. 104

Reference: 108

Vita 117

LIST OF TABLES

Table 1.1 List of Abbreviations……22

Table 3.1 Voltage dependence of current activation Boltzmann fit of $V_{1/2}$ and k for $Ca_V1.2\Delta1733$ and $Ca_V1.2\Delta1801$..... 49

Table 4.1 Steady state inactivation of cardiomyocyte $I_{Ba,L}$..... 76

Table 4.2 Voltage dependence of current activation Boltzmann fit of $V_{1/2}$ and k for cardiomyocytes..... 77

LIST OF FIGURES

Figure 1.1 L-type Calcium channels are part of a voltage gated superfamily..... 23

Figure1.2 Structure of $Ca_V1.2$ 24

Figure 1.3 Fundamental components of Excitation contraction coupling..... 25

Figure 1.4 Relationship of Action potential to Po and Ca2+ driving force..... 26

Figure 1.5 $Ca_V1.2$ Proximal and Distal Carboxyl-terminus..... 27

Figure 1.6 Proposed model of DCT function..... 28

Figure 2.1 HEK current voltage protocol..... 37

Figure 2.2 Cardiomyocyte current voltage protocol 38

Figure 2.3 Cardiomyocyte gating current protocol..... 39

Figure 2.4 Cardiomyocyte steady-state inactivation protocol..... 40

Figure 3.1 DCT decreases IBa,L, but not ICa,L from CaV1.2 Δ 1733 truncation expressed in HEK 293 cells..... 50

Figure 3.2 CaM relieves DCT decreased $I_{Ba,L}$, but not $I_{Ca,L}$ from $Ca_V1.2$ Δ 1733 truncation expressed in HEK 293 cells..... 51

Figure 3.3 Raw current trace kinetics in HEK 293 cells 52

Figure 3.4 Fractional remaining current for $Ca_V1.2$ Δ 1733 truncation expressed in HEK 293 cells 53

Figure 3.5 DCT decreases $I_{Ba,,L}$ and $I_{Ca,L}$ from $Ca_V1.2$ Δ 1801 truncation of $Ca_V1.2$ expressed in HEK 293 cells 54

Figure 3.6 CaM relieves DCT decreased $I_{Ba,L}$, and $I_{Ca,L}$ from $Ca_V1.2$ Δ 1801 truncation expressed in HEK 293 cells 55

Figure 3.7 Raw current trace kinetics in HEK 293 cells 56

Figure 3.8 Fractional remaining current for $Ca_V1.2$ Δ 1801 truncation expressed in EK 293 cells 57

Figure 3.9 CaM_{1234} blocks $I_{Ba,L}$, and DCT block is not additive in HEK cells 58

Figure 3.10 Fractional remaining current after 300ms comparing CaM_{1234} in HEK cells 59

Figure 3.11 Time to peak expressing CaM_{1234} in HEK cells 60

Figure 3.12 DCT co-expression requires a double Boltzmann equation for a successful fit in Ca^{2+} measured currents 61

Figure 4.1 DCT decreases $I_{Ba,L}$, but not $I_{Ca,L}$ in ventricular cardiomyocytes 78

Figure 4.2 DCT decreases $I_{Ba,L}$, but not $I_{Ca,L}$ in ventricular cardiomyocytes 79

Figure 4.3 DCT enhances voltage-dependent inactivation in cardiomyocytes. 80

Figure 4.4 DCT enhances voltage-dependent inactivation (VDI) in cardiomyocytes. 81

Figure 4.5 Ca^{2+} and Ca^{2+}-CaM requirement for diastolic blockade in co-expressed CaM_{1234} cardiomyocytes 82

Figure 4.6 Voltage-dependent inactivation of cardiomyocytes plus $Ca_V1.2$-DCT 83

Figure 4.7 Channel number is unaltered by DCT over-expression in cardiomyocytes. 84

Figure 4.8 DCT-RNAi over-expression in cardiomyocytes 85

Figure 4.9 Ca^{2+}transients for DCT-RNAi over-expression in cardiomyocytes 86

Figure 4.10 Ca2+ transients for DCT-RNAi over-expression in E18 mouse cardiomyocytes. 87

Figure 4.11 L-type Calcium single channel events increase with phosphatase 2Ac inhibition 88

Figure 4.12 The null fraction of 48 hour Verapamil treated mice decreases with the db-cAMP stimulation and Okadaic Acid phosphatase inhibition 89

Figure 4.13 DCT reduces quiescent cytosolic Ca^{2+} and increases the dynamic frequency response range 90

Figure 4.14 Representative Ca_{2+} transients for 3 Hz and 0.5 Hz stimulation 91

Figure 4.15 Representative Ca2+ transients for 3 Hz and 0.5 Hz stimulation. 92

Figure 4.16 Pooled mean diastolic Ca^{2+} level normalized to quiescent value for 0.5, 1, 2, and 3 Hz. 93

Figure 4.17 Response range manifested as difference between 3Hz and 0.5 Hz..... 94

Figure 4.18 DCT decreases diastolic calcium in cardiomyocytes 95

Figure 4.19 DCT decreases diastolic calcium in cardiomyocytes and increases systolic calcium transients 96

Figure 4.20 Model 97

Figure 5.1 Cardiomyocytes respond to ISO when co-expressed with DCT 106

Figure 5.2. Raw Ca^{2+}-transients using Cardiomyocytes paces at 1Hz.....107

Chapter 1: Background

1.1 Introduction

Sydney Ringer published a series of papers from 1882 to 1883 that established the role of Ca^{2+} in contraction of the heart[3, 4]. Calcium through the L-type Ca^{2+} channel triggers contraction in cardiomyocytes[5, 6]. Auto-inhibition of the L-type calcium channel can be controlled by its proteolytically cleaved distal carboxyl-terminus[1]. The focus of this thesis centers around cardiomyocyte Ca^{2+} homeostasis underlying the functional role of the L-type calcium channel distal carboxyl-terminus (DCT). The introduction outlines the molecular and functional characteristics of the L-type calcium channel (LTCC) expressed in cardiomyocytes. First, I will introduce the channel, associated subunits, functional assays, distribution, and physiological/pathophysiological functions in cardiomyocytes. Then, I will detail each description in its own sub-section. Finally, I will outline the thesis research project aims at the end of the chapter.

1.2 The L-type Calcium channel

The L-type calcium channel was first purified from skeletal muscle transverse tubules by Curtis and Catterall in 1984[7]. L-type calcium channels provide the main pathway for Ca^{2+} entry into cardiomyocytes (Figure 1.1) [8]. The *CACNA1C* gene encodes the protein $Ca_V1.2$, the LTCC in cardiomyocytes[2]. The $Ca_V1.2$ L-type channel coding region was first isolated in rabbit heart[2]. $Ca_V1.2$ is a voltage-gated calcium channel made up of a pore forming $Ca_V1.2$ α-1-subunit that is

part of a multi-protein complex. This complex is made up of the $Ca_V1.2$ α-1-subunit and accessory subunits α2δ and $Ca_V\beta$ and sometimes γ[2, 5, 9, 10]. There are four $Ca_V\beta$ subunit genes that have been detected in the heart with $Ca_V\beta_2$ and $Ca_V\beta_3$ as the predominate isoforms that interact with $Ca_V1.2$ [11]. The $Ca_V\beta$ subunit can modify L-type calcium channel currents in an isoform and splice variant specific manner [12]. The cardiac isoform and splice variant $Ca_V\beta_2a$ increases L-type current densities in HEK over-expression systems and slows the inactivation kinetics of the channel[13, 14] [15]. $Ca_V\beta_2a$ hyperpolarizes the voltage-dependence of activation resulting in channel openings at more negative membrane potentials[16]. The primary interaction site for the $Ca_V\beta2$ subunit is the conserved α1-interaction domain (AID) on the $Ca_V1.2$ I-II linker[11, 16]. $Ca_V\beta_2a$ functional effects on the Cav1.2 channel include increased peak amplitude, faster rate of activation, modification in rate of inactivation, hyperpolarizing shift in inactivation[17]. $Ca_V\beta_2a$ increases current amplitude by either by increased open probability and/or increasing the number of channels at the plasma membrane by masking an unidentified endoplasmic retention signal on the $Ca_V1.2$ α-1-subunit cytoplasmic I-II linker[16-18]. The accessory subunits α2δ is transcribed from a single gene[11, 19]. Then α2δ is post-transnationally cleaved into α2 and δ.[11, 19]. The subunits α2-δ remains associated by a disulfide linkage. α2δ-1 cloned from skeletal muscle is one of the four known isoforms including α2δ-2 & α2δ-3 cloned from brain, and α2δ-4 from non neuronal cells[19]. α2δ-1 subunit isoform has been detected in cardiac muscle[19]. This subunit binds to extracellular Domain III regions of the $Ca_V1.2$

subunit[19]. The main effect of the combined α2-δ in HEK cells increases current amplitude and can modify gating kinetics[11, 19]. Yet, the role in the heart has not been closely studied[11]. Early experimental designs used minimal components in HEK cells co-expressing $Ca_V1.2$ and $Ca_V\beta2a$ and omitting α2δ to determine the functional role of $Ca_V1.2$ carboxyl-terminus[20]. However, co-expression of α2δ has a practical advantage and a real disadvantage. First, co-expression of α2δ increases $I_{Ba,L}$ current 2-fold in my hands (data not shown). Yet, when considering co-expressing multiple cDNAs into a HEK system, I elected, like others, to use the minimally required subunit expression of channel, beta subunit, and proteins tested[20].

The L-type calcium channel is part of a superfamily. Voltage gated channels are classified by voltage dependence of activation. High voltage activated (HVA) gated channels are called L-, P/Q-, and N-type[8]. L- signifies long lasting currents when Ba^{2+} is the charge carrier, N- for Neural, P- for cerebellar Purkinje cells, Q- & R- cerebellar granule cells[2]. Low voltage activated (LVA) channels are called T-type for transient current (Figure 1.1) [21, 22]. Distribution of L- and T-type voltage gated Ca^{2+} channels are both tissue specific and development dependent. For example, in mouse fetal ventricular myocytes (FVM), there are two L-type calcium channels and one T-type channel expressed, $Ca_V1.2$, $Ca_V1.3$ and Cav3.1 respectively. $Ca_V3.1$ represents the T-type calcium channel expressed during early development in fetal ventricular myocytes. $Ca_V1.3$ and $Ca_V3.1$ are the dominant calcium channels

expressed up to embryonic day 16, then $Ca_V1.2$ expression becomes dominant[23-25].

1.3 $Ca_V1.2$ is a voltage gated calcium channel

The earliest cardiac calcium channel currents were recorded in purkinje fibres from sheep and calf hearts[26]. Functional assays for L-type calcium channels include whole-cell and single channel patch-clamp, calcium imaging, cardiac or smooth muscle contraction, and hormone secretion[2, 27]. Ca^{2+} through the L-type calcium channel is called Ca^{2+} current ($I_{Ca,L}$)[2, 28]. $Ca_V1.2$ ion selectivity increases from Ca^{2+} >Sr^{2+} >Ba^{2+} >>Mg^{2+}. Experimentally, Ba^{2+} (25pS) is routinely used for recording currents ($I_{Ba,L}$) given its greater conductivity than Ca^{2+} (9pS)[29]. However, $Ca_V1.2$ is more selective for Ca^{2+}. Ca^{2+} coordinating with acidic side chains projecting into the pore achieves selectivity. Thus ions, Ca^{2+} ions bind tightly and will have the lowest conductance[29].

The $Ca_V1.2$ subunit is a 190-250 kDa protein made of 4 repeats (DI-DIV) of six transmembrane regions (S1-S6) each with a pore loop (S5-S6)[5, 9, 30, 31]. The hydrophilic pore of the $Ca_V1.2$ subunit comprises the ion selectivity filter (Figure 1.2). Depolarization of the membrane favors transitions of the $Ca_V1.2$ subunit from closed state (C) to an open state (O)[8]. The molecular transitions are termed channel gating, and Markovian models capture channel gating. In many models, the voltage dependent activation gating is delayed, and described as a two-closed-state reaction, such as: C ←→ C←→O. The transition rate constants (k) are functions of

voltage whereby depolarization speeds activation (right to left transition, C→C→O); conversely repolarization speeds closing (O→C)[8]. Channel gating, is controlled by the $Ca_V1.2$ voltage sensor in the S4 transmembrane segment of each repeat. The α-helical transmembrane S4 segment contains positive charges in register (Arg, Lys) that sense transmembrane potential. Depolarization moves S4 up, that is towards the extracellular space upon depolarization [25]. By definition, the movement of charge through an electric field generates current. Such current is termed gating current, in contrast to the ionic current generated by movement of ions through the pore of the channel. Macroscopic current *(I)* is equal to the product of unitary channel current *(i)* by the number of channels *(N)* and by the open probability of the channel *(Po)*. Single channel recordings allow direct assessment of *Po* and *i*. The single channel currents with short open (O) times are called mode 1[8]. Single channel currents with long open times (O) are called mode 2. Single channel current mode 0 means no opening at all[8]. Although gating current occurs on average prior to ionic current, the stochastic nature of channel opening results in some overlap of gating and ionic current. Therefore, measurements of gating current over the entire voltage range require complete blockade of transmembrane ionic conductance. Alternatively, macroscopic current waveforms measured at the reversal potential isolates the gating charge, the movement of the charged S4 segment[8]. Gating charge is a metric for the number of channels with movable voltage sensors in the membrane[32]. Moreover, the ratio of gating charge to ionic current is a readout for coupling between voltage-sensing and channel opening.

L-type calcium current in cardiac myocytes is a major determinant of calcium-induced Ca^{2+} release (CICR) (Figure 1.3) [5] . The Ryanodine receptor (RyR_2) on the SR is gated by Ca^{2+} from the LTCC[33]. More LTCC Ca^{2+}entry leads to more SR Ca^{2+} release [34, 35]. Upon depolarization, LTCCs increase the Ca^{2+} concentration in the dyadic cleft between the LTCC and the RyR_2. As dyadic cleft Ca^{2+} concentration increases, Ca^{2+} binds to RyR_2, in turn causes RyR_2 to open for SR Ca^{2+} release[33]. Normally, negative potentials limit openings of the LTCC that could trigger Ca^{2+} gated RyR_2 openings. RyR_2 mediated release of SR Ca^{2+} in a spatially and temporally restricted mode is called a Ca^{2+} spark. An ensemble of Ca^{2+} sparks increase Ca^{2+} concentration in the dyadic cleft that can trigger a global SR Ca^{2+} release. Next, I will break down the determinants of LTCC channel currents to expand the relationship between voltage control and channel opening.

As mentioned above, $I_{Ca,L}$ is the product of single channel currents ($i_{Ca,L}$), channel number (N), and open probability (Po);[36, 37]

$$I_{Ca,L} = i_{Ca,L} \times N \times P_o$$

Po is dependent on membrane voltage (Vm)[37]. N can be regulated but assumed to be unchanged on short time scale. The gating and voltage sensing of the LTCC define Po. Finally, unitary $i_{Ca,L}$ (noted by lower case i) is assumed unchanged for any given potential. For an open channel the magnitude of $I_{Ca,L}$ is determined by the Ca^{2+} electrochemical gradient[37]. LTCC Po is comparatively low during diastole, thus limiting CICR at relatively low voltages[35, 38]. Conversely, LTCC Po is

relatively higher as voltage increases. The electrochemical gradient creates a greater driving force for Ca^{2+} at more negative voltages. High driving force of Ca^{2+} through the LTCC increases the probability of RyR_2 openings (Figure 1.4). Relatively low Po of LTCC at very negative voltages protects the cytosol from potentially pathological external Ca^{2+} entry. Conversely, driving force for Ca^{2+} through the LTCC is low at high voltages, thus low driving force of Ca^{2+} decreases the probability of RyR_2 openings[37]. SR Ca^{2+} release and $I_{Ca,L}$ amplitude track a similar bell shaped dependence on membrane voltage[37, 39]. As membrane voltages becomes more positive, Po increases and more Ca^{2+} entry is available to stimulate RyR_2 opening (Figure 1.4) [37]. The ratio of LTCCs to RyR_2s in adult myocytes is ~12 : 100[33, 37, 40]. The amplification of the $I_{Ca,L}$ by SR Ca^{2+} release (SR Ca^{2+} release/$I_{Ca,L}$) is measured by Ca^{2+} imaging transients and Vm of $I_{Ca,L}$[37]. Increased $I_{Ca,L}$ amplification is observed at more negative Vm. In summary, Po at negative potentials are more infrequent, but for a given opening $I_{Ca,L}$ is greater[37]. This in turn activates Ca^{2+} gated RyR_2 to open, releasing the Ca^{2+} store from the SR.

$Ca_V1.2$ inactivation limits Ca^{2+} entry across the cell membrane during prolonged depolarization[41]. Channel inactivation is a transition from opening to a non-conducting state[42]. $Ca_V1.2$ inactivation determines action potential duration and refractory period of excitable cells[42]. Excessive Ca^{2+} entry can contribute to pathological cytosolic calcium overload[43]. Therefore, Ca^{2+} entry inactivation is crucial for normal function, and is tightly controlled by two distinct processes, voltage dependence or intracellular calcium dependence[41, 44, 45]. $Ca_V1.2$ structure-function studies suggest that the elements of

voltage dependent inactivation (VDI) are in the domain I-II linker and the S6 segments of the four transmembrane repeats[46]. $Ca_V1.2$ VDI is experimentally isolated from calcium dependence inactivation (CDI) by using Ba^{2+} as the charge carrier $I_{Ba,L}$. Hence, $Ca_V1.2$ $I_{Ba,L}$ peak current decay is governed by voltage. A consequence of VDI loss of function is seen in the cardiac $Ca_V1.2$ mutation, G406R that is located on S6 of domain I. This mutation found in Timothy Syndrome leads to prolongation of QT intervals causing multiple arrhythmias and sudden death[43]. In my dissertation work, I examine the consequence of $Ca_V1.2$ proximal carboxyl-terminal interacting proteins on inactivation using both VDI and CDI.

$Ca_V1.2$ calcium dependent inactivation (CDI) is modulated by Ca^{2+}/calmodulin which is critical for $I_{Ca,L}$ dependent feedback[47]. The structural underpinning of CDI is a result of Ca^{2+} binding the pre-associated calmodulin protein (CaM) on the $Ca_V1.2$ proximal carboxyl-terminus at the CB/IQ domain[44, 48-55]. Calmodulin is constitutively associated with the $Ca_V1.2$ proximal carboxyl-terminus (PCT)[11]. CaM binds the $Ca_V1.2$ motif at amino acid 1653-1663 rabbit sequence[56] [57]. CaM is made up of an N- and C-lobe. Each lobe contains two Ca^{2+} binding EF hand motifs[55]. $Ca_V1.2$ $I_{Ca,L}$ is modulated by CaM when Ca^{2+} binds these four sites[55]. Calcium activated CaM reorients its attachments that causes a conformational change of the carboxyl-terminus 3D structure enhancing the decay of $I_{Ca,L}$[44, 58]. Studies have shown specificity of CDI though CaM mutagenesis. At the level of $Ca_V1.2$ current, disruption of CaM interaction with the CB/IQ domain may result in reduced CDI effect[58]. For example, engineered CaM_{1234} is Ca^{2+} insensitive by mutation of the EF motifs on the N- and C- Lobe[51]. Over-expression of CaM_{1234} in

rat ventricular cardiomyocytes results in prolonged action potential durations (APD)[59]. Removing the Ca^{2+} dependent feedback by a modified CaM prolonged the action potential duration 4- 5-fold[51]. Functional CaM is essential for cardiac cytosolic Ca^{2+} homeostasis as a negative feedback control of Ca^{2+} entry through $Ca_V1.2$[57, 58]. Another example of CaM interaction, $Ca_V1.2$ co-express with small GTPase Rem in HEK 293 cells results in relatively slow CDI[60]. Rem interacts with a $Ca_V1.2$ proximal C-terminal peptide segment including the CB/IQ domain [60]. Over-expression of calmodulin (CaM), a CB/IQ interacting protein, disrupts the Rem-$Ca_V1.2$ peptide segment interaction in a Ca^{2+} dependent manner [60]. Together, co-expression of exogenous CaM using CDI as a readout of CaM interaction on $Ca_V1.2$ proximal carboxyl-terminus, can be used to evaluate the functional interaction of associated proteins.

1.4 L-type Calcium channel modulation by kinases

The large intracellular $Ca_V1.2$ carboxyl-terminus is a target for regulation by Ca^{2+}, CDI, facilitation, kinase regulation, and transcriptional regulation of the $Ca_V1.2$ channel (Figure 1.5) [24, 25, 61]. $Ca_V1.2$ is the substrate of regulation by interacting proteins. Some examples of interacting proteins and effects in cardiomyocytes are; 1.) CaM activated calmodulin/kinase II; $I_{Ca,L}$ facilitation, 2.) protein kinase C (PKC) Ca^{2+} mediated channel phosphorylation, 3.) protein kinase A, activated through adenylyl cyclase by β-adrenergic agonist, 4.) and protein kinase D (PKD) activated through adenylyl cyclase by α-adrenergic agonist. CaM mediated CaMKII activation

increases Ca^{2+} dependent facilitation (CDF) of L-type Calcium channels and is tethered to the Cav1.2 proximal carboxyl terminus[62]. Increased heart rate enhances inward $I_{Ca,L}$ in a positive force frequency relationship[11]. CaMKII changes modal gating of the L-type calcium channel similar to β-adrenergic enhancement of $I_{Ca,L}$[11]. Recent reports show PKD regulates human Cav1.2 through Ser1884 on the Cav1.2 carboxyl-terminus[63]. Finally, enhanced L-type calcium current by β-adrenergic stimulation has been a focus of study for several decades[11]. Protein kinase A (PKA) is activated by β-adrenergic agonists[11]. PKA stimulation of the L-type calcium channel changes modal gating by longer and more frequent channel openings, mode 2[11]. The $Ca_V1.2$ carboxyl-terminus (Ser^{1928} and Ser^{1700}) and the β_{2a} subunit (Ser478 and Ser^{479}) are specific targets for PKA phosphorylation[11, 64]. However, Ser^{1928} may not be necessary for β-adrenergic enhancement $I_{Ca,L}$ in cardiomyocytes and may also be a substrate for PKD phosphorylation[63, 65]. Cav1.2 over-expression in HEK cells have not always been able to recapture PKA phosphorylation. A kinase anchoring protein 15 (AKAP15) is required in heterologous systems to recapitulate β-adrenergic enhancement $I_{Ca,L}$[11, 65]. AKAP is associated with the $Ca_V1.2$ distal carboxyl-terminus at a.a.2057-2115 and mediates association with PKA signaling of the channel[66, 67]. Calcium activated Protein Kinase C (PKC) has been demonstrated to phosphorylate $Ca_V1.2$ Ser1928 in vivo yet the role of Cav1.2-Ser1928 has yet to be determined[68].

1.5 L-type calcium channel distal carboxyl-terminus

The L-type calcium channel found in native tissues often have a truncated $Ca_V1.2$ subunit at the distal carboxyl-terminus (DCT)[30, 59, 69]. Cardiac $Ca_V1.2$, the main pore-forming subunit, is an ~2171 amino acid protein with a predicted molecular mass of ~250kDa [70-72]. The precise length varies with species [72] and splice variants [73]. A conserved feature of $Ca_V1.2$ is that the carboxyl terminus is located in the cytosol space. The $Ca_V1.2$ distal carboxyl-terminus (DCT) is a protein with a predicted mass of ~37 kDa [1, 74]. Spectroscopy studies show that the closely related $Ca_V1.1$ isoform is truncated at ~ amino acid 1800 in the carboxyl-terminus[1, 74]. $Ca_V1.2$ heterologously expressed in non-excitable cells are not processed as in cardiomyocytes, rather it functions as a full-length ~250kDa protein. Western blot studies of $Ca_V1.2$ in cardiomyocytes consistently show $Ca_V1.2$ migrating as a 190 and a 240kDa protein. DCT is also found to be localized to the nucleus where it can modify gene expression in neurons [75] or cardiomyocytes[24]. The Cav1.2 carboxyl-terminus domains continue to be defined since it was initially reported to auto-regulate L-Type currents [76].

1.6 Regulation of $Ca_V1.2$ by DCT

In 1994 Wei et. al. reported that modifications to the $Ca_V1.2$ carboxyl-terminus resulted in a change in channel Po[76]. They assessed the functional role for the 665 amino acid carboxyl-terminus by constructing deletion mutants of the rabbit cardiac $Ca_V1.2$[76]. As a result of deleting ~70% ($Ca_V1.2\Delta1733$) of the distal carboxyl-terminus, inward $I_{Ba,L}$ increased 4-6 fold[76]. $I_{Ba,L}$ increased without

change to charge movement during voltage dependent gating suggesting no change in $Ca_V1.2$ channel expression[76]. In addition, single channel recordings did not reveal any change in unitary conductance[76]. As defined in an earlier section, the whole cell current density *(I)* is described as *I=i x N x Po,* with *i* as single channel conductance, *N* as the number of channels, and *Po* as the open probablility[25,26,][76]. The combination of unaltered (*i)* and (*N)* suggests that 70% deletion of the $Ca_V1.2$ carboxyl-terminus increased current (*I)* density leading to increased Po[76]. It is noted in this paper that additional deletion of the carboxyl-terminus including $Ca_V1.2\Delta1623$ results in loss of channel expression[76]. The next refinement in $Ca_V1.2$ carboxyl-terminus functional role is examining the 665 amino acid segment membrane targeting and L-type current inhibitory domain.

Gerhardstein et.al. generated a set of rabbit $Ca_V1.2$ carboxyl-terminus deletion mutants to identify a proline rich domain amino acid region 1623-1666 that mediates membrane targeting[77]. Dubuis delivered a short rat Cav1.2 carboxyl-terminal peptide with residues 1973-2001 by whole cell patch pipette and recorded a decrease in L-type calcium channel current density in adult rat cardiomyocytes[78]. Furthermore, Gao applied $Ca_V1.2$ carboxyl-terminus fragments to the pipette solution to recapitulate the inhibition of $I_{Ba,L}$ whole cell patch clamp currents in HEKs expressing $Ca_V1.2\Delta1905$ and $Ca_V1.2\Delta2024$ truncated channels compared to $Ca_V1.2\Delta1733$, 1905, & 2024 alone[30]. As a result of these findings plus the findings above, a map of the $Ca_V1.2$ carboxyl-terminus functional role was beginning to emerge[20, 30, 77, 79]. The $Ca_V1.2$ distal carboxyl-terminus included a

region from amino acids 1733-2171 with 1733-~1900 as the DCT binding region, 1974-2000 as the proline rich domain, and finally as Gao's paper revealed 2024-2171 to be the inhibitory domain[30]. Hulme provided the first functional characterization of the $Ca_V1.2$ auto-inhibitory distal carboxyl-terminus[1]. Co-expression of truncated $Ca_V1.2\Delta1821$ with distal carboxyl-terminus 1822-2171 is a re-associated as a molecular complex[1]. DCT 1822-2171 likewise, inhibited $Ca_V1.2\Delta1821$ $I_{Ba,L}$ in HEK 293 heterologous over-expression systems[1]. Formation of the auto-inhibitory complex reduced coupling efficiency of voltage sensing: channel opening, shifting voltage dependence of activation towards positive membrane potentials[1].

1.7 L-type Calcium channel cardiomyocyte cytosolic Ca^{2+} homeostasis

$Ca_V1.2$ channels are found in cardiac muscle, smooth muscle, endocrine cells, and neurons.[2] The physiological function for $Ca_V1.2$ includes excitation-contraction coupling in cardiac or smooth muscle, action potential propagation in sinoatrial and atrioventricular node, synaptic plasticity, and hormone secretion[2].

$Ca_V1.2$ is the main entry for external Ca^{2+} into the cardiomyocyte and its regulation contributes directly to cytosolic Ca^{2+} homeostasis [5, 6, 21, 25, 31, 37]. Disruption of $Ca_V1.2$ expression or function can contribute to pathophysiological cytosolic Ca^{2+}. For example, altered expression of $Ca_V1.2$ is detrimental to heart function and development. $Ca_V1.2^{-/-}$ knockout is embryonic lethal past embryonic day 14 in fetal ventricular mice [80, 81]. Alternatively, increased expression of

$Ca_V1.2$ also greatly alters cardiomyocyte function. L-type calcium channel over-expression transgenic mouse model resulted in an increase in calcium into the cardiomyocyte resulting in an increased contractile force, without modification in expression of accessory subunits. The major findings of this murine model were; 1.) weakened response of beta-adrenergic signaling pathway, and 2.) development of cardiac hypertrophy and severe cardiomyopathy slowly over time with age.[82-84]. Muth et.al. in 1999 postulates that PKC is increased by the increase calcium through the cardiac channel preceding cardiac hypertrophy, suggesting an endpoint example of altered transcription of the L-type calcium channel [82]. Enhanced $Ca_V1.2$ Ca^{2+} through the channel can be mediated by kinases indirectly by increasing $Ca_V1.2$ channel number subunit [85, 86]. Stimulation of PKA has also been shown to change transcriptional regulation of L-type calcium channels with a 404% increase in transcription rate initiation for the Ca_V1 subunit [85, 86]. Finally, $Ca_V1.2$ Ca^{2+} currents can be increased by mutations in the channel. Timothy syndrome is a de novo mutation in the $Ca_V1.2$ G406R that causes incomplete channel voltage inactivation[43, 87, 88]. In summary, $Ca_V1.2$ expression and function is essential for cardiomyocyte cytosolic Ca^{2+} homeostasis.

1.8 Summary

Ca^{2+} is essential for cardiac contraction [4, 26]. The cardiac L-type calcium channel coding region was first isolated in rabbit for $Ca_V1.2$ [2]. Cardiomyocyte $Ca_V1.2$ is part of a heteromultimeric complex composed of a pore forming $Ca_V1.2$ α-1-subunit, $Ca_V\beta2$ subunit, $\alpha_2\delta$, and sometimes ϒ [22, 69, 79, 89, 90]. $Ca_V1.2$ α-1-

subunit comprises four homologous repeats containing six transmembrane segments (Figure 1.2) [89]. $Ca_V1.2$ is a high voltage gated channel with a voltage sensor on the S4 segment. $Ca_V1.2$ selectivity for Ca^{2+} is achieved by S5-S6 pore segment on each repeat [91]. Macroscopic $I_{Ca,L}$ through the $Ca_V1.2$ is defined as current $I=i*N*Po$ [8]. LTCC initiates calcium induced calcium release (CICR) by Ca^{2+} through the LTCC binding nearby RyR_2 on the SR Ca^{2+} store [35]. Relaxation is mediated through clearance of the cytosolic Ca^{2+} by SR re-uptake, NCX, and Ca^{2+}ATPase. In order to maintain Ca^{2+} homeostasis, LTCC inactivate by voltage dependence (VDI) or Ca^{2+} dependence (CDI). Loss of function of either inactivation can lead to increased pathological cytosolic Ca^{2+} resulting in prolonged action potentials that may cause arrhythmias [41, 55]. Kinases enhance LTCC function by shifting the activation curve more negative and increasing the frequency and duration of channel openings. The $Ca_V1.2$ carboxyl-terminus is a substrate for kinase association and regulation [59, 64, 66-68]. Cardiac $Ca_V1.2$ channels are expressed as full length ~250kDa protein or a truncated ~190 kDa [59]. $Ca_V1.2$ carboxyl-terminal deletion studies show increased 4-6 fold increase in $I_{Ba,L}$ when ~70% of the $Ca_V1.2$ channel is truncated[76]. The remaining $Ca_V1.2$ carboxyl-terminus was later shown to re-associate with the $Ca_V1.2$ proximal-carboxyl-terminus (PCT) to recapitulate block of $I_{Ba,L}$ similar to full length $Ca_V1.2$ [1].

The contribution of LTCC to cardiomyocyte cytosolic Ca^{2+} homeostasis on a beat-to-beat basis has been an area of intense focus[5, 6, 25, 31, 34, 35, 38, 40, 45, 57]. The LTCC multiple roles include Ca^{2+} signaling gene regulation that can set the

diastolic resting Ca^{2+} between beats. The goal of this thesis is to examine the auto-regulatory function of $Ca_V1.2$ carboxyl-terminus. The function of LTCC channel segments such as the $Ca_V1.2$ carboxyl-terminus is an active ongoing field of research[63]. Although, LTCC channels have been studied extensively in heterologous over-expression systems, the number of studies on how the distal carboxyl-terminus of the $Ca_V1.2$ channel regulates function in a native system is limited.

1.9 Dissertation Overview

In Summary, the $Ca_V1.2$-DCT(1821-2171) blocks LTCC Ba^{2+} currents ($I_{Ba,L}$) in heterologous-expression systems [1, 76, 92]. Early studies of deletion analysis of $Ca_V1.2$ expressed in oocytes and HEK cells promoted the current view that DCT inhibits LTCC current[76, 77]. These previous studies showed that the shorter the $Ca_V1.2$ channel truncation, the larger the resulting current [92]. Subsequently, Hulme et al. showed that co-expression of DCT with truncated $Ca_V1.2$ reduced $I_{Ba,L}$ [1]. Moreover, DCT re-associates with $Ca_V1.2$ near the CB/IQ domain on the proximal carboxyl terminus (PCT). It is notable that the DCT interaction on $Ca_V1.2$ PCT site is juxtaposed to CaM interaction domains[93]. Therefore it is plausible to suggest that CaM may interact with DCT-LTCC function (Figure 1.6). To date, there are no reports of DCT effects on $I_{Ca,L}$ in HEK 293 studies, nor is there a demonstration of DCT effects on LTCC function in cardiomyocytes [94].

The overlying goal of this thesis is to examine the hypothesis that DCT is an important mediator of cell Ca^{2+} homeostasis in cardiomyocytes and functions in a calcium concentration dependent manner. The dissertation attempts to elucidate modulation of L-type calcium currents based on findings suggesting the cleaved $Ca_V1.2$(1821-2171) distal c-terminal domain of the L-type calcium channel can serve as a direct channel modulator and transcription factor[1, 23, 24, 75, 76, 95]. My overall hypothesis is that L-type calcium currents contribute to dynamic Cav1.2 distal carboxyl-terminus (DCT) $I_{Ca,L}$ block, acting as a reverse use-dependent inhibitor that increases current block under relatively low Ca^{2+} (Figure 1.6).

My simplified cartoon represents (Figure 1.6) physiological conditions of the $Ca_V1.2$ channel in ventricular myocytes. $Ca_V1.2$ is the main pore forming subunit with a predicted mass of 250kD and the exact length varies with species and splice variants [96]. The large ~665 amino acid $Ca_V1.2$ carboxyl terminus is located in the cytosolic space [25]. The cartoon does not depict accessory proteins such as $Ca_V\beta2a$ or $\alpha2\delta$ fo simplicity. Spectroscopic studies of the related skeletal muscle L-type Ca^{2+} channel isoform, $Ca_V1.1$, is cleaved at a site on the carboxyl terminus [1]. $Ca_V1.2$ distal carboxyl-terminus (DCT) has a predicted mass of ~37 kDa [1]. Therefore, the $Ca_V1.2$ remaining mass is < 200 kDa in the cardiomyocyte complex. The $Ca_V1.2$ length is reported as ~190 kDa in human [97]. Antibodies against full length $Ca_V1.2$ show singlets and doublets, but some of the literature figures are incomplete because the blots were cut off either above 190 or below 250 kDa limiting the data description. The model starts with the channel-closed in low membrane potential

hyperpolarized approximately -80 mV (left top). Middle panel Po diagram (Figure 1.5), NPo is relatively low and Ca^{2+} driving force is relatively high. Apo-CaMs (Ca^{2+} free form of CaM) is constitutively pre-associated with the channel and up to two CaMs can bind to the $Ca_V1.2$ carboxyl-terminus on the Pre-IQ C-region and the IQ domain respectively[98]. In non-physiological conditions where DCT and/or CaM is over-expressed in the cardiomyocytes, CaM may functionally compete with proteins that can interact with the $Ca_V1.2$ proximal carboxyl-terminus. We tested this in our previous paper demonstrating with biochemistry and electrophysiology that Rem, a small GTPase could interact with the $Ca_V1.2$ PCT and then be functionally displaced by CaM. We noted a recovery from zero current, the main effect of Rem co-expression with channel, and a slowing of CDI which implies Rem may functionally compete with CaM[60]. I propose a general concept that Cav1.2 has many binding partners and those proteins may have binding partners. Moreover, if channels are in clusters they will gate faster than low-density clusters or individual channels suggesting a cooperative gating. Now, take the well described interaction of a Ca^{2+} sensing protein CaM as tool to functionally dissect proteins dynamically interacting with the proximal carboxyl-terminus in cardiomyocytes. Rem demonstrated a case for using CaM as a functional readout of association backed up by biochemistry data. Building on the concept of CaM functional displacement of $Ca_V1.2$ PCT interacting proteins, I will test if excess CaM functionally disrupts DCT current inhibition in cardiomyocytes and HEK over-expression systems. I will use a similar analysis from the Rem experiment predicting DCT will slow CDI. Since CaM is a localized channel

Ca^{2+} sensor, I postulate that DCT functional inhibition maybe affected by cytosolic Ca^{2+} concentration. Ba^{2+} used as the charge carrier in electrophysiology experiment with Ca^{2+} buffering EGTA in the pipette solution will test a nominal Ca^{2+} environment when DCT and CaM are over-expressed. I predict DCT will functionally inhibit $I_{Ba,L}$ as published in previous literature and the co-expression of CaM to interrupt DCT current block. Now to test the effect of increased Ca^{2+} on DCT inhibition of $I_{Ca,L}$, I will use physiological bath solutions. As Ca^{2+} is readily available, I predict the pre-associated CaMs will bind Ca^{2+}, change conformation, and reduce the ability of DCT to functionally inhibit the channel. However, in intact myocytes I postulate that DCT may lower NPo at negative potential. Whole cell patch clamp $I_{Ca,L}$ are relatively small at peak current, assessing current at low voltages requires a different approach to test this hypothesis. I will use intact cardiomyocytes and assess the resting diastolic Ca^{2+} using a calcium ratio metric dye. The cells can then be electrically stimulated at different frequencies to test a range of systolic Ca^{2+}, as pacing frequency increases so does diastolic Ca^{2+}. As NPo increases, diastolic Ca^{2+} increases, and DCT inhibition is relieved.

1.9.1 Regulation of $Ca_V1.2$ function by DCT and CaM (in Chapter 3)

Specific Aim 1: Establish DCT block on $I_{ca,L}$ in a reconstituted system.

Rationale: The LTCC distal carboxyl-terminus (DCT) is proteolytically cleaved, and re-associates with the LTCC complex to regulate Ca^{2+} channels[1]. DCT reduces LTCC barium current ($I_{Ba,L}$) in reconstituted complexes, and mediated by the fight or flight

response[64]; yet the contribution of DCT to $I_{Ca,L}$ in reconstituted systems is unexplored. This study examines the contribution of DCT to LTCC function in the HEK model.

Specific Aim 2: Functionally compete with DCT block on $I_{ca,L}$ in a reconstituted system.

Rationale: CaM is a calcium sensor pre-associated with the PCT on the LTCC, and DCT re-associates with the LTCC complex to regulate Ca^{2+} channels[1, 76, 77]. CaM partially restores PCT associated Rem block LTCC calcium current ($I_{Ca,L}$) in reconstituted complexes, and slows the calcium dependent inactivation kinetics. Over-expression of CaM may functionally compete with DCT block to restore LTCC $I_{Ba,L}$ and $I_{Ca,L}$. in reconstituted systems. This study examines the contribution of CaM to functional DCT block on LTCC function in the HEK model.

1.9.2 $Ca_V1.2$-DCT as a reverse use dependent inhibitor (in Chapter 4)

Specific Aim 1: Establish DCT block on $I_{Ba,L}$ and $I_{Ca,L}$ in a native cardiomyocyte system.

Rationale: The LTCC distal Carboxyl-terminus (DCT) is proteolytically cleaved, and re-associates with the LTCC complex to regulate Ca^{2+} channels[1]. DCT reduces LTCC barium current ($I_{Ba,L}$) in reconstituted complexes; however the contribution of DCT to $I_{Ba,L}$ and $I_{Ca,L}$ in native cardiomyocyte systems is unexplored. This study examines the contribution of DCT to LTCC function in the cardiomyocyte model.

Specific Aim 2: Functionally compete with DCT block on $I_{Ba,L}$ and $I_{Ca,L\ L}$ in a cardiomyocyte.

Rationale: CaM is a calcium sensor pre-associated with the PCT on the LTCC, and DCT re-associates with the LTCC complex to regulate Ca^{2+} channels[1, 76, 77]. CaM partially restores PCT associated Rem block LTCC calcium current ($I_{Ca,L}$) in reconstituted complexes, and slows the calcium dependent inactivation kinetics. Over-expression of CaM may functionally compete with DCT block to restore LTCC $I_{Ba,L}$ and $I_{Ca,L}$. in a native cardiomyocyte system. This study examines the contribution of CaM to functional DCT block on LTCC function in the native cardiomyocyte model.

Specific Aim 3: Establish DCT block as a function of low to high frequency electrical pacing of the cardiomyocytes *in-vitro.*

Rationale: Increasing diastolic calcium is sufficient to induce pathological hypertrophy, reduced contraction, and arrhythmias. Electrical pacing depolarized the membrane opening LTCC increasing cytosolic Ca^{2+} concentration beat to beat. As frequency of electrical stimulation is reduced, LTCC contribution to the cytosol is decreased. Since DCT does not block $I_{Ca,L}$ but does $I_{Ba,L}$ in whole cell Ca^{2+} buffered patch clamp recordings, I postulate that cytosolic Ca^{2+} is high when Ca^{2+} currents are recorded and cytosolic Ca^{2+} is nominally low when Ba currents are recorded. Over-expression of DCT may functionally block at very low cytosolic Ca^{2+} in an intact native cardiomyocyte system. This study examines the contribution of cytosolic Ca^{2+} to functional DCT block on Ca^{2+} transients in the native cardiomyocyte model.

Table 1.1 List of Abbreviations

Name	Abbreviation	Name	Abbreviation
Proximal Carboxyl-terminus	PCT	Calmodulin	CaM
Distal Carboxyl-terminus	DCT	Fetal Ventricular myocyte	FVM
L-type Calcium channel	LTCC	L-type Calcium channel	LTCC

	Current Type	Protein	Gene	Former name	Expression	Function
HVA	L	$Ca_v1.1$	*CACNA1S*	α1S	Skeletal muscle	EC-coupling
	L	$Ca_v1.2$	*CACNA1C*	α1C	Cardiac myocytes	EC-coupling
	L	$Ca_v1.3$	*CACNA1D*	α1D	Atrial cardiac myocytes	Pacemaking
	L	$Ca_v1.4$	*CACNA1F*	α1F	Retina	Neurotransmitter release
	P/Q	$Ca_v2.1$	*CACNA1A*	α1A	Neural	Neurotransmitter release
	N	$Ca_v2.2$	*CACNA1B*	α1B	Neural	Neurotransmitter release
LVA	R	$Ca_v2.3$	*CACNA1E*	α1E	Neural	Dendritic Ca^{2+} transients
	T	$Ca_v3.1$	*CACNA1G*	α1G	Embryonic Cardiac myocytes	Pacemaking
	T	$Ca_v3.2$	*CACNA1H*	α1H	Embryonic cardiac myocytes	Pacemaking
	T	$Ca_v3.3$	*CACNA1I*	α1I	Neural	Pacemaking

Modified from Hille B. *Ion channels of excitable membranes*. Sunderland, Mass.: Sinauer; 2001. and Catterall, W.A., et al., *International Union of Pharmacology. XLVIII. Nomenclature and structure-function relationships of voltage-gated calcium channels*. Pharmacol Rev, 2005. **57**(4): p. 411-25.

Figure 1.1 L-type Calcium channels are part of a voltage gated superfamily. The table represents a brief overview of channels and function, for complete details see excellent reviews from Catterall [2]. The gene CACNA1C encodes for the protein $Ca_V1.2$. L-type calcium channels are high voltage activated (HVA) channels.(highlighted box). $Ca_V1.2$ channels are expressed in heart, smooth muscle, neurons, and endocrine cells. $Ca_V1.2$ is the predominant protein expressed in ventricular cardiomyocytes. $Ca_V1.2$ triggers excitation-contraction coupling (EC-coupling) and can act as a transcription factor.

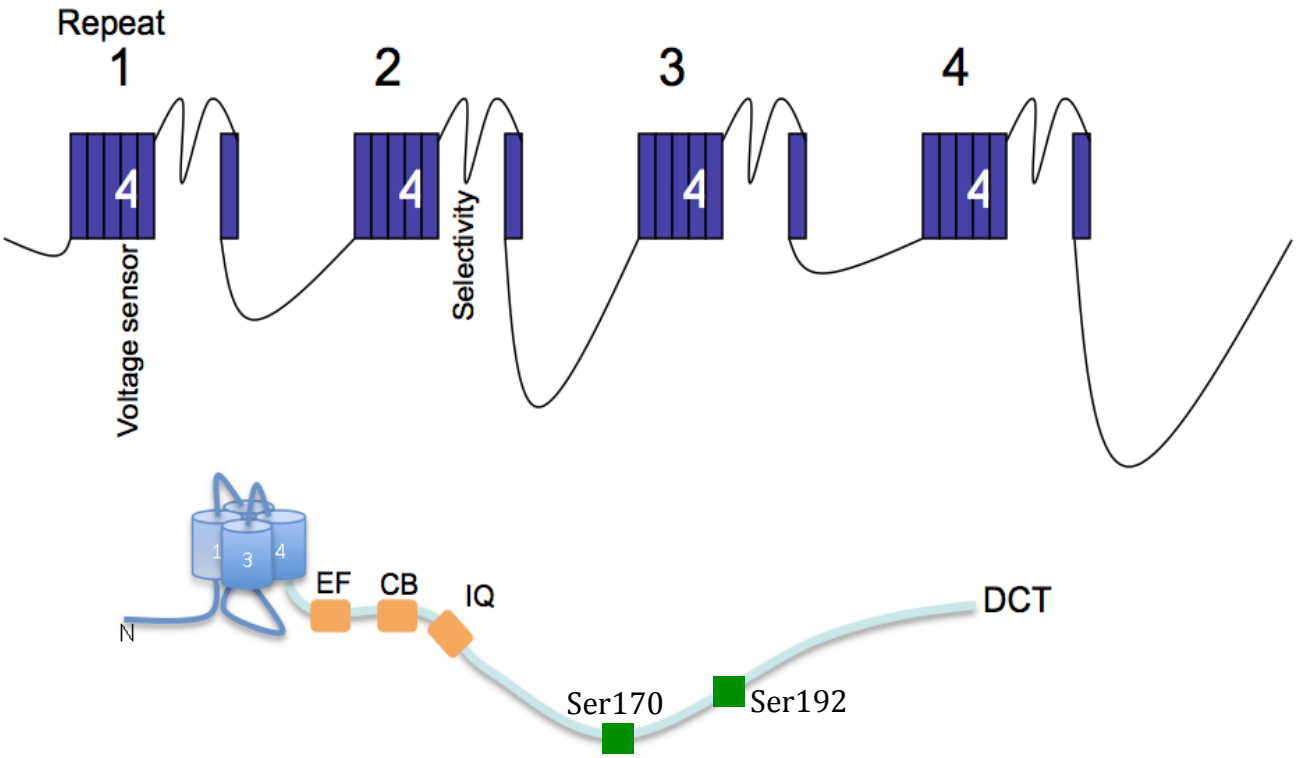

Figure 1.2 Structure of $Ca_V1.2$. $Ca_V1.2$ is made up of 6 transmembrane segments with 4 repeats. Segment 4 (S4) is the voltage sensor and the hairpin loop between S5-S6 confers ion selectivity for the pore. $Ca_V1.2$ forms a complex with many interaction partners, however $Ca_V\beta$ subunit co-expression with the channel is sufficient for recording $I_{Ca,L}$ and $I_{Ba,L}$. DCT is thought to be associated with PCT through electrostatic interaction. Ser1700 and Ser1928 are described substrates for kinase phosphorylation.

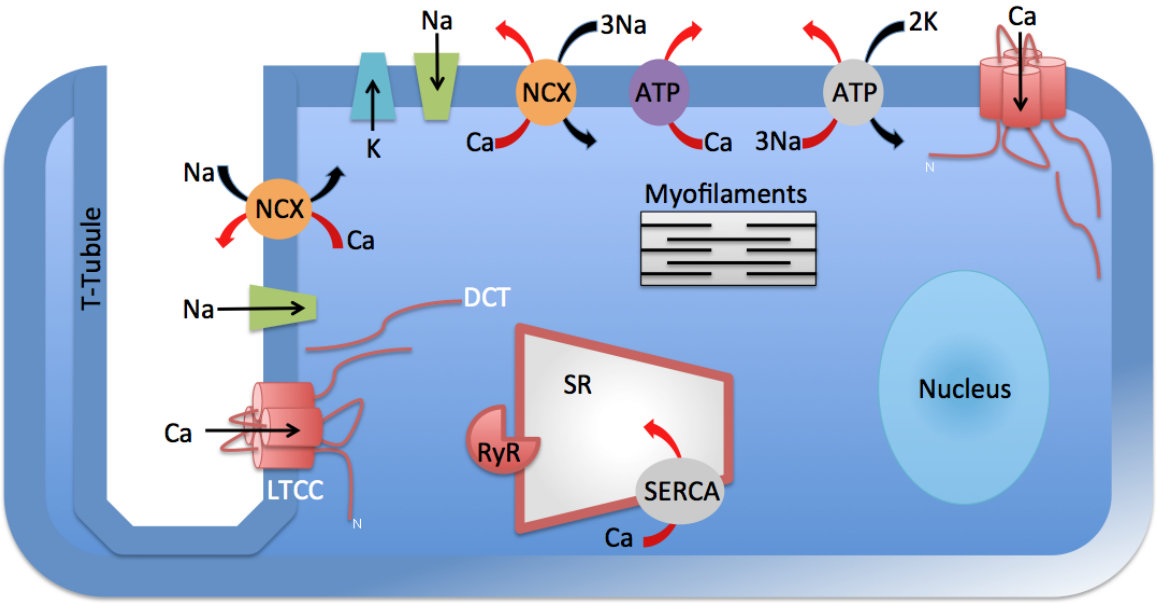

Figure 1.3 Fundamental components of excitation contraction coupling. A simplified picture of the CICR with the major components for excitation-contraction and relaxation. $Ca_V1.2$ channel (LTCC) opens upon membrane depolarization. Ca^{2+} goes through the channel and binds RyR_2 on the Sarcoplasmic reticulum (SR), globally releasing Ca^{2+} into the cytosol. As cytosolic Ca^{2+} concentrations increase, Ca^{2+} binds Troponin C followed by contraction. Ca^{2+} is cleared from the cytosol through multiple actions. Most notably, Ca^{2+} is extruded by NCX, Ca^{2+}-ATPase, and by SR Ca^{2+} re-uptake to lower Ca^{2+} concentration resulting relaxation.

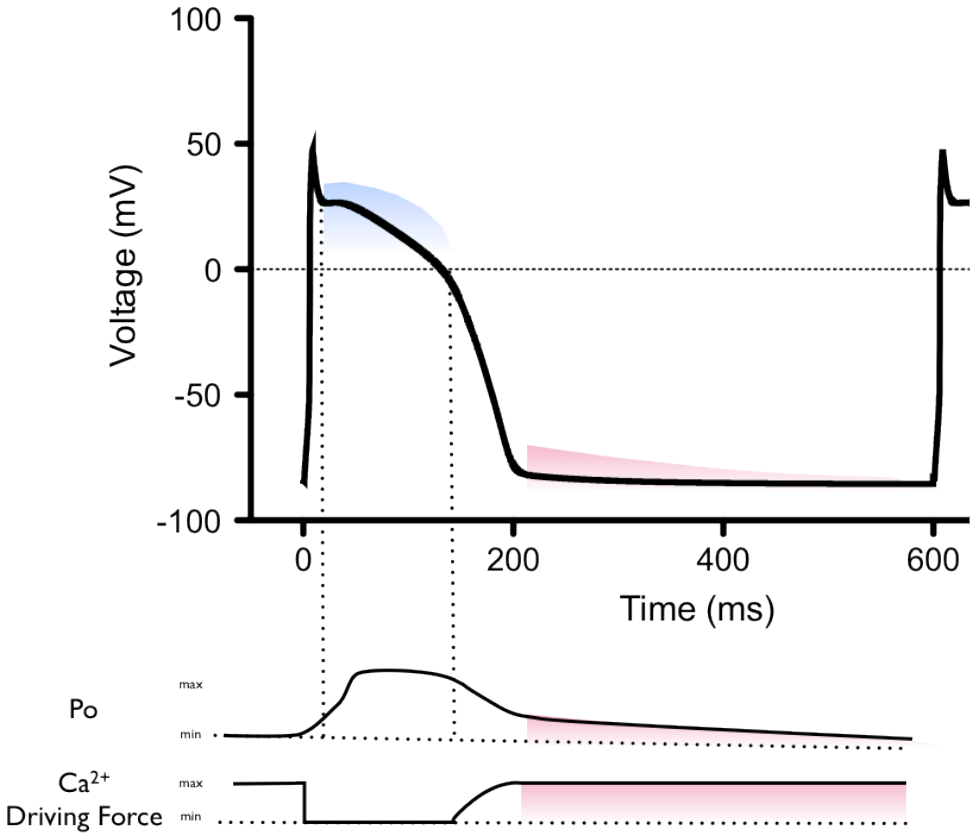

Figure 1.4 Relationship of Action potential to Po and Ca^{2+} driving force. When membrane potential is negative, $Ca_V1.2$ channel Po (blue) is low and Ca^{2+} electrochemical driving force is high. I propose DCT lowers Po comparatively. As Po increases Ca^{2+} driving force is rapidly reduced.

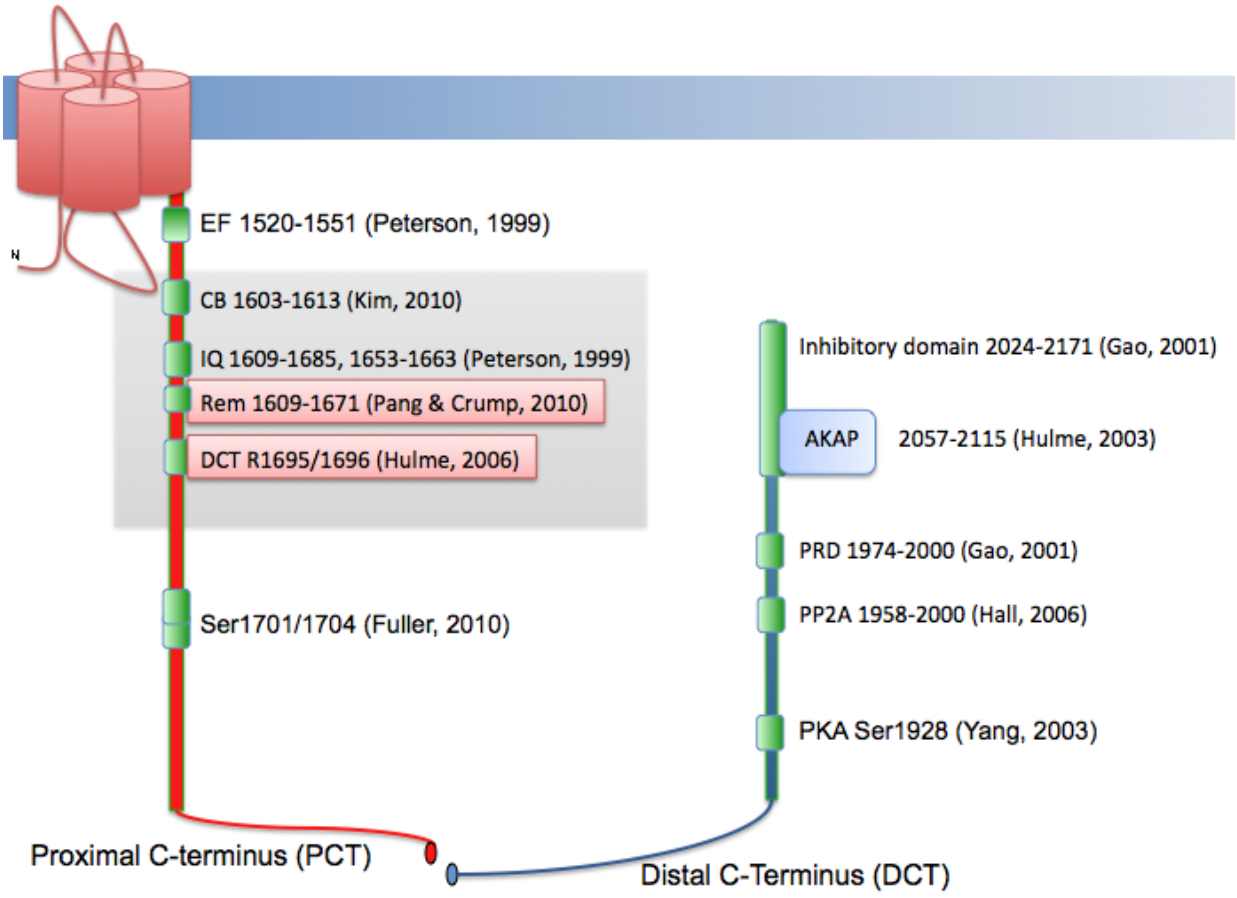

Figure 1.5 $Ca_V1.2$ Proximal and Distal Carboxyl-terminus. $Ca_V1.2$ proximal carboxyl-terminus (PCT) contains the IQ domain with CaM pre-associated. DCT can functionally re-associate with the channel to inhibit $I_{Ba,L}$ in HEK cells . PCT and DCT are substrates for kinase regulation at Ser1701 and Ser1928. DCT contains an inhibitory domain from amino acids 2024-2171 in rabbit sequence.

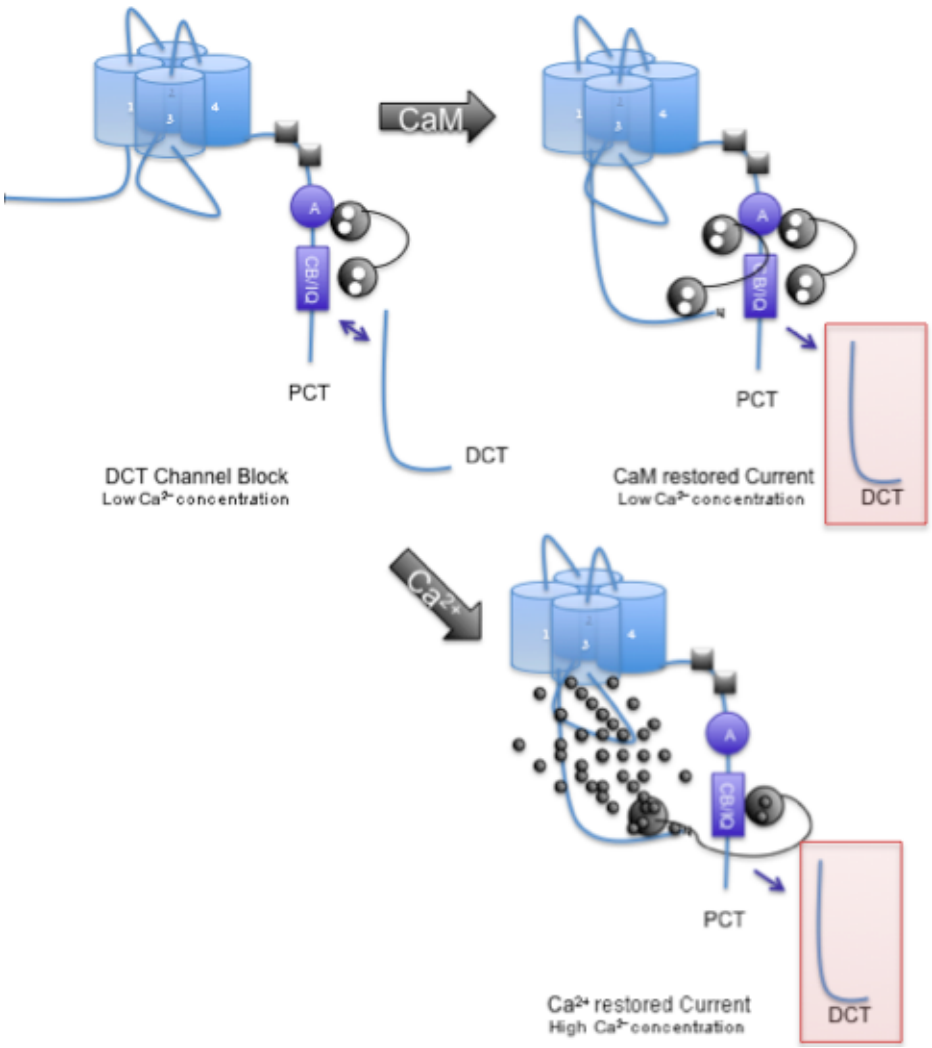

Figure 1.6 Proposed model of DCT function. DCT blocks $Ca_V1.2$ Ba^{2+} current in cardiomyocytes and HEK 293 cells. CaM (tethered black circles) over-expression completely reverses DCT functional inhibition of Ba^{2+} current. When membrane potential is negative, $Ca_V1.2$ channel Po is low, and addition of DCT lowers Po comparatively. As the channel opens and Ca^{2+} enters the cytosol increasing concentration around the channel and, DCT no longer functionally inhibits the channel (bottom right). If Ca^{2+} remains low and Ba^{2+} is used as the charge carrier, CaM over-expression relieves DCT functional block (top right).

Copyright © Shawn M. Crump 2012

Chapter 2: Materials and methods

2.1 HEK cell culture

Cells were maintained at 37° Celsius and 5% CO_2. Cells were split when the division reached 70% confluence in 10 cm tissue culture plate. Cells were washed with PBS, and then incubated with 5 mL of trypsin for 3 minutes. Addition of 5mL 10% FBS tissue culture media neutralized the trypsin. Cells were collected and centrifuged for 3 minutes at 500 rpm. The supernatant was removed and 10mL of fresh media was added to the cell pellet. 5-10 drops of the re-suspended cells were added to new 10 cm tissue culture plates containing 10mL of fresh tissue culture media with 10% FBS. Cells were not split less than three days at a time and new cells were thawed once passage number exceeded 20 to maintain a range in heterologous transfection efficiency.

2.2 E18 primary cell isolation

ICR (outbred Charles Rivers mice, CD-1®) mice were housed in a pathogen-free facility and handled in accordance with standard use protocols, animal welfare regulations, and the NIH *Guide for the Care and Use of Laboratory Animals*. All protocols were approved by the University of Kentucky Institutional Animal Care and Use Committee (IACUC protocol #00963M).

Fetal ventricular cardiomyocytes were isolated as described previously[99]. Timed pregnant dams of embryonic day 16-19 (E16-19) were anesthetized with ketamine (90mg/kg) + xylazine (10mg/kg) intraperitoneal injected . Litters were removed. Fetuses were decapitated and hearts excised. While under anesthesia the dam was euthanatized by heart excision. Below outlines the isolation in detail.

2.2.1 Solutions

1. 50 mL 1xPBS+25microL 2M MgCl2, filter with 0.45micron filter (white) 2. Add 10micrograms of Worthington Collagenase II to 20mL of PBS+MgCl2. Add 10 mL to a 10 mL syringe and add a 0.2 micron filter. 3. Add 2.5mL freshly thawed FBS to a 50mL tube and bring to 50mL volume with 5% FBS/DMEM

2.2.2 Isolation Protocol

Place embryo sac containing pups in 50mL tube with ~5-10mL of PBS + $MgCl_2$ (250 microL of 2mM $MgCl_2$ added to 500mL PBS). Extract pups, remove all from embryonic sac. In sequence, decapitate, cut down chest from neckline, spread with forceps and press cavity until heart pops up, pull heart and place in separate dish with ~3mL PBS+$MgCl_2$. Grab atria or aorta with forceps and cut away with scissors. Press hearts to push any remaining blood out of the vessels or arteries and place ventricle in 15mL tube with ~ 10mL of PBS+$MgCl_2$. Spin ~ 5min at 500 rpm. Re-suspend in ~ 1mL of filtered Collagenase. Cut the tip off a 1000 μL tip and transfer the pellet to a culture dish lid with ~ 1 mL of filtered Collagenase II (Worthington). Tear the hearts apart using forceps. Transfer hearts back into the 15mL tube and

bring to 10mL volume with filtered Collagenase. Set tube on its side in the 37 degree incubator for 10 min, then spin down for ~5 minutes at 500 rpm. Re-suspend in fresh filtered Collagenase. Cut the tip off a 1000 μL tip and transfer the pellet to a culture dish lid with ~ 1 mL of filtered Collagenase. Bring to 10mL volume with filtered Collagenase. Set tube on its side in the 37° incubator for 10 min, then spin down for ~5 at 500 rpm. Based on pellet size, re-suspend with 5-10 mL of 10% FBS/DMEM. Break apart the pellet using a 3mL syringe + 18 gauge needle. Setup a 24 well plate with pre-treated coverslips (Poly-L, Lamimin, or Fibronectin for at least 30 min under UV light). Add 0.5 mL of media in each well and use serological pipette to submerse all coverslips. Swirl plate to rinse coverslips well. Remove media and add 500 μL of fresh 10% FBS/DMEM to each well. Place plate in incubator (This step can be done during the second 10 minute incubation with Collagenase). To the first 3 wells, add 1 drop, then 2 drops to the second well, and 3 drops to the third well. Compare wells under the microscope and choose the desired plating density. The method described produces the best results. For electrophysiology experiments, plate ~ 5000 cell per 35mm dish. Plating with less cells will result in poor transfection efficiency. To account for this variation, I plated half the wells with one drop and the other half of the wells with 2 drops. Plating > 5000 cells/35mm well were used for Fura-2 calcium imaging or confocal experiments.

2.3 Adult ventricular myocyte isolation

Single adult ventricular myocytes were isolated using a Alliance for Cellular Signaling protocol PP00000125 with modifications[24]. Four to six month old female ICR mice were anesthetized. Chest was opened to expose the lungs and heart. The heart was excised, hung on a blunted needle in less than 1 min, then retrogradely perfused at 3 mL/min at 37°C for 4 to 8 minutes with a Ca^{2+}-free bicarbonate based perfusion buffer containing (in mmol/L) NaCl 113; KCl 4.7; KH_2PO_4 0.6; $MgSO_4$ 1.2; NaH_2PO_4 0.6; glucose 5.5; $NaHCO_3$ 12; $KHCO_3$ 10; HEPES 10; phenol red 0.032; 2,3-butanedione mon- oxime 10; and taurine 30. Before the heart was perfused, the perfusion buffer was gassed with 95% O_2/5% CO_2 for at least 30 minutes. Enzymatic digestion began using 0.25 mg/mL liberase blendzyme (Roche), and 12.5 μmol/L $CaCl_2$ was added to the perfusion buffer for approximately 10-15 minutes until the heart was swollen and pale in color. The heart was then cut from the cannula. Ventricular tissue was placed in a dish with enzyme buffer and gently dissociated for several minutes. After the addition of stop buffer (perfusion buffer containing 10% FBS and 12.5 μmol/L $CaCl_2$), dissociation continued until large pieces of heart tissue were gently dispersed into the cell suspension. Cells were allowed to sediment by gravity for 10 minutes followed by centrifugation at 500 rpm for 1-3 minutes. Cells were re-suspended in perfusion buffer containing 5% FBS/DMEM and 12.5 μmol/L $CaCl_2$. External Ca^{2+} was added in four segments to the solution with a final concentration of 2.0 mmol/L. Only rod-shaped, square ended,

quiescent myocytes with clear striations were selected for current recordings or Ca^{2+} imaging.

2.4 Plasmids

Full length $Ca_V1.2$ plasmid (provided by Dr. T. Kamp, University of Wisconsin) was identical to the cloned full-length rabbit cardiac α1C-subunit[100, 101] except for alternative splicing in domain IV S3[101]. Rat $Ca_V\beta2a$ plasmid (provided by Dr. E. Perez-Reyes, University of Virginia)[10] contains two cysteine residues within the D1 domain associated with palmitoylation. CaM_{1234} was provided by David T. Yue (Johns Hopkins University), and $Ca_V1.2\Delta1801$ was provided by Henry Colecraft (Columbia University).

2.5 Lipofectamine transfection

HEK-293 cells were transiently transfected with plasmids 4-6 hours using Lipofectamine® 2000 transfection (Invitrogen Corporation), then recordings were performed 24-48 hours after transfection, as previously described [102]. Transfected cells were identified by the expression of eGFP.

2.6 Ca^{2+} imaging

E18 fetal mouse cardiomyocytes were used 24-72 hours after Lipofectamine® 2000 transfection (Invitrogen Corporation). Myocytes plated on Poly-L-Lysine 25mm square glass coverslips were incubated with 2micoM of freshly mixed Fura-2, AM (Molecular Probes, F-1221, from stock 2.5mM in DMSO) + 10% FBS media for 8 minutes at 37°C without Pluronic (as sometimes used to aid adult

myocyte Fura-2 loading). Coverslips were transferred to a custom-designed microscope chamber system containing physiological salt solution with 1.8mM $CaCl_2$. Transfected cells were identified by the eGFP or eGFP fused $Ca_V1.2$ (1821-2171) at the N-term. Cells were measured initially for 20 seconds without pacing, and then paced at 1Hz, 2Hz, 3Hz, 0.5 Hz, and 0Hz for 20-60 seconds at each frequency. Diastolic F_{340}/F_{380} (F/F_o) ratios were determined using Clampfit 9.2. Ca^{2+} calibrations were performed as in reference [103]. All recordings were performed at room temperature (20–22°C) using IonOptix Myocyte Calcium Recording System, Myopacer Field Stimulator, and IonWizard 4.4 revision 13 (IonOptix LLC, Milton, MA). I used unpaired Students t-test to test for significance between control and experimental groups.

2.7 Electrophysiology

Transfected cells were identified by the expression of eGFP. The whole cell configuration of the patch-clamp technique was used to measure ionic current. Patch electrodes with resistances of 1–2.5 MΩ contained pipette solution consisting of: (in mM) 110 K-gluconate (or 110 TEA-Cl), 40 CsCl, 3 EGTA, 1 $MgCl_2$, 5 Mg-ATP, and 5 HEPES, pH to 7.36 with CsOH. The bath solution for HEK cells consisted of (in mM) 130 (or 112.5) CsCl, 2.5 (or 30) $BaCl_2$ or $CaCl_2$, 1 $MgCl_2$, 10 tetraethylammonium-Cl, and 5 HEPES, 5 glucose, pH 7.4 with CsOH. For fetal ventricular myocytes, the physiological salt solution (PSS) contained 140 NaCl, 1.8 $CaCl_2$, 1 $MgCl_2$, 5.4 KCl, 10 glucose, and 10 HEPES, pH 7.4. The Na-free bath was 150

N-methyl-D-glucamine, 2.5 $BaCl_2$ (or $CaCl_2$), 1$MgCl_2$, 10 HEPES, 10 glucose, and 5 4-aminopyridine, pH 7.4. Signals were amplified with an Axopatch 200B amplifier, with series resistance compensation, and captured at 333 kHz A/D system (Axon Instruments, Union City, CA). For HEK 293 cells, current-voltage curves were generated by voltage clamp protocols consisting of: V_{hold}= -80 mV followed by 320 ms V_{test} pulse ranging from -80 mV to +80 mV in 5 mV increments (Figure 2.1). For myocytes, current-voltage curves were generated by voltage clamp protocols consisting of: V_{hold} = -80 mV, $V_{pre\text{-}pulse}$ = -40 mV for 100ms, followed by V_{test} for 310 ms ranging from -60 mV to +80 mV in 10 mV increments. The 100 ms $V_{pre\text{-}pulse}$ to -40 mV inactivated voltage-gated Na^+ currents (Figure 2.2). For analysis of gating currents, cardiomyocytes were stepped from -80 mV to a reversal potential determined by the I/V curve for each cell (typically -50 mV) for 400 ms, then stepped to +50 mV for 20 ms, then back to -60 mV for tail current (Figure 2.3). For analysis of voltage dependence of steady state inactivation, myocytes were held at -80 mV and subjected to a 50 ms pre-pulse at 0 mV, followed by a 2-sec steady state inactivation pulse from -80 mV to +20 mV in 10 mV increments, then a test-pulse to 0 mV for 300 ms. 8-sec intervals elapsed between each recording sweep (Figure 2.4). Whole cell recordings used P/4 leak subtraction. Activation voltage dependence parameters were obtained by fitting current voltage curves to a modified Boltzmann distribution of the form: : $I(V) = G_{max}*(V-E_{rev})/(1+\exp(V_{½} - V)/k)$, where Gmax is maximal conductance, Erev is reversal potential, $V_{½}$ is activation midpoint potential, and *k* is the slope factor. Data were analyzed with

Clampfit 9.2 (Axon Instruments), Origin v7 (OriginLab, Northampton, MA), and unpaired t test with Welch's correction and/or one way Student t-test statistics performed with Prism 5 (GraphPad Software, Inc.). Sample sizes are listed in the Figure and Table Legends.

Figure 2.1 HEK current voltage protocol

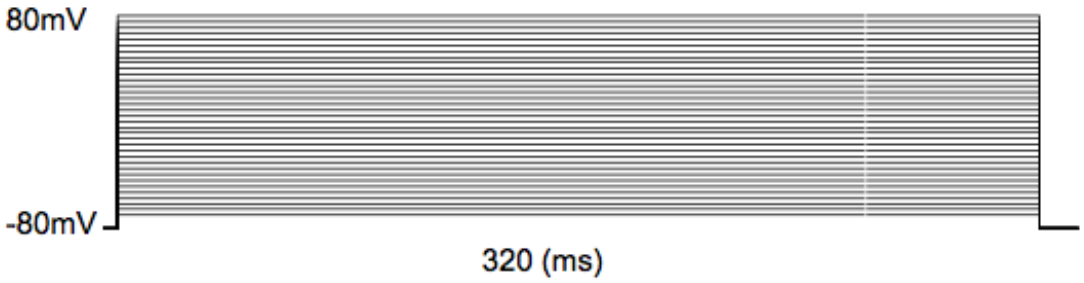

Figure 2.2 Cardiomyocyte current voltage protocol

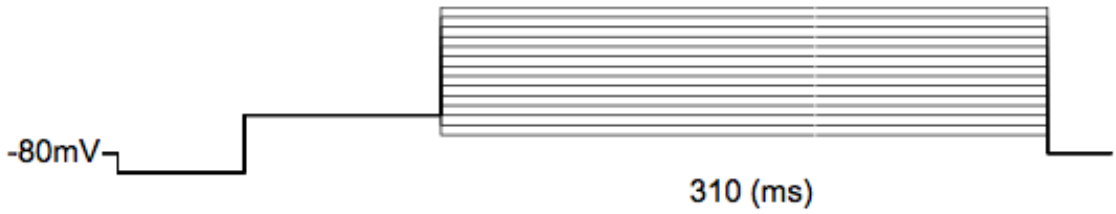

Figure 2.3 Cardiomyocyte gating current protocol

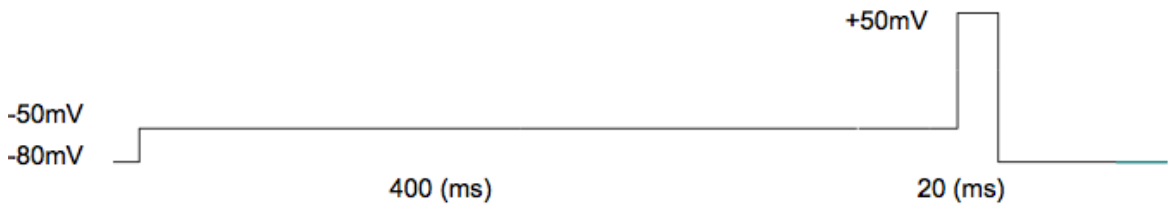

Figure 2.4 Cardiomyocyte steady-state inactivation protocol

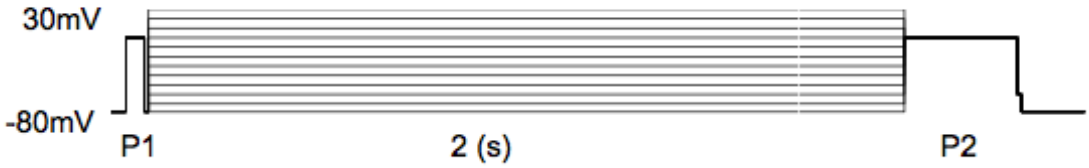

Copyright © Shawn M. Crump 2012

Chapter 3: Regulation of $Ca_V1.2$ function by DCT and CaM

3.1 Introduction

The $Ca_V1.2$ DCT blocks LTCC Ba^{2+} currents ($I_{Ba,L}$) in heterologous expression systems [1, 92]. Early studies of deletion analysis of $Ca_V1.2$ expressed in HEK cells established the current view that DCT inhibits LTCC current. These previous studies showed that the shorter the $Ca_V1.2$ channel truncation, the larger the resulting current [92]. Subsequently, Hulme et al. showed that co-expression of DCT with truncated $Ca_V1.2$ reduced $I_{Ba,L}$ [1]. Moreover, these studies indicate that DCT re-associates with $Ca_V1.2$ near the CB/IQ domain on the proximal carboxyl terminus (PCT). It is notable that the DCT interaction site overlaps the well characterized $Ca_V1.2$ PCT CaM interaction domains [93]. Therefore it is plausible to suggest that CaM may modulate DCT-LTCC function. To date, there are no reports of DCT effects on $I_{Ca,L}$ [94].

3.2 Results

3.2.1 DCT inhibits IBa,L, but not ICa,L in HEKs.

Early clues to the potential inhibitory contribution of DCT were elucidated when studies used $Ca_V1.2$ truncation at amino acid position 1733 ($Ca_V1.2\Delta1733$;[30,

76]). Subsequent studies demonstrated that DCT blocked $I_{Ba,L}$ when DCT was co-expressed with $Ca_V1.2\Delta1801$[1]. I tested both $Ca_V1.2\Delta1733$ and $Ca_V1.2\Delta1801$ co-expressed with $Ca_V\beta2a$ and DCT in HEK 293 cells. $Ca_V1.2\Delta1733$ expressing cells displayed DCT blockade in a similar pattern to that for DCT in cardiomyocytes. DCT reduced peak $I_{Ba,L}$, but not $I_{Ca,L}$ (Figure 3.1). DCT inhibition of $I_{Ba,L}$ was reversed by co-expression of CaM with DCT (Figure 3.2). $I_{Ca,L}$ and $I_{Ba,L}$ was recorded in all cells, and the relative difference between $I_{Ca,L}$ and $I_{Ba,L}$ serves as an internal check that DCT selectively interferes with $I_{Ba,L}$ but spares $I_{Ca,L}$. Note that maximal $I_{Ba,L}$ relative to $I_{Ca,L}$ is distinct with DCT expression compared to other conditions (Figure 3.1 and 3.2), $Ca_V1.2\Delta1801$ expressing cells also exhibited DCT inhibition of peak $I_{Ba,L}$ (Figure 3.5 and 3.6); however, this was accompanied by a corresponding decrease of $I_{Ca,L}$ (Figure 3.5). Thus, in heterologous expression, both $Ca_V1.2$ truncation constructs mimic DCT attenuation of cardiomyocyte peak $I_{Ba,L}$. The absence of $I_{Ca,L}$ effect on peak current is also captured by the $Ca_V1.2\Delta1733$ construct.

DCT did not significantly alter the voltage dependence of activation for $I_{Ca,L}$ or $I_{Ba,L}$ (Table 3.1), with one notable exception. $Ca_V1.2\Delta1733$ $I_{Ca,L}$ required a second Boltzmann distribution to fit data negative to -20mV (Figure 3.12). There is no voltage threshold for LTCC opening. Rather, at relatively negative voltages, open probability (Po) is at very low levels. These results are consistent with the notion that DCT preferentially inhibits LTCC when Po is relatively low. We could not verify these measurements in cardiomyocytes because current amplitudes were too small.

3.2.2 DCT has no effect on LTCC current kinetics

Voltage-dependent inactivation (VDI) of $I_{Ba,L}$ is enhanced by DCT in cardiomyocytes (Figure 3.3 and 3.4). VDI, measured as the remaining $I_{Ba,L}$ of $Ca_V1.2\Delta1801$ or $Ca_V1.2$ $\Delta1733$ channels, co-expressed with DCT, showed indistinguishable (Figure 3.7 and 3.8). CaM co-expression had no effect. $I_{Ca,L}$ decay kinetics was not affected by DCT (Figure 3.3 and 3.4). The consensus finding from these heterologous expression studies is that $I_{Ba,L}$ is blocked by DCT, and this block can be antagonized by CaM co-expression. At limiting Po, DCT blocks better. This raises the notion that elevated Ca^{2+}-entry, perhaps in complex with CaM, modulates DCT blockade.

3.2.3 Role of Ca^{2+}-CaM in CaM-DCT current restoration.

To distinguish between Ca^{2+} and Ca^{2+}-CaM requirement for relief of DCT blockade I co-expressed CaM_{1234} (Ca^{2+} binding deficient mutant CaM) with $Ca_V\Delta1733$ and measured $I_{Ba,L}$ and $I_{Ca,L}$. We focused on $Ca_V\Delta1733$ for this experiment because this construct captured DCT effects on cardiomyocyte $I_{Ba,L}$ and $I_{Ca,L}$. Figure 3.9 shows the results of CaM_{1234} with or without DCT. CaM_{1234} did not restore current in cells co-expressing DCT. Rather, the currents in both control and test group were identical. CaM_{1234} reduced the control $I_{Ba,L}$ and DCT+CaM_{1234} did not result in an additive block. Comparison of $I_{Ba,L}$ and $I_{Ca,L}$ I(V) curves for CaM_{1234} expression (Figure 3.9) to $I_{Ba,L}$ and $I_{Ca,L}$ I(V) curves without CaM_{1234} (Figure 3.9) illustrates that CaM_{1234} preferentially blocked $I_{Ba,L}$ compared to $I_{Ca,L}$. CaM_{1234}

reduced CDI and compared to eGFP control or DCT co-expression (Figure 3.10). Taken together, these results show that CaM_{1234} and DCT individually exert similar action on LTCC current. These results are consistent with a model that limiting channel Po, and limiting Ca^{2+} favors increased DCT blockade.

3.2.4 Role of Ca^{2+} in Time to peak current.

Time to peak comparing CaM_{1234} vs. CaM_{1234}+DCT in Ca^{2+}. Examination of time to peak to test if Ca^{2+} through the Ca^{2+} channel changes the rate of activation, no change was observed except when CaM_{1234} was co-express, then time to peak increases (Figure 3.11).

3.2.5 DCT co-expression requires a double Boltzmann equation

DCT co-expression in HEKs requires a double Boltzmann equation for a successful fit in Ca^{2+} measured currents. (Figure 3.12)- (i) $I_{Ca,L}$ currents measured in control cells are successfully curve fitted with a single Boltzmann fit. (Figure 3.12-(ii)) $I_{Ca,L}$ currents measured in DCT over-expressed cells are failed to curve fit with a single Boltzmann equation in 7/8 cells. Yet could be fitted with a double Boltzmann equation. Note changed aspect ratios to improve comparison to Figure 3.1.

3.3 Discussion

In this dissertation I report a novel mechanisms of action of DCT on $I_{Ca,L}$ in HEK 293 cells that was previously not reported. My first major finding was that DCT inhibited HEK $I_{Ba,L}$, but not $I_{Ca,L}$. DCT blockade of $I_{Ba,L}$ was consistent with earlier studies in HEK 293 cells [1, 76]; however, literature searching earlier studies did not consider $I_{Ca,L}$. Second, my data showed that DCT blockade was antagonized by Ca^{2+}-CaM.

The first major finding of the present study, DCT blocks $I_{Ba,L}$ but not $I_{Ca,L}$ leads to the question: what kind of block? In this section, I discuss the type of block by DCT, open channel block or closed channel block. In simplest terms of voltage gated channels opening and closing, channels are closed at negative potential and open at relatively positive potentials. Set aside inactivation for the moment by VDI and CDI as extensively described in the introduction. During a sequence of closed to open, there may be multiple open and closed channels at the same time, thus shifting from a majority of closed channels to a majority of open channels. With co-expression of DCT, I hypothesized that at negative potentials, even more channels will be closed operating as a closed channel block. Sotalol works as a reverse use dependence potassium channel drug block resulting in longer action potential duration[104]. This drug binds during resting state and action potential duration is prolonged, however as pacing frequency increases, prolongation of the action potential duration decreases[104]. This action is consistent with reverse use dependence. Open block starts with an increased APD and as the pacing frequency increases, prolongation of the APD decreases, the opposite effect of closed

channel block [104]. 4-AP blocks ferret ventricular myocyte Ito only at hyperpolarized potentials and do not need Ito channels to be activated for block, but advances very diminutive block at positive potentials [105]. Dofetilide also acts as a reverse use dependent block of IKr in AT-1 cells exhibiting block at low [K]o but relieved as [K]o increased, similar to our hypothesis that increased cytosolic Ca through the channel relieves ICa,L block by DCT [106].

Closer examination of activation of $I_{Ca,L}$ shows that at relatively low voltages DCT prevents detection of measurable macroscopic $I_{Ca,L}$ (Figure 3.12). Use-dependent inhibition can be generalized as blockade of a voltage-gated ion channel that is in a depolarization-induced open or inactivated state. Conversely, blockade of a channel in a relatively low open probability state suggest a reverse use-dependence. Reverse use-dependence is commonly associated with the rate-dependent action of sotatol [107, 108]. Blockade of $I_{Ca,L,}$ preferentially at low potentials is consistent with a reverse use-dependence inhibitor (RUDI).

DCT and RGK proteins share the common feature of purportedly interfering with $I_{Ca,L}$ and interacting with the $Ca_V1.2$ PCT. Excess CaM interferes with RGK blockade of $I_{Ca,L}$ manifested in alterations of peak current and slowing Ca^{2+}-dependent inactivation [109]. The CaM-RGK findings motivated assessment of CaM-DCT interaction with respect to LTCC function. In common with RGK modulation, CaM also interfered with DCT blockade; however, there was no effect on CDI nor on $I_{Ca,L}$ for that matter. My results highlight the importance of multiple proteins in the native heteromultimeric protein complex that comprises cardiomyocyte LTCC. With this consideration HEK 293

cells serve as a minimal system whereby specific protein expression can be controlled simultaneously; however, missing components from native complexes must be weighed on interpretations of results. The correspondence of DCT blockade of $I_{Ba,L}$, and the incomplete correspondence between HEK 293 and $I_{Ca,L}$ for $Ca_V1.2\Delta1733$ but not $Ca_V\Delta1801$ is not completely surprising nor easily interpreted. Importantly, in all cases DCT effects are competed by excess Ca-CaM. Moreover, as first reported by Fuller et al.[64], we report DCT blockade of $I_{Ba,L}$ for $Ca_V1.2\Delta1801$ expressed in HEK 293 cells (Figure 3.5). Despite quantitative differences, the present results for DCT effects on amplitude and alterations of activation gating are in common with previous reports confirming an auto-inhibitory function of DCT that may be propagated from DCT through the PCT EF-hand to channel gating[110].

The finding that CaM-LTCC PCT tethering is Ca^{2+} dependent [111] raises the idea that apparent DCT block is better conceptualized as a dynamic CaM displacement by DCT. Peptides to the CaM-interacting motif of PCT have auto-agonist [112] function. Conversely, in the absence of CaM, or in the presence of excess CaM_{1234} macroscopic LTCC conductance is decreased[57]. In the present study CaM_{1234} and DCT had similar and non-synergistic effects on LTCC current. I envision that for $I_{Ca,L}$, compared to $I_{Ba,L}$, sufficient Ca^{2+}-entry is achieved to strengthen CaM-PCT interaction and thus prevent DCT from interfering with CaM-PCT function. The exception is low voltage whereby sufficiently low open channel probability limits Ca^{2+}-entry (despite an increased driving force). This effect is subtle in patch-clamp recordings, but I propose to test the CICR which amplifies Ca^{2+} signaling when measurement are made with Ca^{2+} imaging.

The finding that CaM-PCT interaction is Ca^{2+}-dependent provides a logical framework to explain DCT effects. In this scheme, DCT is expected to be a more effective competitor for PCT than CaM at low Ca^{2+}, and LTCC without CaM functional interaction has diminished ability to open. DCT blockade is not complete, and the remaining current has unaltered kinetics (Figure 3.4), consistent with the idea that the open channels have active CaM-PCT complexes.

The emerging concept that DCT is a RUDI has potential physiological significance but first must be confirmed in a native cardiomyocyte. My findings in HEK 293 cell propose a new mechanism of regulation of LTCC function. Yet with a simplified over-expression system, other missing native interacting proteins such as RGKs[109], AKAP15, or $Ca_V\beta_2$, could potentially contribute to LTCC functional regulation. The significance of DCT as a RUDI needs to be extended beyond HEK systems and evaluated in cardiomyocyte physiology.

In conclusion, my data expands current understanding of DCT blockade on LTCC function, but only under conditions when either Ca^{2+} levels are low and at relatively low potentials. My new hypothesis is that DCT is an intrinsic reverse use-dependent inhibitor of LTCC function. The second aim of this study is to test the function of DCT in cardiomyocytes. A logical extension of my findings is that DCT controls Ca^{2+}-entry at diastolic potentials while sparing Ca^{2+}-entry for systole in cardiomyocytes.

Table 3.1 Voltage dependence of current activation Boltzmann fit of $V_{1/2}$ and k for $Ca_V1.2\Delta 1733$ and $Ca_V1.2\Delta 1801$.

$Ca_V1.2\Delta1733+\beta2a+$		eGFP	DCT	CaM	DCT+CaM
30 Calcium	(n)	8	8‡	5	10
	$V_{1/2}$, mV	7.0 ± 0.7	9.8 ± 1.7	8.2 ± 3.0	8.7 ± 0.9
	k, mV	10± 1.1	9.7 ± 0.5	10.1 ± 0.4	9.0 ± .2
30 Barium	(n)	10	8	5	13
	$V_{1/2}$	-3.1 ± 1.1	-1.3 ± 1.6	-6.5 ± 1.5	-2.4 ± 1.8
	k	6.7 ± 0.2	7.7 ± 0.3	7.4 ± 0.6	6.8 ± 0.4

$Ca_V1.2\Delta1801+\beta2a+$		eGFP	DCT	CaM	DCT+CaM
30 Calcium	(n)	4	10	7	11
	$V_{1/2}$	8.6 ± 0.95	3.4 ± 0.69	11.7 ± .65	11.0 ± 0.6
	k	8.8 ± 0.43	9.8 ± 0.28	9.2 ± 0.31	8.9 ± 0..22
30 Barium	(n)	4	10	7	11
	$V_{1/2}$	2.2 ± 0.43	-1.4 ± 0.44	4.6 ± 0.35	-1.5 ± 0.50
	k	6.7 ± 0.25	6.9 ± 0.25	7.2 ± 0.17	6.8 ± 0.3

A double Boltzmann equation was required to satisfy all points for DCT co-expression in 7/8‡ cells with 30mM Ca^{2+} (similar behavior with Ba^{2+} currents was noted by Hulme et.al. [1].

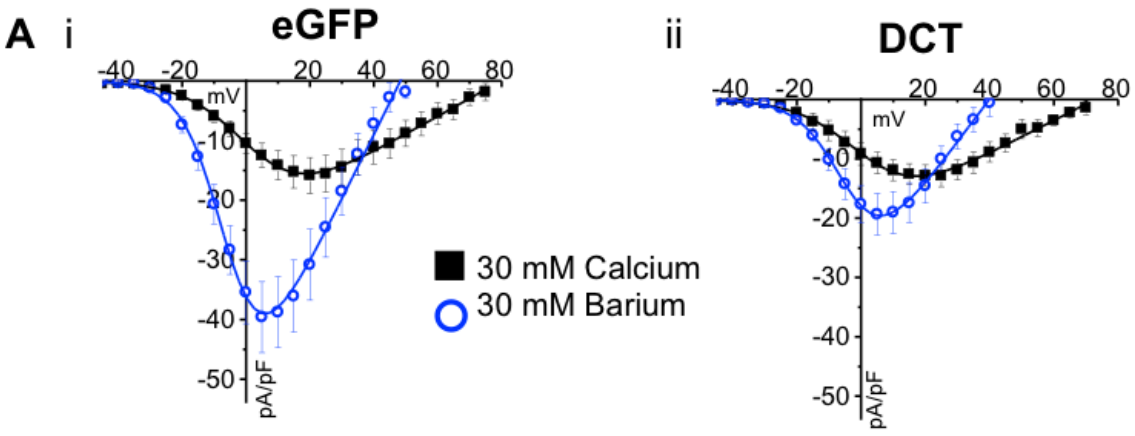

Figure 3.1 DCT decreases $I_{Ba,L}$, but not $I_{Ca,L}$ from $Ca_V1.2\Delta1733$ truncation expressed in HEK 293 cells. A) Current voltage curves for $I_{Ca,L}$ (black squares) and $I_{Ba,L}$ (blue circles) for control (i), DCT over-expression (ii) Note the difference in the relative $I_{Ba,L}$ versus $I_{Ca,L}$ curves for DCT in contrast to all other conditions. (i) Peak $I_{Ca,L}$ density for potential eliciting maximal current (+20mV) shows no significant difference by DCT. (ii) Peak $I_{Ba,L}$ density for potential eliciting maximal current (+5 mV) is significantly reduced by DCT. Unpaired test with Welch's comparison, *p=0.007 & **p=0.006 for DCT versus control and DCT respectively.

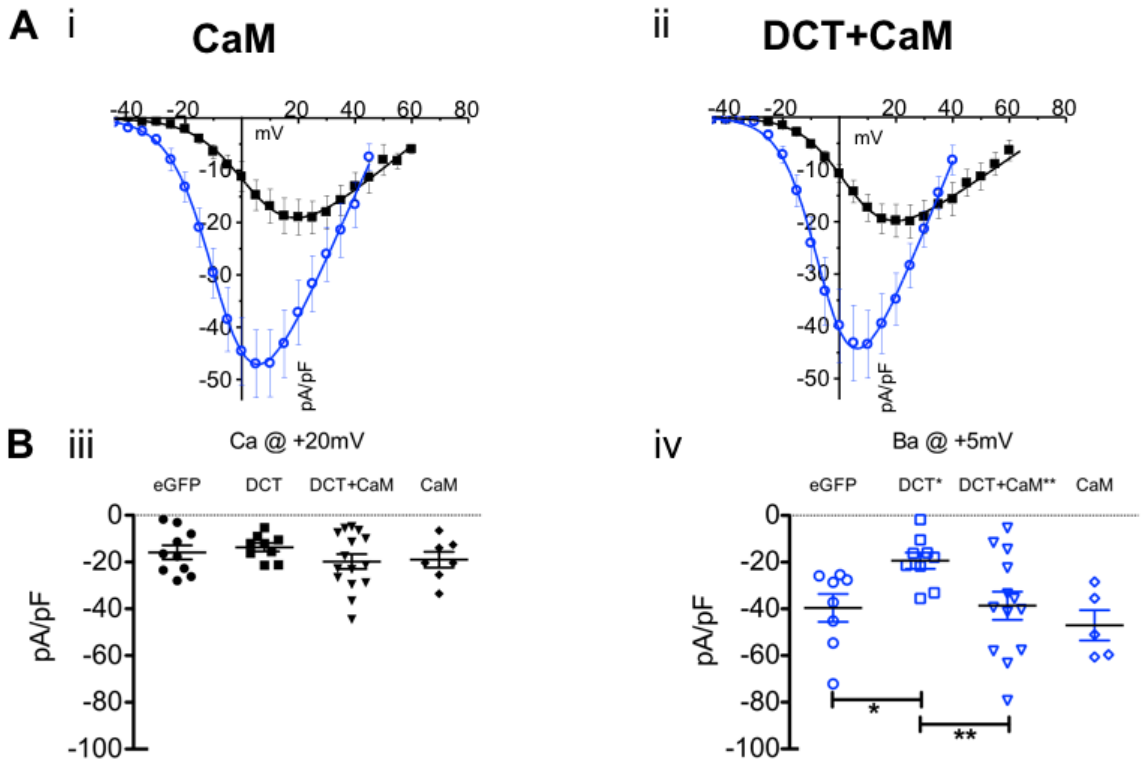

Figure 3.2 CaM relieves DCT decreased $I_{Ba,L}$, but not $I_{Ca,L}$ from $Ca_V1.2\Delta1733$ truncation expressed in HEK 293 cells. CaM over-expression (i), and DCT+ CaM dual over-expression (ii). DCT+CaM completely restores current amplitude. CaM alone has no significant effect. Unpaired test with Welch's comparison, *p=0.007 & **p=0.006 for CaM versus DCT+CaM, respectively.

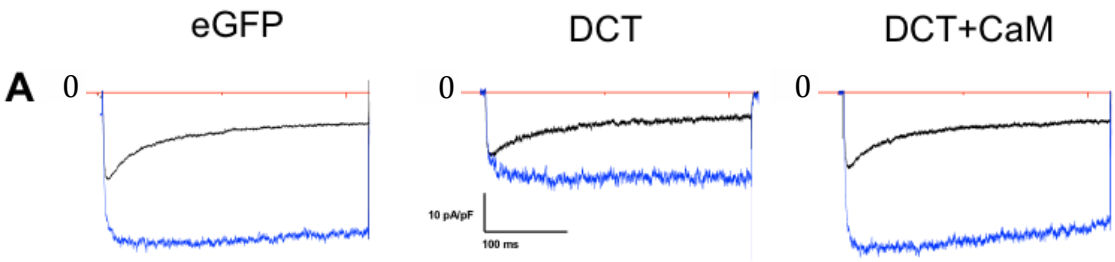

Figure 3.3 Raw current density trace kinetics in HEK 293 cells. A) $Ca_V1.2\Delta1733$ current density traces for V_{hold} -80mV stepped to 0mV for control (left), DCT (center), and DCT+CaM. Ca^{2+} current density represented by black lines and Ba^{2+} current density by blue lines.

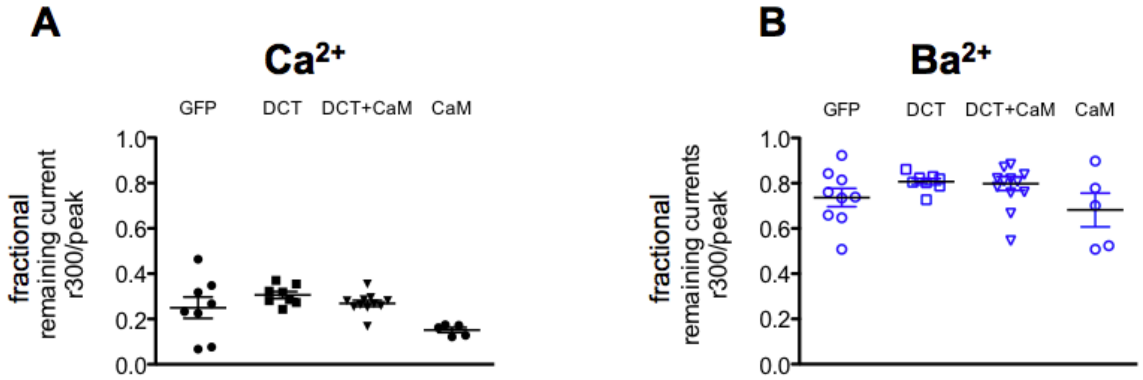

Figure 3.4 Fractional remaining current for $Ca_V1.2\Delta1733$ truncation expressed in HEK 293 cells. Remaining fractional current 300ms after the peak for $I_{Ca,L}$ (A), and $I_{Ba,L}$ (B), respectively. There are no significant differences for $I_{Ba,L}$ VDI or $I_{Ca,L}$ CDI in the heterologous expression systems.

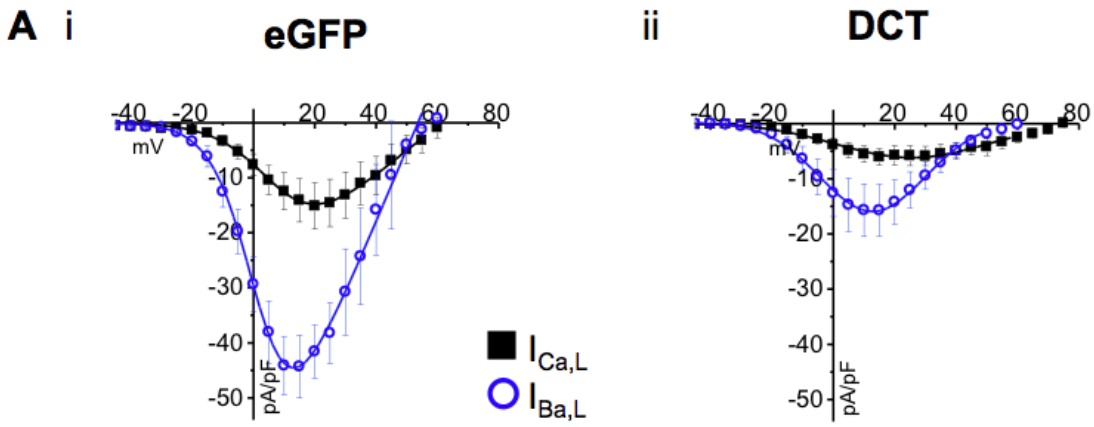

Figure 3.5 DCT decreases $I_{Ba,,L}$ and $I_{Ca,L}$ from $Ca_V1.2\,\Delta\,1801$ truncation of $Ca_V1.2$ expressed in HEK 293 cells. A) Current voltage relationships for $I_{Ca,L}$ (black squares) and $I_{Ba,,L}$ (blue circles) for control (i), DCT over-expression (ii). Peak $I_{Ca,L}$ density for potential eliciting maximal current (+20mV) shows significant current reduction by DCT ($p<0.05$). (ii) Peak $I_{Ba,,L}$ density for potential eliciting maximal current (+10 mV) is significantly reduced by DCT. Unpaired t-test with Welch's comparison, *p=0.01 & **p=0.007 for DCT versus control respectively.

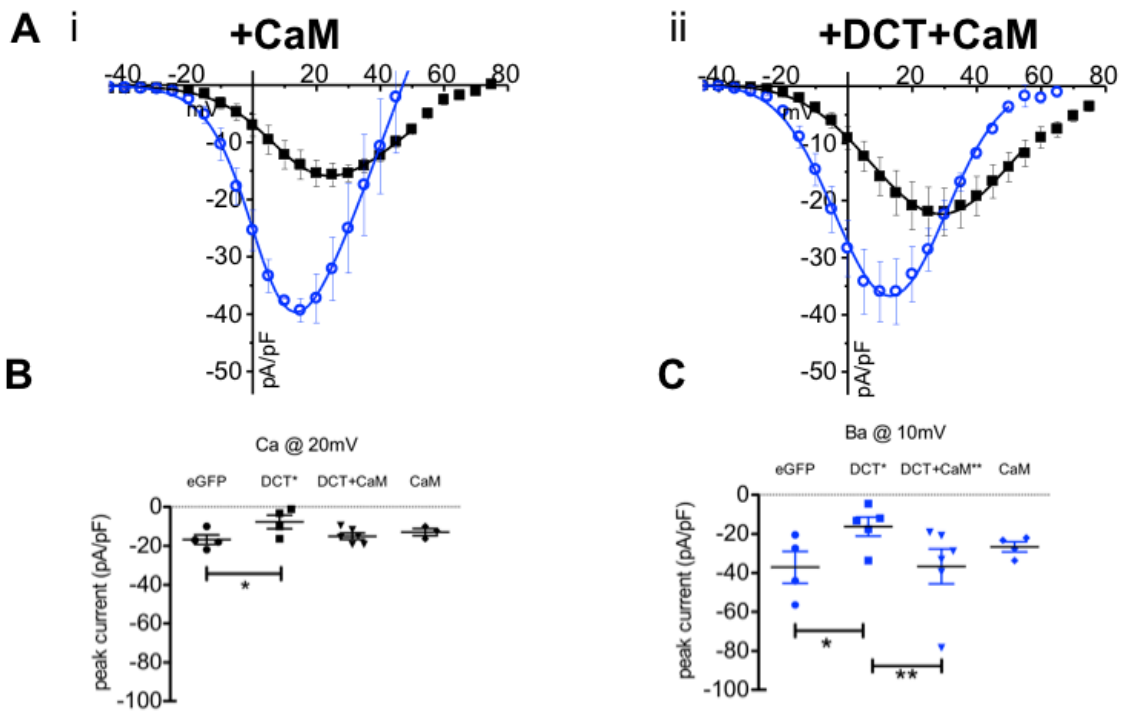

Figure 3.6 CaM relieves DCT decreased $I_{Ba,L}$, and $I_{Ca,L}$ from $Ca_V1.2\,\Delta\,1801$ truncation expressed in HEK 293 cells. A) CaM over-expression (i), and DCT+ CaM dual over-expression (ii). B) Peak $I_{Ca,L}$ density for potential eliciting maximal current (+20mV) shows significant current reduction by DCT ($p<0.05$). C) Peak $I_{Ba,L}$ density for potential eliciting maximal current (+10 mV) is significantly reduced by DCT, and DCT+CaM restores current amplitude. CaM alone has no significant effect. Unpaired t-test with Welch's comparison, *p=0.01 & **p=0.007 for DCT versus control and DCT versus DCT+CaM, respectively

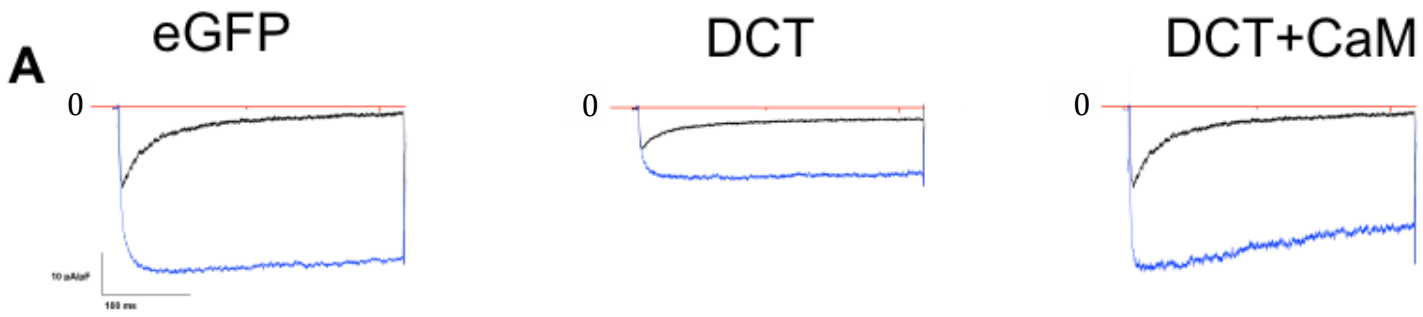

Figure 3.7 Raw current density trace kinetics in HEK 293 cells. A) $Ca_V1.2$ Δ 1801 current density traces for V_{hold} -80mV stepped to 0mV for control (left), DCT (center), and DCT+CaM. $I_{Ca,L}$ density represented by black lines and $I_{Ba,L}$ density by blue lines.

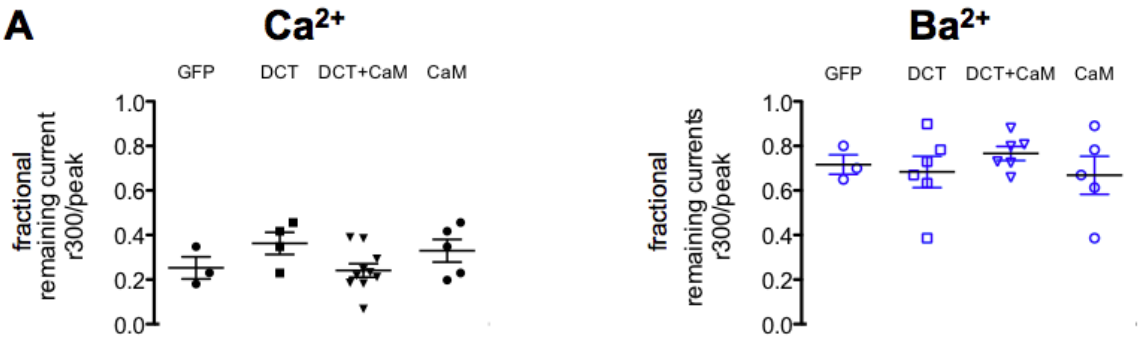

Figure 3.8 Fractional remaining current for $Ca_V1.2\Delta1801$ truncation expressed in HEK 293 cells. Remaining fractional current 300ms after the peak for $I_{Ca,L}$ (A), and $I_{Ba,L}$ (B), respectively. There are no significant differences for $I_{Ba,L}$ VDI or $I_{Ca,L}$ CDI in the heterologous expression systems respectively.

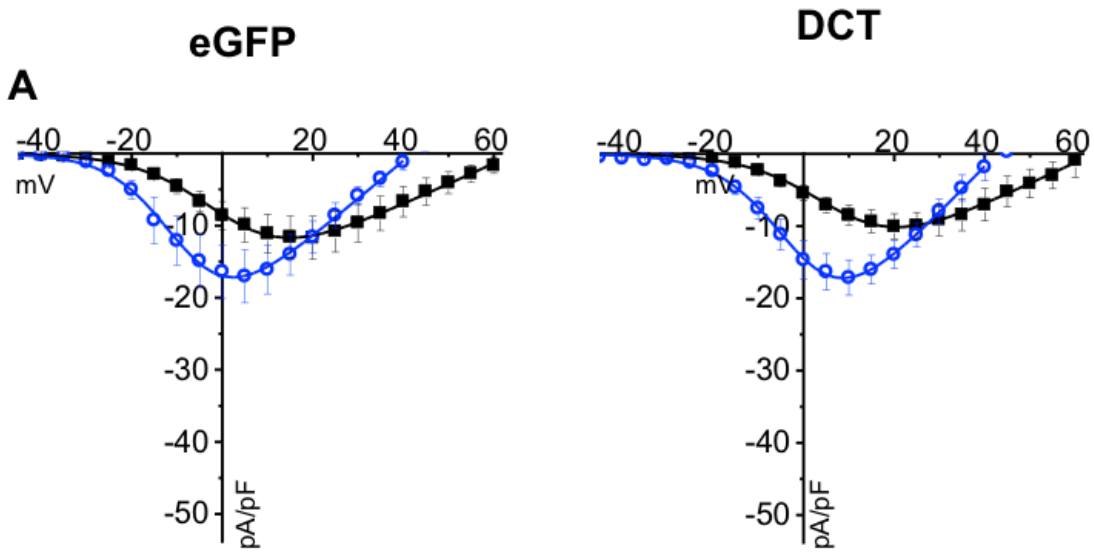

Figure 3.9 CaM_{1234} blocks $I_{Ba,L}$, and DCT block is not additive in HEKs. A) $Ca_V1.2\,\Delta\,1733$ + DCT co-expression with CaM_{1234} decreases $I_{Ba,L}$, but the effect is not additive. Black squares represent the 30mM calcium current density measurement as a change in voltage. Blue circles represent the same cell with bulk flow displacement of 30mM Ca^{2+} with 30mM Ba^{2+}. There is no apparent synergistic effect of DCT+CaM_{1234}.

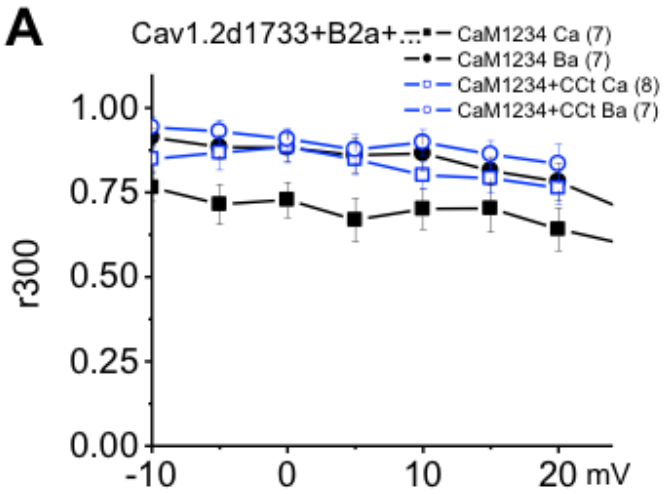

Figure 3.10 Fractional remaining current after 300ms comparing CaM_{1234} in HEKs. A) Remaining current after 300ms comparing CaM_{1234} vs. CaM_{1234}+DCT bulk flow displacement of 30mM Ca^{2+} with 30mM Ba^{2+}. DCT=DCT. Black corresponds to cells without DCT, Blue corresponds to cells co-expressing DCT with CaM_{1234}

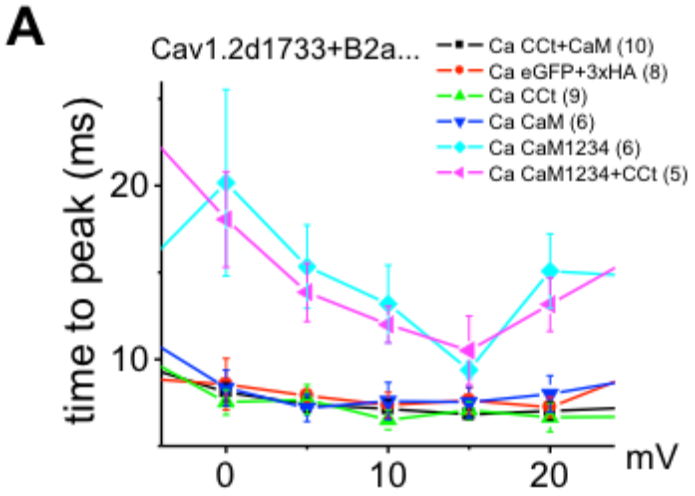

Figure 3.11 Time to peak expressing CaM_{1234} in HEKs. A) Time to peak comparing CaM_{1234} vs. CaM_{1234}+DCT using 30mM Ca^{2+}. No time to peak changes were observed except when CaM_{1234} was co-express, then time to peak increases.

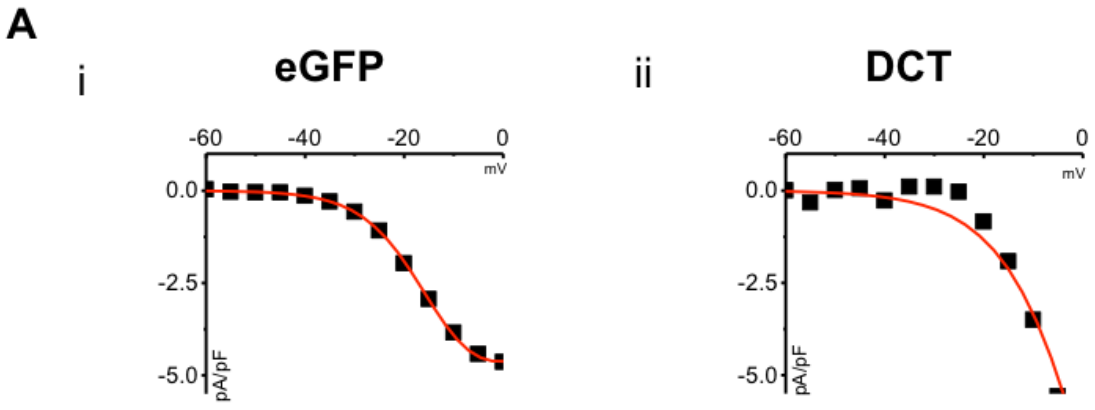

Figure 3.12 DCT co-expression in HEKs requires a double Boltzmann equation for a successful fit in Ca^{2+} measured currents. (i) $I_{Ca,L}$ currents measured in control cells are successfully curve fitted with a single Boltzmann fit. (ii) $I_{Ca,L}$ currents measured in DCT over-expressed cells are failed to curve fit with a single Boltzmann equation in 7/8 cells. Yet could be fitted with a double Boltzmann equation. Note changed aspect ratios to improve comparison to Figure 3.1.

Copyright © Shawn M. Crump 2012

Chapter 4: Regulation of $Ca_V1.2$ function by DCT and CaM in Cardiomyocytes

4.1 Introduction

The $Ca_V1.2$ DCT blocks LTCC Ba^{2+} currents ($I_{Ba,L}$) in reconstituted HEK 293 systems [1, 92]. My current studies in HEK 293 cells suggest that DCT will inhibit LTCC currents. My HEK 293 data matches previous studies using Ba^{2+} as the charge carrier that resulted in larger current with a $Ca_V1.2$ channel truncation [92]. In addition, I show lack of DCT block when using Ca^{2+} as a charge carrier unlike Hulme et al. who only showed that co-expression of DCT with truncated $Ca_V1.2$ reduced $I_{Ba,L}$ [1]. These studies in HEK 293 cells indicate that DCT functionally re-associates with $Ca_V1.2$ near the CB/IQ domain on the proximal carboxyl-terminus (PCT). As stated earlier in chapter 3, the DCT interaction site overlaps the well characterized $Ca_V1.2$-PCT-CaM interaction domains [93]. Therefore it is plausible to suggest that CaM may also modulate DCT-LTCC function in cardiomyocytes. To date, there are no reports of DCT effects on $I_{Ca,L}$, [94] or studies in native cardiomyocytes.

4.2 Results

4.2.1 DCT inhibits $I_{Ba,L}$, but not $I_{Ca,L}$ in ventricular cardiomyocytes.

Heterologous expression studies predict that cardiomyocyte L-type current will be inhibited by DCT [1]. To test this, I isolated ventricular cardiomyocytes and

transfected cells with eGFP-DCT. Ca^{2+} currents ($I_{Ca,L}$) and $I_{Ba,L}$ were measured using 10 mV depolarizing steps from a -50 mV pre-pulse to inactivate I_{Na}. $I_{Ca,L}$ (closed squares) and $I_{Ba,L}$ (open circles) were measured in the same cell (Figure 4.1). As expected, DCT inhibited $I_{Ba,L}$; however, DCT did not significantly reduce $I_{Ca,L}$. Vertical scatter plots of maximal current illustrate the lack of significant difference for $I_{Ca,L}$ between eGFP (control) and eGFP-DCT transfected cells (Figure 4.2 B). By contrast, $I_{Ba,L}$ is significantly reduced by DCT expression (Figure 4.2 C). By extension, I postulated that CaM co-expression with DCT can then functionally compete with DCT block of $I_{Ba,L}$. CaM over-expression alone has no significant effect on cardiomyocyte $I_{Ca,L}$ or $I_{Ba,L}$ (Figure 4.2)-(i); however, CaM exogenous-expression exogenously expressed CaM interferes with the DCT inhibition of $I_{Ba,L}$ (Figure 4.2)-(ii). As expected, $I_{Ca,L}$ was not significantly different following DCT and CaM over-expression (Figure 4.2 B).

4.2.2 DCT has no effect on LTCC current kinetics in cardiomyocytes

Voltage-dependent inactivation (VDI) of $I_{Ba,L}$ is enhanced by DCT in cardiomyocytes (Figure 4.3 and Figure 4.4)–(ii). CaM co-expression had no effect. $I_{Ca,L}$ decay kinetics was not affected by DCT (Figure 4.3 and Figure 4.4)–(ii). The consensus finding from these heterologous expression studies is that $I_{Ba,L}$ is blocked by DCT, and this block can be antagonized by CaM co-expression.. At limiting Po,

DCT blocks better. This raises the notion that elevated Ca^{2+}-entry, perhaps in complex with CaM, abrogates DCT blockade.

4.2.3 Role of Ca^{2+}-CaM in CaM-DCT current restoration in cardiomyocytes.

To distinguish between Ca^{2+} and Ca^{2+}-CaM requirement for diastolic Ca^{2+} transients, I co-expressed CaM_{1234} (Ca^{2+} binding deficient mutant CaM) in cardiomyocytes and measured Ca^{2+} transients. Figure 4.5 shows the results of cardiomyocytes with or without CaM_{1234}. The Ca^{2+} transients in both control (eGFP expressing cells) CaM_{1234} group were identical. CaM_{1234} reduced the Ca^{2+} transient amplitude and did not result in a lower diastolic phase Ca^{2+} transient. In HEK studies CaM_{1234} preferentially blocked $I_{Ba,L}$ compared to $I_{Ca,L}$. Taken together, these results show that CaM_{1234} and DCT individually exert similar action on LTCC current but not Ca^{2+} transients in cardiomyocytes. These results are consistent with a model that limiting channel Po, and limiting Ca^{2+} favors increased DCT blockade.

4.2.4 Role of DCT on Voltage-dependent inactivation

To determine the effect on steady-state inactivation, I voltage-clamped cells to a range of potentials for 2 seconds and measured the available current (Figure 4.6 top panel). Steady-state inactivation curves are described by single Boltzmann distributions. For $I_{Ca,L}$ there are no significant differences between control and DCT-expressing myocytes (Table 4.2). For $I_{Ba,L}$ the midpoint of inactivation is not

different, but the slope factor is significantly steeper in the presence of DCT (Table 4.2). To determine if a reduced duration of the steady-state inactivation affected DCT slope factor, I measured a range of potentials for 250ms (Figure 4.6 bottom panel). The data tracks the 2-second interval measured in the previous figure with no change due to a reduced inactivation interval.

4.2.5 DCT does not change the channel number at the surface

To test if the channel number is changed by DCT over-expression, I measured gating charge movement. There was no significant difference among control, DCT, CaM, or DCT+CaM groups (Figure 4.7). Similarly, gating charge normalized to ionic current was unchanged (Figure 4.7 B). These results are consistent with the notion that DCT has no significant effect on surface expression of $Ca_V1.2$

4.2.6 DCT-RNAi reduces LTCC current in cardiomyocytes

To test if current increases with reduced endogenous DCT in cardiomyocytes I co-expressed DCT-RNAi. $I_{Ba,L}$ was drastically reduced comparing control versus DCT-RNAi. However, the possibility that DCT-RNAi may also knock down the full-length channel must be considered. I will test this by examining the full length knockdown RNAi using calcium transient studies since $I_{Ba,L}$ and $I_{Ca,L}$ would be too diminished in whole cell recordings for a valid comparison. I examined voltages from -10 mV, 0 mV, and 10 mV (Figure 4.8). LTCC $I_{Ca,L}$ were too small to make a valid summary analysis (data not shown).

4.2.7 DCT-RNAi reduces LTCC Ca^{2+} transients in cardiomyocytes

To test if reduced endogenous DCT in cardiomyocytes alter Ca^{2+} transients, I transfected cardiomyocytes with DCT-RNAi. When comparing control versus DCT-RNAi, Ca^{2+} transients twitch amplitude are reduced for DCT-RNAi over-expression in cardiomyocytes and for Full length $Ca_V1.2$-RNAi. **(**Figure 4.9 A) we also tested the diastolic and systolic range by electrically stimulated myocytes from 0.5 Hz to 3 Hz for control, DCT RNAi, & $Ca_V1.2$-RNAi (Figure 4.10). The frequency-Ca^{2+}-transient amplitude relationship is not apparent in DCT RNAi treated cells. The DCT-RNAi and $Ca_V1.2$-RNAi had reduced twitch amplitudes. These results suggest a reduction in the channel number with DCT-RNAi when the results are combined with the electrophysiology data in the previous figure. Careful characterization of mRNA expression in DCT-RNAi and $Ca_V1.2$-RNAi treated cells showed that both treatments indistinguishably coordinately reduced mRNA encoding DCT and $Ca_V1.2$. Hence, I conclude from this experiment that DCT cannot be selectively reduced relative to pore-forming $Ca_V1.2$.

4.2.8 Long-term Ca^{2+} channel block in cardiomyocytes

Since DCT-RNAi results are consistent with overall channel knock down, I chose an alternative complementary approach to quantify the change in the channel number

expression when cells are blocked pharmacologically for 48 hours. If DCT reduces diastolic Ca^{2+}, long term remodeling may occur as part of the signaling cascade from lower diastolic Ca^{2+} and even channel expression feedback loop. A testable hypothesis is that L-type calcium currents contribute to L-type calcium protein expression. I support this hypothesis with following observations from 48-hour in-vivo calcium channel block in adult mice cardiomyocytes, 1.) increased L-type channel protein expression, and 2.) increased phosphatase protein expression[1]. If the DCT plays a role on L-type calcium channel currents as a direct modulator of current and as a result, changes channel transcription factor in cardiomyocytes, this provides a novel study of feedback to L-type calcium channel currents. Decreases in the number of L-type channel representative by multichannel recordings null events after verapamil treated mice were treated with a phosphatase inhibitor okadaic acid (OA) and db-cAMP of adult mouse ventricular myocytes stepped from a -80 mV holding potential to plus 10mV potential (Figure 4.11). Representative history plots of events over time represented as successive sweeps (Figure 4.12 A). Summary bar graph of nPo comparison of vehicle (ascorbic acid, AA) vs. verapamil treated mice treated with phosphatase inhibitor OA applied to myocytes during recording (Figure 4.12 B). The null fraction of Verapamil treated mice decreases with the cAMP stimulation and OA phosphatase inhibition (Figure 4.12C). In Figure 4.12 A) Single channel recordings graphed as history plot of nPo with the addition of db-cAMP after 300 sweeps and the OA after 600 sweeps. Summary bar graphs of nPo averages with standard error bar (Figure 4.12 B.) Summary null fraction averages

with standard error bars (Figure 4.12 C.) The null fraction of Verapamil treated mice decreases with the cAMP stimulation and OA phosphatase inhibition. Positive controls for whole cell patch clamp in ascorbic acid controls did not respond to increase in current with OA, rather currents decreased and then increased with 8Bromo-cAMP. 48 hour Verapamil treated myocytes had no change with OA, and increased similar to controls with 8 Bromo-cAMP. Western blots (not shown) by Dr. Schroder indicate an increase in proposed PP2a activity, which is near the consensus phosphorylation site Ser1928 suggesting LTCC currents are initially suppressed with a high basal dephosphrylation of the channel. In attempts to unmask the increase in channel density due to channel number increase, OA was used to block phosphatase activity. PLB-Ser16 is an index for PKA phosphorylation and was reduced with Verapamil treated mice in phosphor specific western blots performed by Dr. Schroder. I hypothesized that basal cAMP levels were low in Verapamil treated mice and designed a test using PLB Ser16-P as a readout for reversal with 20 min treatment of 8 bromo-cAMP. PLB Ser 16-P was restored to ascorbic acid controls (blots performed by Dr. Schroder). However, when measuring SCR or whole cell patch clamp, I was not able to see a statistically significantly different increase in nPo or LTCC current with OA+8Bromo-cAMP, however the data trend followed an increase.

4.2.9 DCT increases the dynamic range of Ca^{2+} transients by lowering diastolic Ca^{2+}.

My results are consistent with DCT preferential inhibition of LTCC under conditions of relatively low Ca^{2+}. In other words, DCT blocks best when the channel is relatively inactive. I defined this as a reverse use-dependent inhibitor (RUDI). It is very difficult to directly measure LTCC blockade at low open probabilities. However, LTCC pre-amplifies CICR in cardiomyocytes. I postulate that during quiescence, or at low pacing frequencies, diastolic Ca^{2+} might be sufficiently low to create a detectable effect of DCT. To test this I measured cytosolic Ca^{2+} from fura-2 loaded cardiomyocytes. Cardiomyocytes transfected with DCT have significantly less cytosolic Ca^{2+} during quiescence (Figure 4.13). Cells were then field paced at frequencies ranging from 0.5 to 3 Hz (Figure 4.14 and 4.15). In all cases a positive staircase for Ca^{2+} transients was observed. Normalizing the diastolic Ca^{2+} Ratio in paced cells to that during quiescence reveals that DCT significantly increased the dynamic range of responses (Figure 4.16). The diastolic Ca^{2+} ratio difference between 0.5 Hz and 3 Hz is significantly greater in DCT transfected cardiomyocytes (Figure 4.17). I also compared diastolic and systolic ratios converted to nM Ca^{2+} (Figure 4.18). In 1.8 mM bath Ca^{2+} DCT significantly reduces diastolic $[Ca2+]_i$ (Figure 4.18 and Figure 4.19). I superimposed data from Frampton, et al, 1991 for reference (Figure 4.19, light grey filled squares). Taken together, DCT reduction of quiescent Ca^{2+} levels and increased dynamic range of Ca^{2+} transients are consistent with my new hypothesis that DCT acts as a RUDI.

4.3 Discussion

Cardiomyocytes contain DCT separate from the LTCC [24, 59, 69]. In the present body of work, I report novel mechanisms of action of DCT on $I_{Ca,L}$ in cardiomyocytes. The first major finding was that DCT inhibited cardiomyocyte $I_{Ba,L}$, but not $I_{Ca,L}$. HEK 293 cells responded similarly to over-expressed DCT. DCT blockade of $I_{Ba,L}$ and tracked earlier studies by others labs using HEK 293 cells [1, 76]; however, as previously stated, earlier studies did not consider $I_{Ca,L}$. Again, my data showed that DCT blockade was antagonized by Ca^{2+}-CaM as seen in my HEK 293 studies. The second major finding is that my results are consistent with the novel model that DCT blocks channels best at conditions of low Ca^{2+} corresponding to low open probabilities with the Ca^{2+} imaging studies. In essence, the data suggests that DCT is a reverse use-dependent inhibitor (RUDI) of LTCC in cardiomyocytes. The physiological significance of DCT RUDI is revealed by the increase of dynamic range of Ca^{2+}-transients to DCT as a function of stimulation frequency.

The first major finding of the present study, DCT blocks $I_{Ba,L}$ but not $I_{Ca,L}$ leads to the problem: how can $I_{Ba,L}$ selective block be physiologically relevant? Closer examination of activation of $I_{Ca,L}$ in the HEK studies shows that at relatively low voltages DCT prevents detection of measurable macroscopic $I_{Ca,L}$ (Figure 3.12). Use-dependent inhibition can be generalized as blockade of a voltage-gated ion channel that is in a depolarization-induced open or inactivated state. Conversely, reverse use-dependence (RUDI) posits blockade of a channel in a relatively low open

probability state. Blockade of $I_{Ca,L,}$ preferentially at low potentials, and low-frequency dependent attenuation of Ca^{2+}-transients are consistent with RUDI.

My third major finding was excess exogenous CaM interferes with DCT blockade of $I_{Ba,L}$ without alterations of slowing Ca^{2+}-dependent inactivation and peak current in cardiomyocytes [109]. The CaM-DCT findings in HEK 293 system motivated assessment of CaM-DCT interaction with respect to LTCC function in cardiomyocytes. In cardiomyocytes, CaM also interfered with DCT blockade; however, there was no effect on CDI nor on $I_{Ca,L}$ as in HEK 293 data. My results highlight the importance of multiple proteins in the native heteromultimeric protein complex that comprises cardiomyocyte LTCC. DCT effects are competed by excess Ca^{2+}-CaM.

As a logical extension to the long-term Rem block, l tested verapamil, a calcium channel blocker in adult mouse cardiomyocytes. Since we observed an increase in $Ca_V1.2$ protein with Rem over-expression in cardiomyocytes, I predicted that DCT block would have a similar effect as Verapamil calcium channel block for 48hrs. Although LTCC protein increased and whole cells currents increased [24], I was not able to quantify SCR of increased nPo in the Ver treated adult myocytes. DCT-RNAi was used conversely to test if the relief of block would increase LTCC currents. Unfortunately, whole cell LTCC decreased in combination with the decreased Ca^{2+} transient amplitude data. The DCT-RNAi treated cardiomyocytes results in very small currents. Both $I_{Ca,L}$ and $I_{Ba,L}$ currents were reduced. I_{Na}

currents were voltage inactivated but still contaminated the Ca^{2+}/Ba^{2+} currents up to 200 pA. To resolve this, I applied 30uM TTX to the PSS for the Ca^{2+} current recordings. The resulting currents were either zero or no currents at all. The peak currents were negative shifted from 20mV to -10mV with Ca^{2+} and similar with Ba^{2+}. Although, with the other data of intact cells using Ca^{2+} imaging, we note a increase in Diastolic levels with RNAi compared to control, fitting with the RUDI hypothesis and RNA/protein analysis correlate with a diminished DCT in RNAi-DCT treated cells. Our lab measured a decrease in $Ca_V1.2$ RNA, but protein was not quantitated. Second, RNAi-DCT reduces both current and Ca^{2+} twitch amplitude similar to RNAi-$Ca_V1.2$. This may suggest that RNAi-DCT is also knocking down full length $Ca_V1.2$ on the background of reduced $Ca_V1.2$, evaluating the effects of DCT with such a low measurable current makes the data unreliable separating it from contaminating currents and data noise.

The new data with cardiomyocytes support the finding that CaM-LTCC PCT tethering is Ca^{2+} dependent [111] supports the indication that seeming DCT block is hypothesized as a functional CaM displacement by DCT. The cardiomyocyte data suggests that for $I_{Ca,L}$, ample Ca^{2+}-entry is achieved to increase CaM-PCT interaction and DCT may no longer interfere with CaM-PCT function. However, at low voltage where low open channel probability limits Ca^{2+}-entry. This effect was observed in patch-clamp recordings in HEK studies but currents were too small to make the measure in cardiomyocytes. I then chose to utilize the mechanism of CICR, which amplifies Ca^{2+} signaling. Reverse-use dependence manifested as low frequency

dependent DCT attenuation of Ca^{2+} transients illustrates potential physiological relevance DCT modulation of LTCC activity.

The supporting data in cardiomyocytes that CaM-PCT interaction is Ca^{2+}-dependent provides a logical framework to explain DCT effects. As suggested with the HEK 293 data, DCT is likely to be a more effective competitor for PCT than endogenous CaM at low Ca^{2+}, and LTCC without functionally interacting CaM will have lessened ability to open. As with the HEK 293 data, DCT inhibition is not complete, and the remaining current has unaltered kinetics, coherent with the notion that the open channels have active CaM-PCT complexes.

A developing mouse model system was adopted for the contribution of DCT to cardiomyocyte physiology. Specifically, my study addresses the effect of DCT on $I_{Ca,L}$ in a native cell environment. Developing cardiomyocytes have an advantage over adult myocytes in addressing this specific aim. First, developing myocytes have relatively large $I_{Ca,L}$[113]. Second, developing cardiomyocytes can be transfected for exogenous protein expression such as DCT and CaM demonstrated in this paper. Finally, developing cardiomyocytes can be cultured for several days in contrast to adult cardiomyocytes, which adult cardiomyocytes in vitro undergo a de-differentiation process resulting in a reduced I and do not culture well. Although mouse developing myocytes are not a substitute for human adult myocytes, they fit the criteria for asking questions about $I_{Ca,L}$ current regulation by DCT. The

advantages of using a developing cardiomyocyte (CM) as a model system is outlined below.

Developing CMs have a relatively slow heart rate (HR), compared to mature cells. Consequently the diastolic interval is relatively prolonged[114, 115]. Developing CMs have a comparatively long action potential duration (APD)[113, 116]. Developing CMs are a pliable model system. Developing CMs in vitro can be pharmacologically treated, or genetically modified[102]. Secondary to the reduced HR and prolonged APD, excitation-contraction coupling is more reliant on external Ca^{2+} compared to adult rodents [5, 33, 117]. Thus, developing CMs use a mixture of external and SR Ca^{2+} for ECC approximately large mammalian systems. The use of mouse cells in cultures allows proof of principle for future genetically modified animal studies. The use of native developing cells approximates immature phenotype of embryonic stem cell, and induced pluripotent stem cell derived cardiomyocytes[118]. In Summary, a mouse is not a large mammal, nor a human. A developing cardiomyocyte is not an adult cell; however, it must be recognized that in a developing myocytes emphasis on LTCC Ca2+ flux is greater than SR Ca^{2+} flux vs adult myocytes. In rodents, 90% of Ca^{2+} handling is SR, where as adult human and larger mammals it is 50%[116]. Our study seeks to understand the role of DCT on L-type Ca^{2+} currents, thus a model system where predominant Ca^{2+} flux is trough the LTCC is desired as found in the developing CM mouse model[117].

DCT as a RUDI has potential physiological significance. The purpose of this study is to test the function of DCT in cardiomyocytes. As a result of my findings, I propose a new mechanism of regulation of LTCC function. Determining the degree of inherent RUDI that can be attributed to DCT in a cardiomyocyte will require further careful study requiring simultaneous control of stoichiometries of CaM, LTCC and DCT. Also, consideration of other PCT interacting proteins, such as RGKs[109], AKAP15, or $Ca_V\beta_2$, could potentially contribute to LTCC functional regulation. The significance of DCT as a RUDI extends beyond cardiomyocyte physiology. From a therapeutic perspective, over-expression of DCT is posited to have the beneficial impact of decreasing Ca^{2+}-entry during diastole, yet sparing Ca^{2+}-entry during systole. A key future stumbling block for application of DCT as a therapeutic is of course the requirement for cytosolic delivery.

In conclusion, my data identify DCT blockade of LTCC function, but only under conditions when either Ca^{2+} levels are low and at relatively low potentials. I show that DCT increases the stimulation frequency-dependent dynamic range of Ca^{2+} transients in cardiomyocytes leading us to the new hypothesis that DCT is an intrinsic reverse use-dependent inhibitor of LTCC function. A logical extension of my findings is that DCT may provide a novel therapeutic benefit by controlling Ca^{2+}-entry at diastolic potentials while sparing Ca^{2+}-entry for systole.

Table 4.1 Steady state inactivation of cardiomyocyte $I_{Ba,L}$.

Cardiomyocytes		eGFP	DCT
2.5mM Barium	(n)	8	7
	$V_{1/2}$	-31 ± 1.1	-28 ± 1.1
	k	7.3 ± 0.52	6.1 ± 0.25*
	offset	0.035 ± 0.01	0.1 ± 0.021**

p=0.03* for DCT vs eGFP k, p<0.01 for DCT vs eGFP offset.**

Table 4.2 Voltage dependence of current activation Boltzmann fit of $V_{1/2}$ and k for cardiomyocytes.

		DCT	DCT+CaM
1.8-2.5 Calcium			
	$V_{1/2}$	-8.7 ± 3.4	-8.5 ± 0.6
	k	7.5 ± 1.3	6.7 ± 0.3
2.5 Barium			
	$V_{1/2}$	-10.0 ± 1.2	-7.5 ± 0.6
	k	5.9 ± 0.5	5.2 ± 0.4

Figure 4.1 DCT decreases $I_{Ba,L}$, but not $I_{Ca,L}$ in ventricular cardiomyocytes. A) Current voltage curves for $I_{Ca,L}$ (black squares) and $I_{Ba,L}$ (blue circles) for control (i), DCT over-expression (ii). Note the difference in the relative $I_{Ba,L}$ versus $I_{Ca,L}$ curves for DCT in contrast to all other conditions.

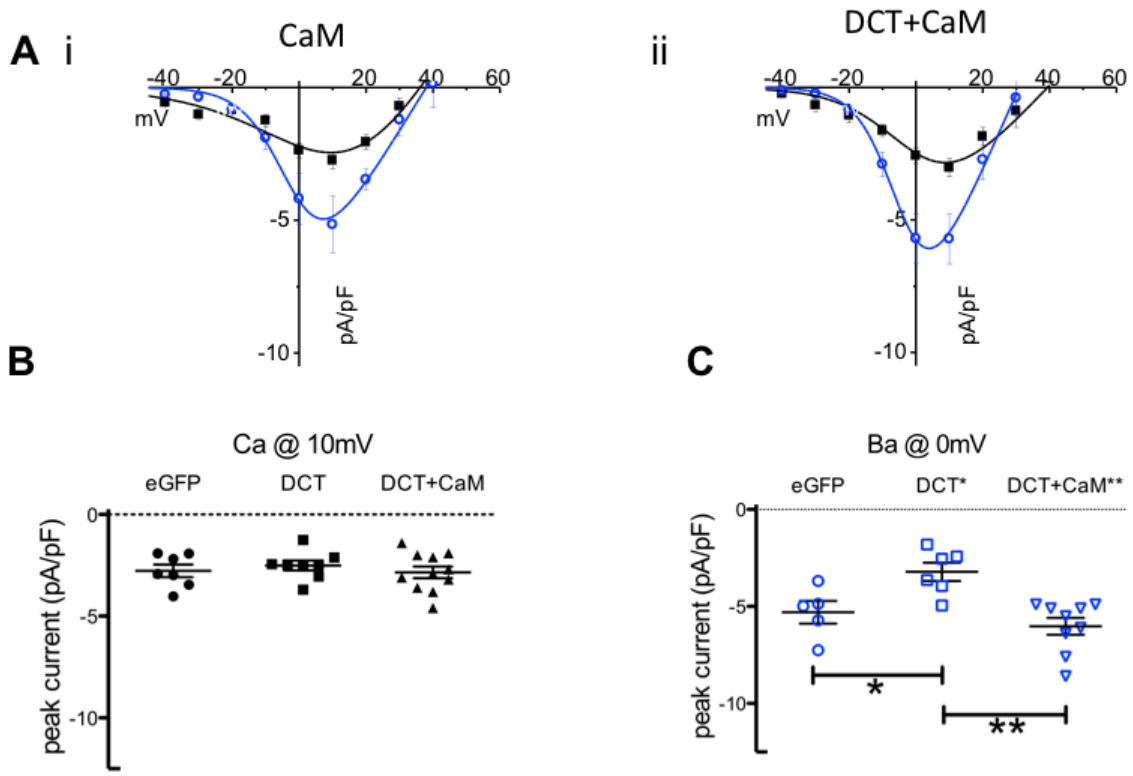

Figure 4.2 DCT decreases $I_{Ba,L}$, but not $I_{Ca,L}$ in ventricular cardiomyocytes. A) Current voltage relationships for $I_{Ca,L}$ (black squares) and $I_{Ba,L}$ (blue circles) for CaM over-expression (i), and DCT+ CaM dual over-expression (ii). B) Peak $I_{Ca,L}$ density for potential eliciting maximal current (+10mV) shows no significant difference by DCT. C) Peak $I_{Ba,L}$ density for potential eliciting maximal current (0 mV) is significantly reduced by DCT, and DCT+CaM restores current amplitude. Unpaired test with Welch's comparison, p=0.01*,**; n = 5, 6, and 9 for control, DCT, and DCT+CaM, respectively.

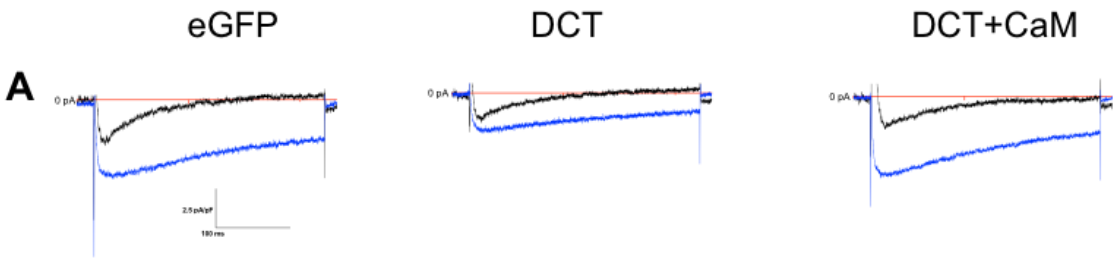

Figure 4.3 DCT enhances voltage-dependent inactivation in cardiomyocytes. Current traces for V_{hold} -50mV stepped to 0mV for control (Left), DCT (center), and DCT+CaM (right) in cardiomyocytes. Black lines for $I_{Ca,L}$ and Blue for $I_{Ba,L}$.

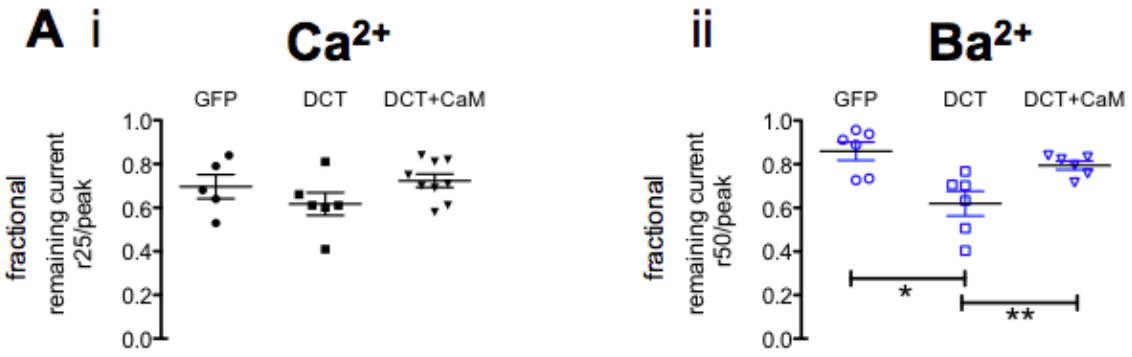

Figure 4.4 DCT enhances voltage-dependent inactivation (VDI) in cardiomyocytes. A) Remaining fractional current 25ms and 50ms after the peak for $I_{Ca,L}$ (i), and $I_{Ba,L}$ (ii), respectively. DCT over-expressing cells showed a significantly greater VDI than control or DCT+CaM. Unpaired test with Welch's comparison, *p=0.04 for control versus DCT, and **p=0.01 for CaM+DCT versus DCT.

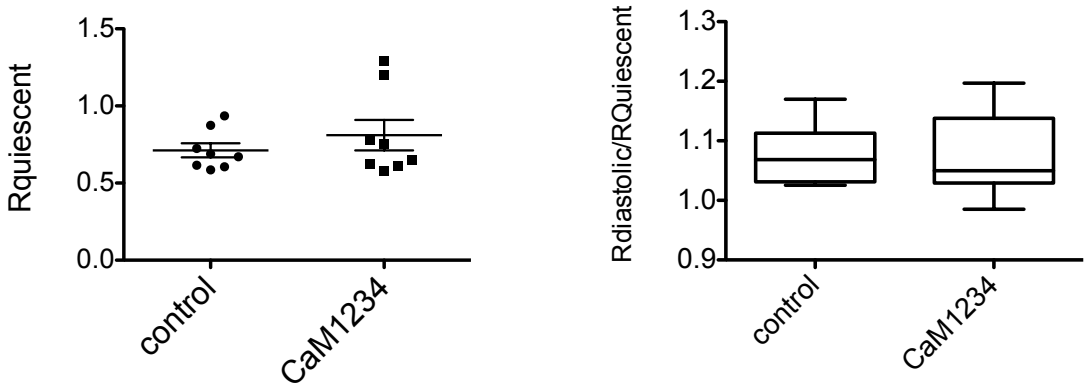

Figure 4.5 Ca^{2+} and Ca^{2+}-CaM requirement for diastolic blockade in co-expressed CaM_{1234} cardiomyocytes. With and without CaM_{1234} co-expressed in cardiomyocytes and measured Ca^{2+} transients. Left panel shows the results of cardiomyocyte diastolic resting ratio with or without CaM_{1234}. CaM_{1234} did not change diastolic phase Ca^{2+} transients. Rather, the Ca^{2+} transients in both control and CaM_{1234} group were identical. CaM_{1234} reduced the Ca^{2+} transient twitch amplitude and CaM_{1234} did not result in a lower diastolic phase Ca^{2+} transient.

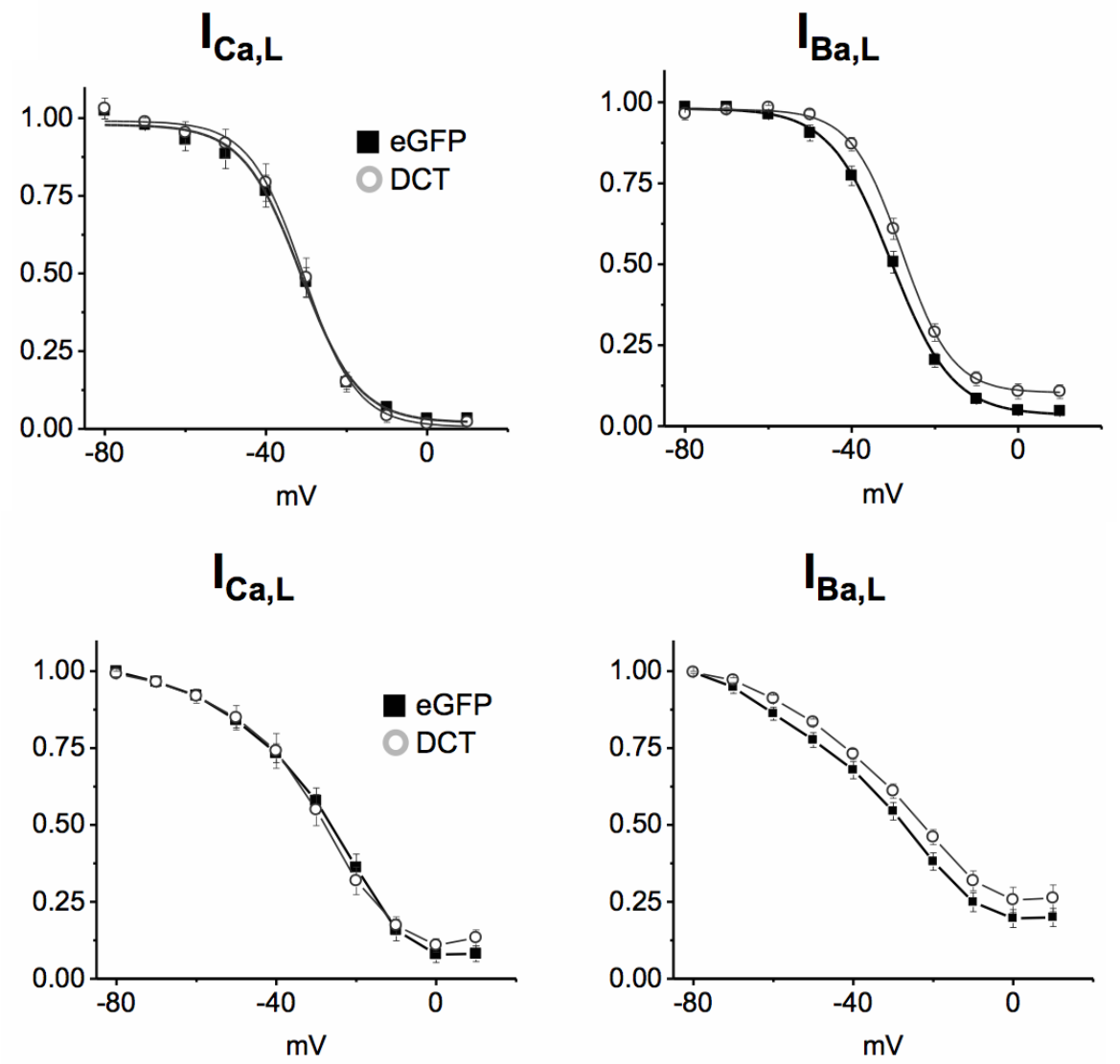

Figure 4.6 Voltage-dependent inactivation of cardiomyocytes plus $Ca_V1.2$ distal carboxyl terminus 1821–2171. A 20 ms pre pulse to 0 mV was followed sequentially by a series of 2 second (top panel) or 250 ms (bottom panel) or conditioning pulses to the indicated potentials and then by a 50 ms post-test pulse to 0 mV. Normalized data points were obtained by dividing the post test-pulse currents by the peak values of the test-pulse currents. Smooth black curves through the data points were generated from a single Boltzmann function as described in Methods. Midpoint of activation was shifted positive for cardiomyocytes + DCT in Ba^{2+}. Steepness of the slope increases with over-expression of DCT compared to control. Boltzmann fit parameters and sample sizes in Table 4.2.

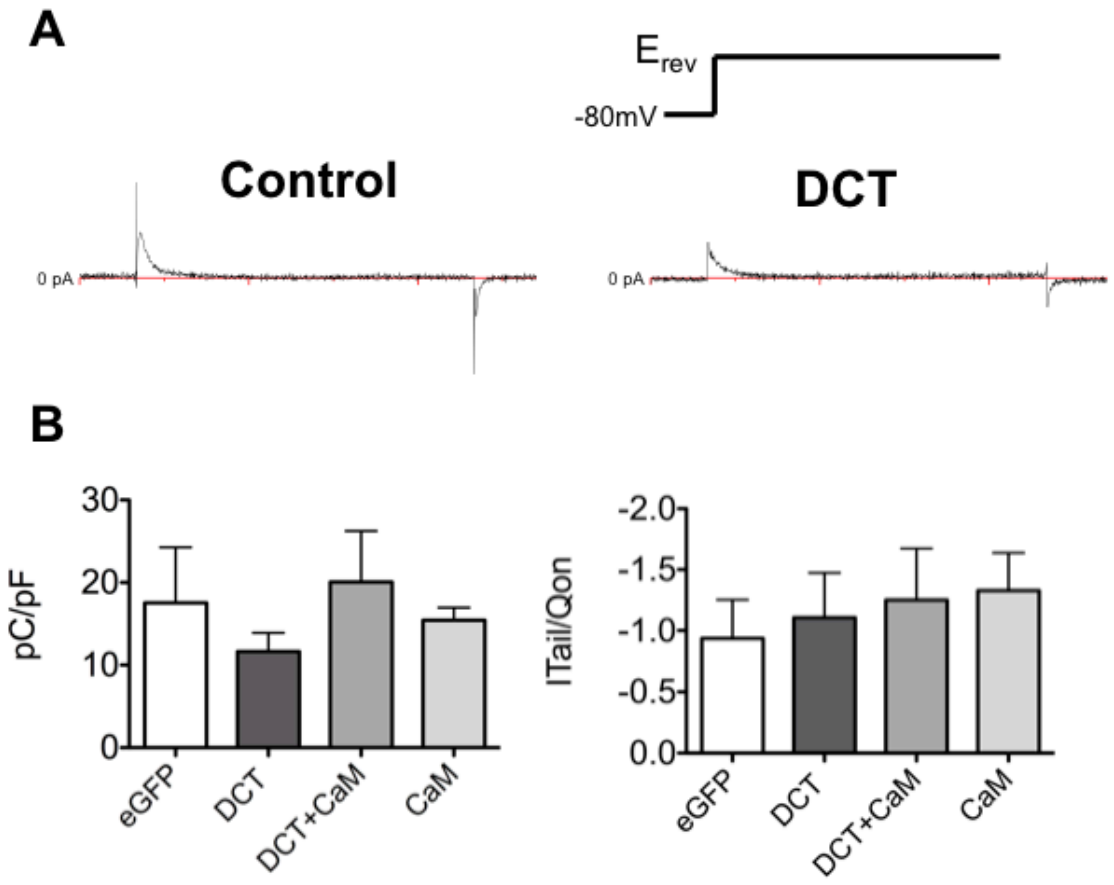

Figure 4.7 Channel number is unaltered by DCT over-expression in cardiomyocytes**.** A.) Upper current traces show representative gating current measured by a voltage step to E_{rev} for control (left) and cardiomyocytes expressing DCT (right). B) Lower panels: (left), gating charge density is not significantly different among control, DCT, CaM, and DCT+CaM recordings. B) Lower panels (right), Ratio of gating charge to tail current is not different among control, DCT, CaM, and DCT+CaM recordings. n = 4, 3, 4, and 3 for control, DCT, CaM, and DCT+CaM, respectively.

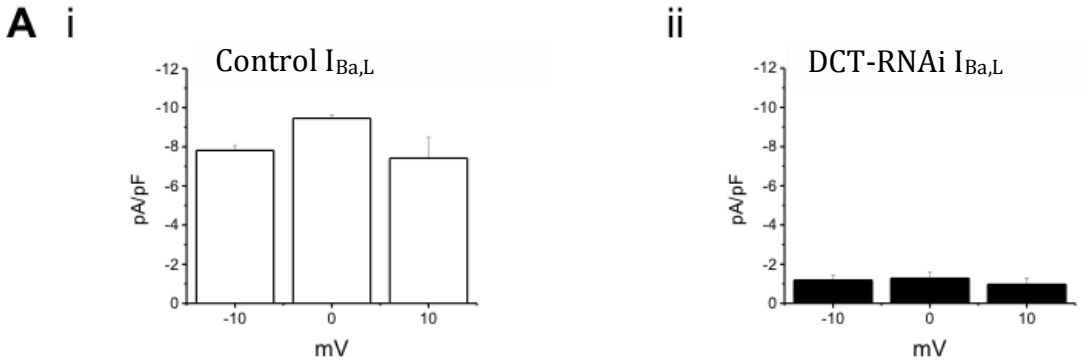

Figure 4.8 DCT-RNAi over-expression in cardiomyocytes**.** Control $I_{Ba,L}$ (i) vs DCT –RNAi (ii) expressed in cardiomyocytes. Our lab measured a decrease in $Ca_V1.2$ RNA, but protein was not quantitated. DCT-RNAi cells had greatly reduced $I_{Ba,L}$ versus control, n=3 and n=2 respectively.

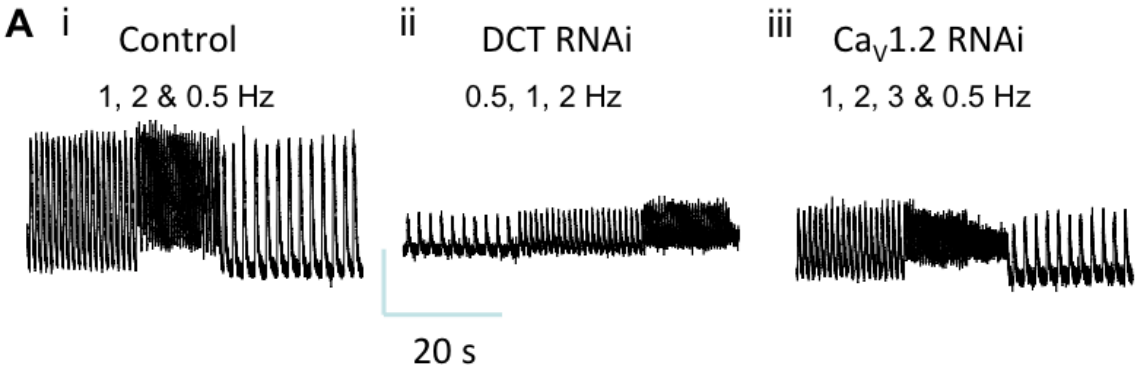

Figure 4.9 Ca^{2+}transients for DCT-RNAi over-expression in cardiomyocytes. A) Electrically stimulated myocytes from 0.5 to 3Hz for control, DCT RNAi, & $Ca_V1.2$ RNAi. Negative frequency-amplitude relationship is not apparent in DCT RNAi treated cells. Scale bars, 0.25 Ratio & 20s.

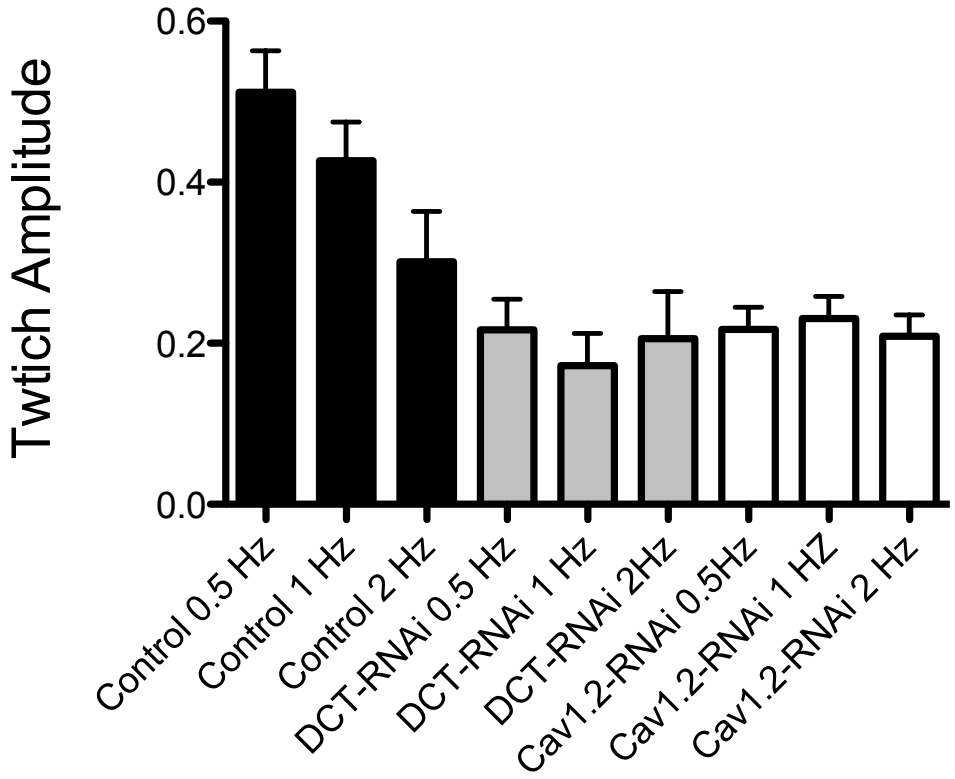

Figure 4.10 Ca^{2+} transients for DCT-RNAi over-expression in E18 mouse cardiomyocytes. DCT (grey) or $Ca_V1.2$ RNAi (white) reduces twitch amplitude. DCT reduces frequency dependence. All data show cells driven by field stimulation. Pooled data for 0.5 Hz, 1 Hz, and 2 Hz. N=10, 10, 5, 11, 12, 6, 9, 9, and 8 respectively on the x-axis. Control 0.5 Hz versus DCT-RNAi, p=0.0001. DCT-RNAi 0.5 Hz versus $Ca_V1.2$-RNAi is not significant.

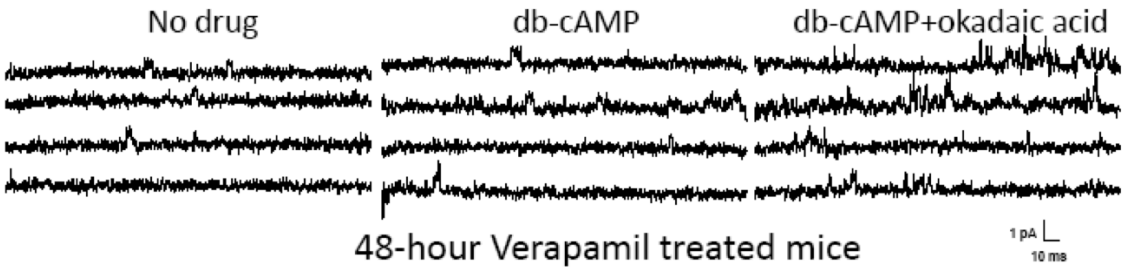

Figure 4.11 L-type Calcium single channel events increase with phosphatase inhibition. Representative single channel recordings from a the same cardiomyocytes before drug (left), then elevating cAMP with 300 microM db-cAMP (middle), and finally adding 1 microM okadaic acid (right) a phosphatase inhibitor, in 48-hour verapamil pre-treated mice. Voltage protocol; 250 ms depolarization from -80mV to +10mV using 100 microM barium as the charge carrier. Inward raw currents plotted as positive inflections. Scale bars; indicate 10ms and 2pA (unitary currents).

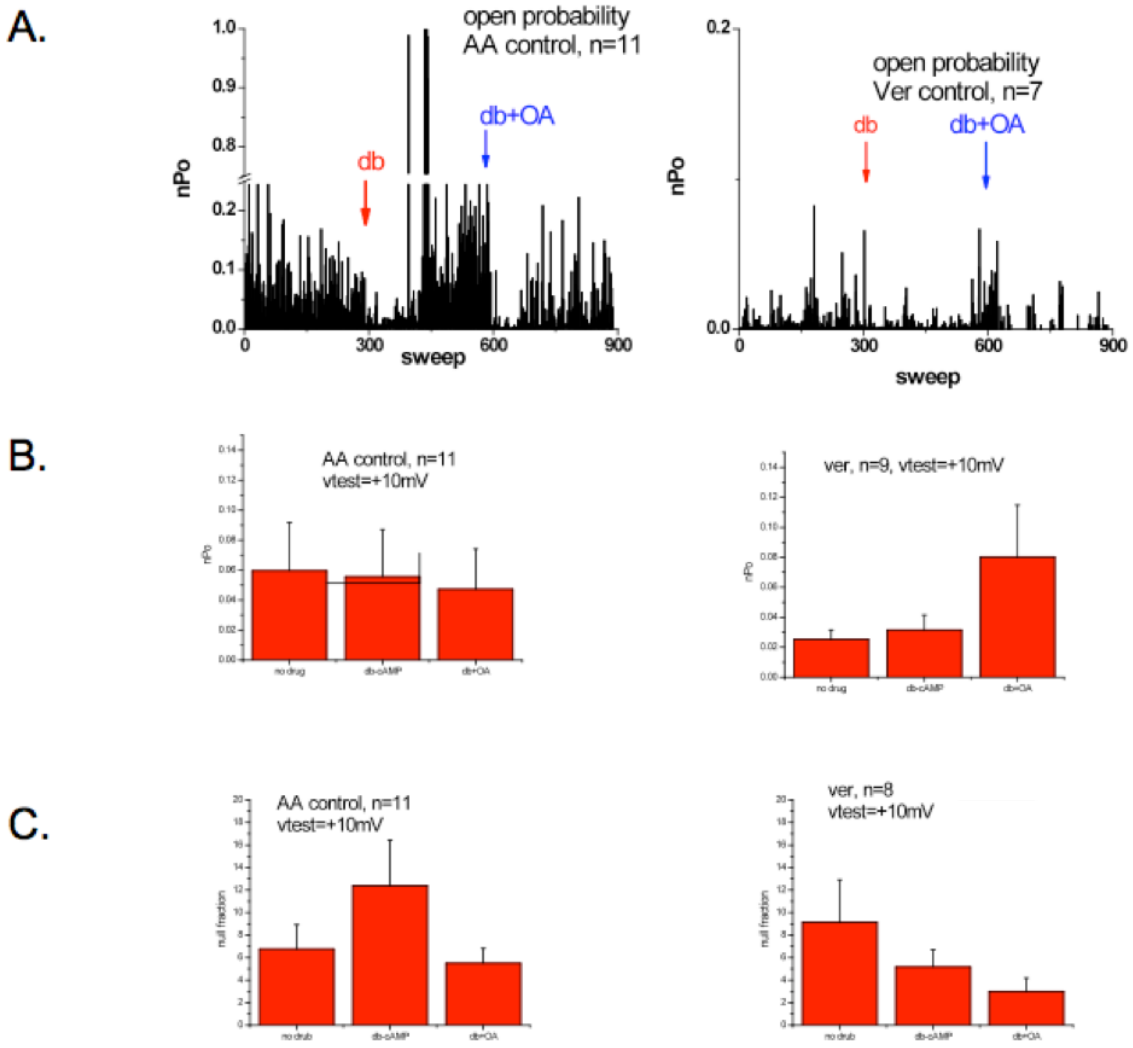

Figure 4.12 The null fraction of 48 hour Verapamil treated mice decreases with the db-cAMP stimulation and Okadaic Acid phosphatase inhibition. A.) Single channel recordings graphed as history plot of nPo with the addition of db-cAMP after 300 sweeps and the OA after 600 sweeps. B.) Summary bar graphs of nPo averages with standard error bars. C.) Summary null fraction averages with standard error bars.

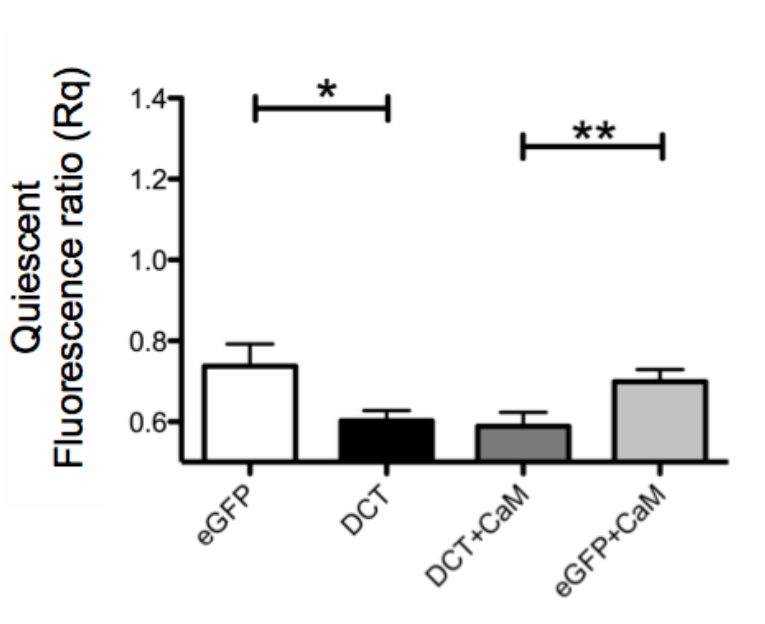

Figure 4.13 DCT reduces quiescent cytosolic Ca^{2+} and increases the dynamic frequency response range. A) Quiescent cytosolic Ca^{2+}-level is reduced by DCT expression (p=0.03; n=9 control, n=14 DCT).

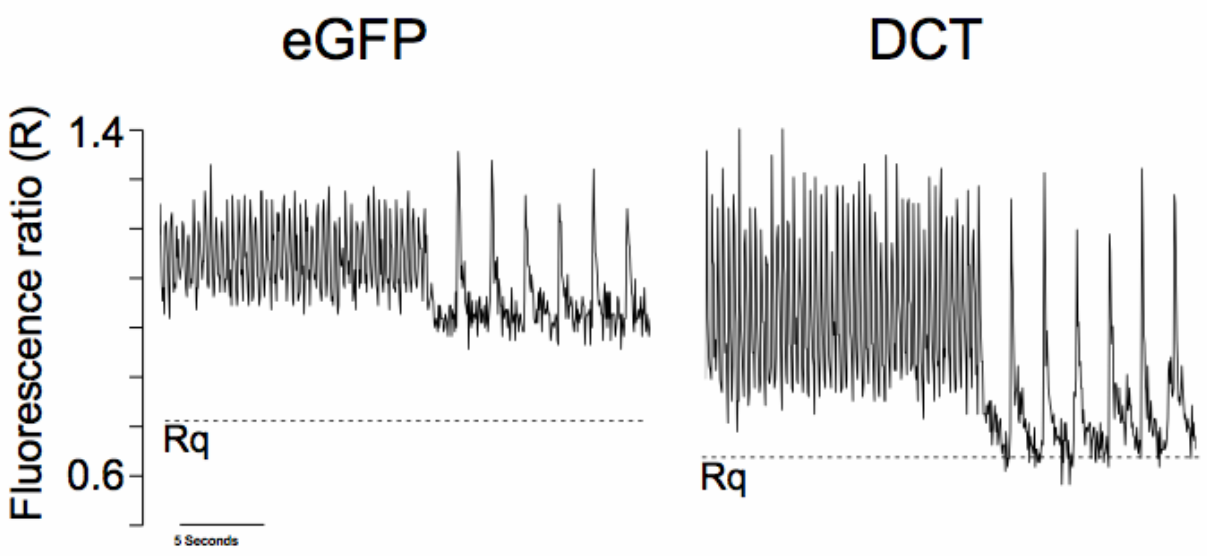

Figure 4.14 Representative Ca^{2+} transients for 3 Hz and 0.5 Hz stimulation. Control (left panel) vs DCT (right panel) in cardiomyocytes. C) Pooled mean diastolic Ca^{2+} level normalized to quiescent value for 0.5, 1, 2, and 3 Hz. Note the increase in dynamic response range for DCT-transfected cardiomyocytes.

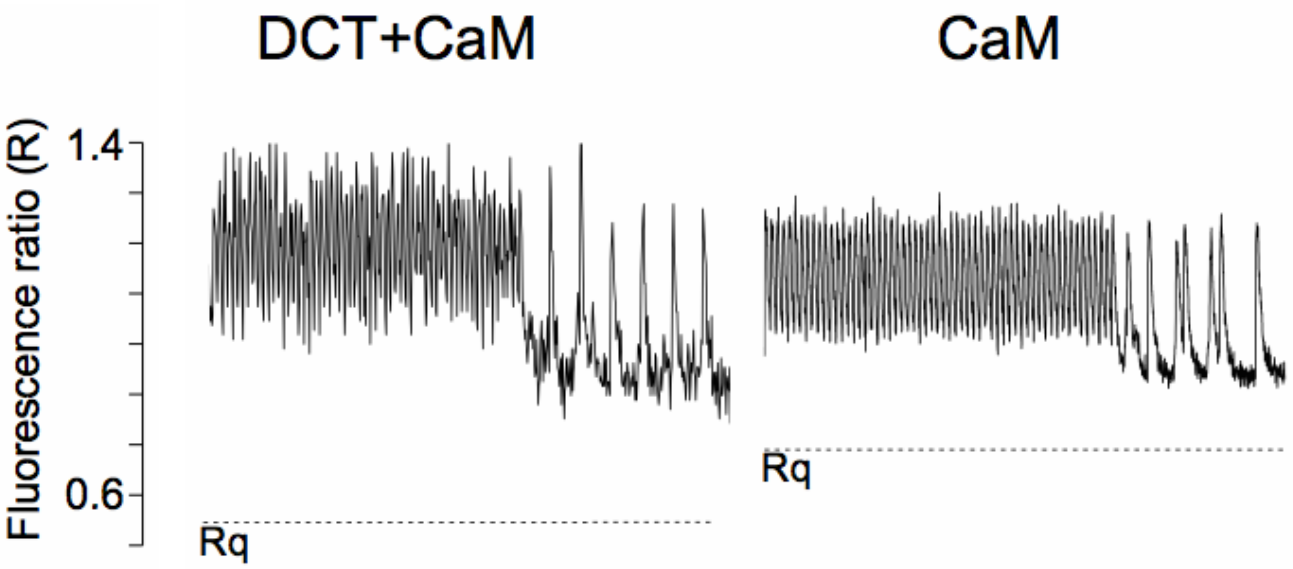

Figure 4.15 Representative Ca^{2+} transients for 3 Hz and 0.5 Hz stimulation for DCT+CaM versus CaM in cardiomyocytes. DCT+CaM also reduces quiescent cytosolic Ca^{2+} and increases the dynamic frequency response range. Quiescent cytosolic fura-2 fluorescent ratio (Rq) is reduced by DCT+CaM expression. The horizontal dashed line is the Rq from Figure 4.13. Pooled mean diastolic fura-2 ratio ($R_{diastolic}$) normalized to Rq for 0.5, 1, 2, and 3 Hz.

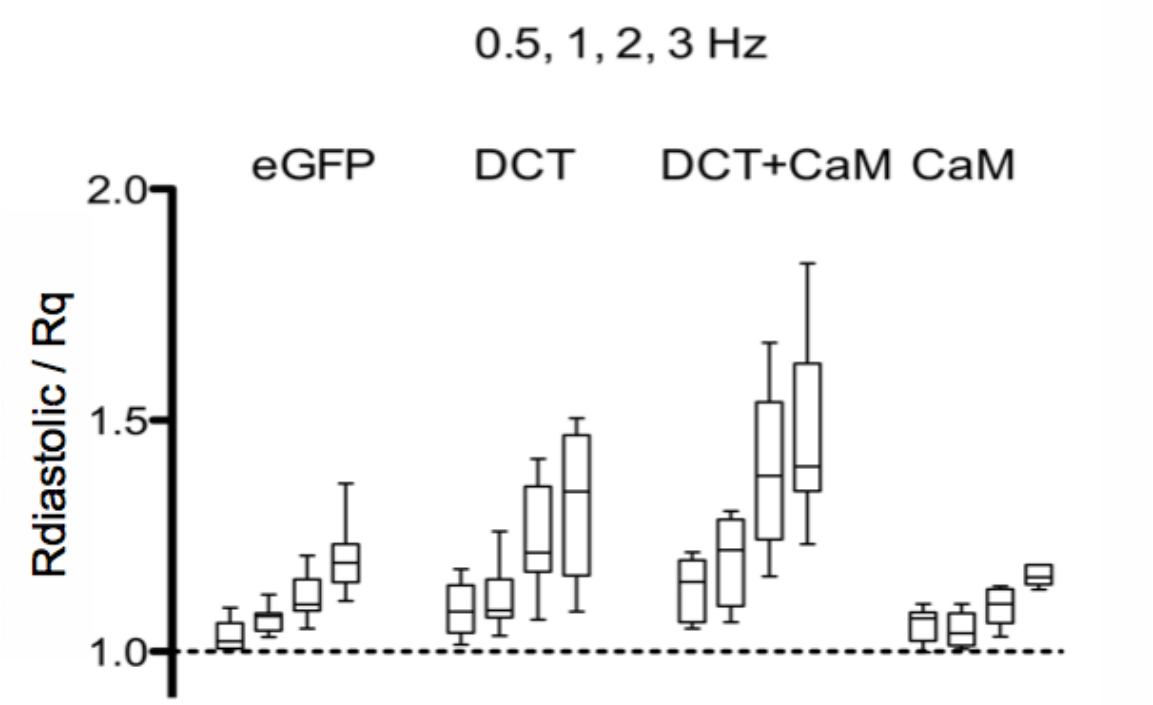

Figure 4.16 Pooled mean diastolic Ca^{2+} level normalized to quiescent value for 0.5, 1, 2, and 3 Hz. Rdiastolic values from Figures 4.14 & 4.15 were divided by Rq values in Figure 4.13. Note the increase in dynamic response range for DCT-transfected cardiomyocytes.

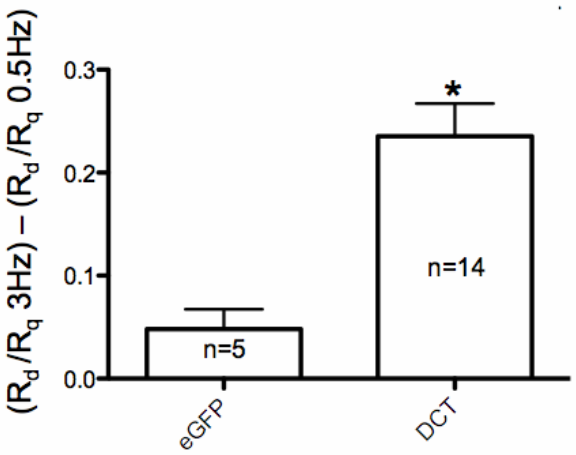

Figure 4.17 Response range manifested as difference between 3 Hz and 0.5 Hz. DCT significantly increased response range *(p=0.0100) compared to eGFP controls.

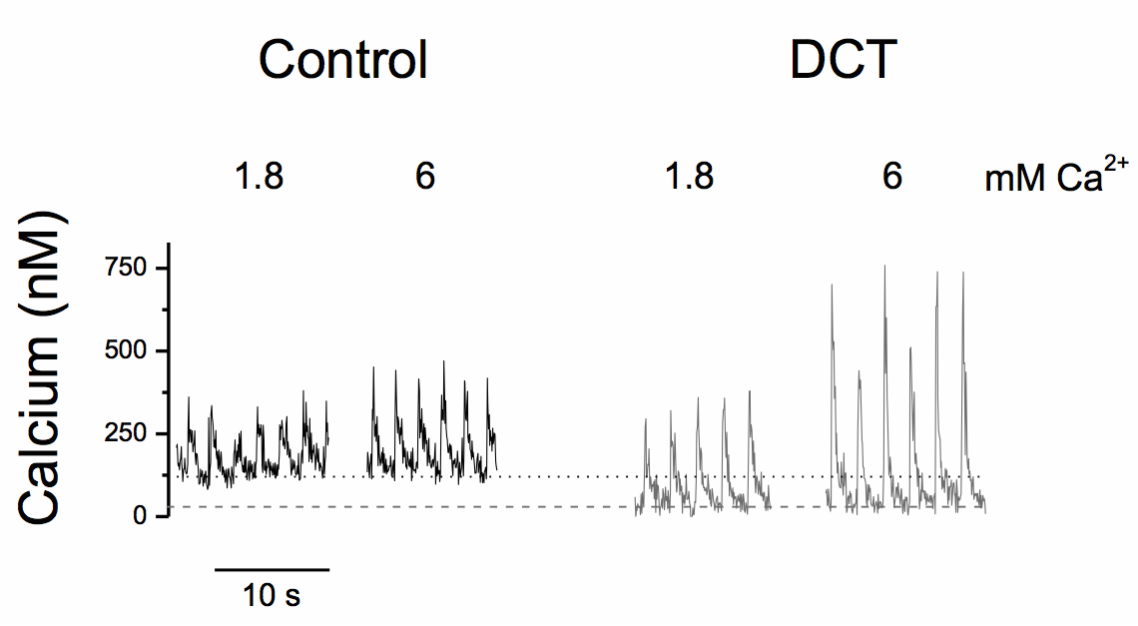

Figure 4.18 DCT decreases diastolic calcium in cardiomyocytes. **A)** Calcium transients induced by 0.5 Hz electrical field stimulation from 1.8mM bath Ca^{2+}, and 6mM Ca^{2+}. Horizontal dashed lines shown for referencing diastolic Ca^{2+} level. Diastolic DCT versus control (n=12 and n=6, respectively).

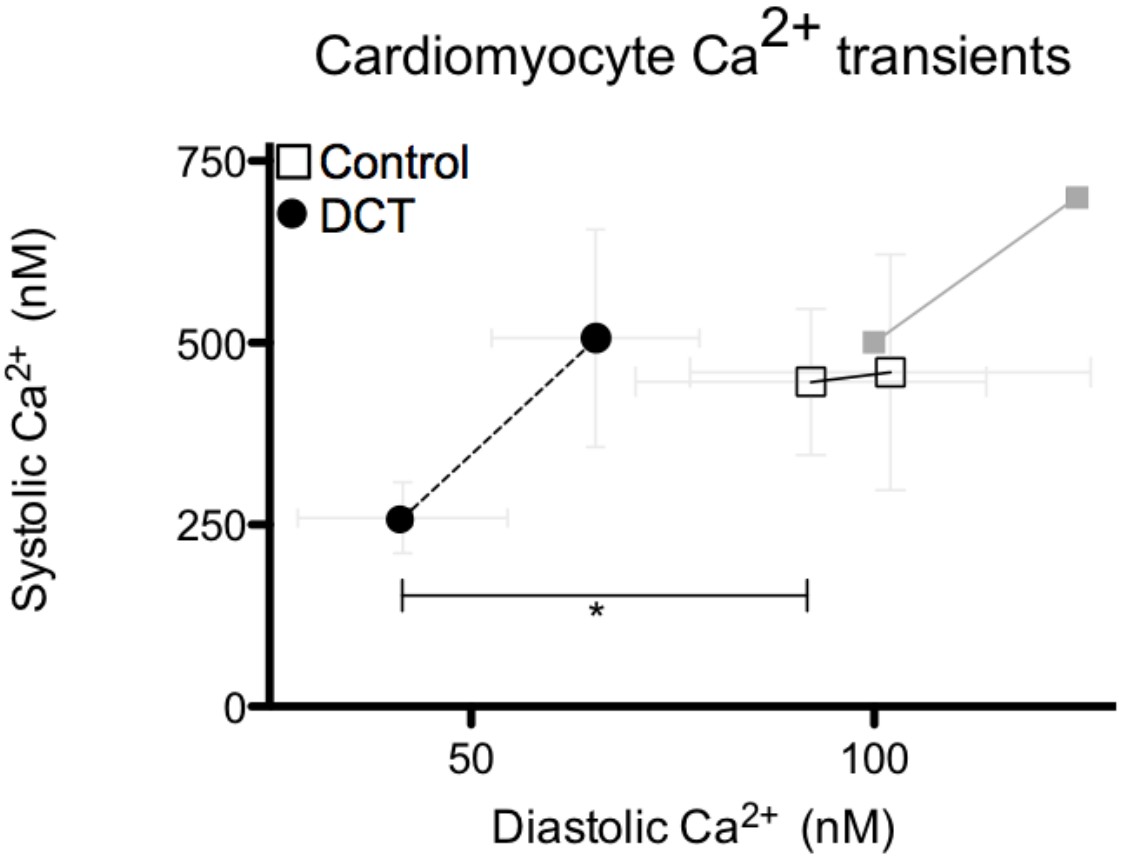

Figure 4.19 DCT decreases diastolic calcium in cardiomyocytes and increases systolic calcium transients. Calcium transients induced by 0.5 Hz electrical field stimulation from 1.8mM bath Ca^{2+}, and 6mM Ca^{2+}. The relationship between diastolic and systolic calcium transients in cardiomyocytes over-expressing DCT (closed circles, dashed line) vs. control (open squares, solid line) at 1.8 and 6mM calcium respectively. The light gray solid squares shows data from Frampton, Orchard, and Boyett (1991) for 2 and 6mM Ca^{2+} for reference. *p=0.04 for diastolic DCT versus control (n=12 and n=6, respectively).

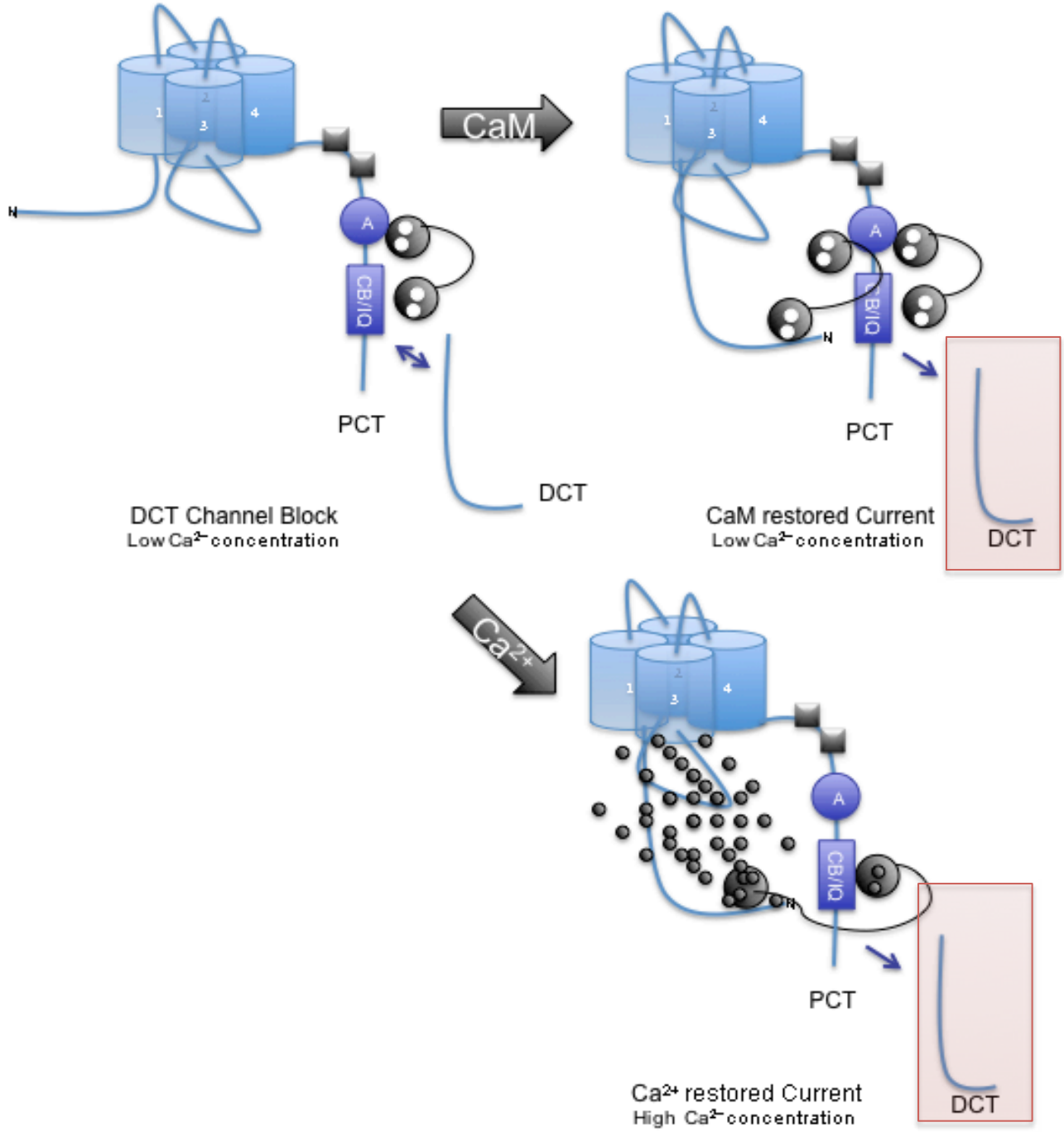

Figure 4.20 Model of DCT inhibition. CaM over-expression completely reverses DCT function inhibition at Low Ca^{2+} (using Ba^{2+} as the charge carrier in whole cell electrophysiology) concentrations (top left to right). Electrically pacing cardiomyocytes elevates cytosolic Ca^{2+} and relieves DCT functional block in diastolic phase of the transients (top left to bottom right).

Copyright © Shawn M. Crump 2012

Chapter 5. Dissertation Summary

The data presented in this dissertation provides supporting evidence of the global hypothesis that low cytosolic calcium enhances DCT auto-inhibition of $Ca_V1.2$ L-type calcium currents in cardiomyocytes. When channel Po is low at low voltages, DCT acts to lower Po further, thus reducing the amount of calcium through the calcium channel.

5.1 Major Findings

5.1.1 DCT blocks Ba^{2+} current, not Ca^{2+} current in HEKs

Chapter 3 describes the first novel finding of this dissertation project. Co-expression of a truncated $Ca_V1.2$ channel with DCT lowers channel Po at low voltages. The result of studies showed that DCT inhibited HEK $I_{Ba,L}$, but not $I_{Ca,L}$. DCT blockade of $I_{Ba,L}$ was consistent with earlier studies in HEK 293 cells [1, 76]; however, I was the first to consider $I_{Ca,L}$. Second, my data showed that DCT blockade was antagonized by Ca^{2+}-CaM. Our labs previous findings demonstrated CaM could interfere with another protein associated with the $Ca_V1.2$-PCT. RGK, a small GTPase, can strongly inhibit $Ca_V1.2$ current and associates with the $Ca_V1.2$-PCT. The RGK studies showed CaM over-expression in HEK cells with $Ca_V1.2$ plus Rem could rescue Rem current block. Since the $Ca_V1.2$-PCT near the CB/IQ is the site of dynamic protein interactions, it was proposed that CaM might also interfere with

Cav1.2-PCT—DCT functional interaction. However, in chapter 4 I did not see reversal of CaM-DCT diastolic ratio in cardiomyocyte Fura-2 experiments. An alternative explanation to the HEK and cardiomyocyte whole cell current data maybe that CaM increases Po by binding CB/IQ domains, and reversing DCT block. Po increases with increased CaM-binding IQ domain mimetic peptide (IQmp) in LTCC [112]. Low $[Ca^{2+}]_i$ is a requirement for the observed increase in LTCC Po [112]. Another proximal-carboxyl terminus CaM-binding domain mimetic peptide (CBmp) added to isolated rabbit ventricular myocytes increased single channel Po on LTCC in a CaMKII and Ca^{2+}/CaM independent manner [112]. My result with CaM reversing $I_{Ba,L}$ fits the criteria of 1.) excess CaM is available to bind IQ or CB domain, and 2.) low cytosolic Ca^{2+} through pipette buffers EGTA and using a Ca^{2+} free bath solution with Ba as the main charge carrier conducting through LTCC.

I postulate that DCT block of LTCC current is a closed state block. I will describe some open and closed state blockers with examples of reverse use dependence. A simple model of channel opening and closing is a channel closed at negative potential and open at positive potentials. I hypothesized that DCT will block a greater number of channels at negative potentials, resulting in more channels remaining closed and DCT operating as a closed channel block. Sotalol works as a reverse use dependence potassium channel drug block, thus resulting in longer action potential duration. Sotalol binds during resting state and action potential duration is prolonged, however as pacing frequency increases, prolongation of the action potential duration decreases[104]. This action is

consistent with reverse use dependence. Open block starts with an increased APD and as the pacing frequency increases, prolongation of the APD decreases, the opposite effect of closed channel block [104]. 4-AP blocks ferret ventricular myocyte Ito only at hyperpolarized potentials and do not need Ito channels to be activated for block, but advances very diminutive block at positive potentials [105]. Dofetilide also acts as a reverse use dependent block of IKr in AT-1 cells exhibiting block at low $[K^+]o$ but relieved as $[K^+]o$ increased, similar to our hypothesis that increased cytosolic Ca^{2+} through the channel relieves $I_{Ca,L}$ block by DCT [106].

5.1.2 DCT blocks Ba^{2+} current, not Ca^{2+} current in cardiomyocytes.

Chapter 4 describes the novel findings of DCT regulation of L-type calcium channel currents in cardiomyocytes. This is the first time DCT has been evaluated on a background of native $Ca_V1.2$. As predicted by my heterologous studies, DCT over-expression blocks $I_{Ba,L}$, but not $I_{Ca,L}$ in whole cell electrophysiology experiments using cardiomyocytes. Since my hypothesis predicts that DCT lowers an already low Po, detection of the DCT inhibition in electrophysiology experiments was below measurable detection. I therefore used intact cardiomyocytes over-expressing DCT in electrically field-stimulated cells using calcium imaging. By controlling the pacing stimulation rate from quiescent cells to 0.5 Hz up to 3 Hz, I was able to increase cytosolic calcium concentrations. The novel finding shows that DCT lowers diastolic calcium at rest and increases the dynamic range for twitch amplitude as frequency

of electrical pacing is increased. A follow-up experiment to directly test the effect of DCT on Po would test cardiomyocytes in the cell-attached configuration. I would measure the single channel openings and predict that DCT co-expression would increase the null fraction versus controls. However, the charge carrier would be limited to Ba^{2+} because single channel currents in Ca^{2+} are indistinguishable from noise. My next major finding was excess exogenous CaM interferes with DCT blockade of $I_{Ba,L}$. However, there was no effect on CDI nor on $I_{Ca,L}$ as in HEK 293 data. My results highlight the importance of multiple proteins in the native heteromultimeric protein complex that comprises cardiomyocyte LTCC. DCT effects are competed by excess Ca^{2+}-CaM.

The combined results from Chapter 3 and Chapter 4 supports a hypothesis that DCT auto-inhibition is relieved when cytosolic calcium increases. I define this as a reverse use dependent inhibitor, or RUDI. The significance of DCT as a RUDI contributes a new approach in understanding cardiomyocyte physiology and reconstituted HEK 293 systems. Based in these studies, over-expression of DCT is postulated to decrease Ca^{2+}-entry during diastole, yet spare Ca^{2+}-entry during systole. Lowering diastolic calcium is a key beneficial therapeutic approach, but current cytosolic delivery systems limit the application of DCT as a therapeutic.

In conclusion, first my data refines the role of DCT blockade of LTCC function, but only under conditions when either Ca^{2+} levels are low and at relatively low potentials. Second, I show that DCT increases the stimulation frequency-dependent

dynamic range of Ca^{2+} transients in cardiomyocytes leading us to the new hypothesis that DCT is an intrinsic reverse use-dependent inhibitor of LTCC function. In summary, DCT may provide a novel therapeutic benefit by controlling Ca^{2+}-entry at diastolic potentials while sparing Ca^{2+}-entry for systole.

5.2 Future Directions

5.2.1 DCT Ser1928 modifies Ca^{2+} transient response to Isoproteranol

To establish if modulation of DCT inhibition is regulated by the consensus phosphorylation site on the DCT, I tested DCT with a phospho-deficient target at Ser1928. This is a logical extension to test if auto-inhibition of LTCC by DCT over-expression in cardiomyocytes could be overcome by increasing the Po of the channel by β-adrenergic expression. Cardiomyocytes were loaded with Fura-2 AM, 2uM for 8 minutes then paced at 1Hz for 1 minute, then exposed to 2uM iso, paced for 2 min (Figure 5.1). Means represent average steady state of more than 40 points, or transients. Serine (S or Ser) to Glutamate (Glu or E) mimics phosphorylated Ser1928 and Ser to Ala mimics phosphor-deficient Ser1928. The twitch amplitude actually increased with the phospho-deficient Ser1928 and resembled DCT twitch amplitudes with Ser1928Glu. One interpretation is that phosphorylated DCT does not reduce the diastolic Ca^{2+} phase of the transient, while the dephosphorylated DCT is associated with the channel and can increase the dynamic range by lowering diastolic Ca^{2+} phase transient levels. This would be consistent with low Ca^{2+} entry

through the LTCC retaining DCT auto-inhibition. Yet once phosphorylated, DCT is not longer associated with the channel and does not lower diastolic Ca^{2+}, but amplitude is increased by more Ca^{2+} coming through the channel and β-AR response with enhanced CDI.

Next I consider the other possibility of β-AR regulation that both my preliminary data from future studies support as well as recent reports by Fu and Ganesan[65] [119]. First I must determine the role of DCT on β-AR response in adult myocytes. I propose to develop a mouse with knock in fluorescent GFP of the Cav1.2-DCT. This will allow delineation between DCT and non-DCT associated Cav1.2 channels. Then I can monitor the activity of each channel in the presence of β-AR stimulation to see if DCT indeed plays a role in the signal transduction of the β-AR stimulation. Ca^{2+} sparks provide the ideal readout for this experiment with a localized Ca^{2+} event tied to a given local channel complex's response. Highly localized spatial and temporal increases in Ca^{2+} during the low activity of Ca^{2+} channels are called sparks[120]. I predict that in the absence of β-AR response, that DCT will lower the Po and in turn reduce the spark number and frequency measured. Second, if I measure a $Ca_V1.2$ without DCT associated, I predict an increase in spark number and frequency. Third, I predict that the phosphorylation by β-AR stimulation in the presence of DCT will be equal or greater than the spark frequency of β-AR stimulated channel in the absence of DCT associated with $Ca_V1.2$ channel. If the last result is negative, I must consider the stoichiometry of DCT and

AKAP15 that plays a role in PKA localization to the channel[64]. Furthermore, I can introduce trypsin or carboxylpeptidase A to enhance currents from a predicted increase in proteolytic processing of $Ca_V1.2$ in vivo [119]. To address the shortcomings of the Fu paper, I must design a test to address if DCT is required for cell surface localization of the $Ca_V1.2$ channel in cardiomyocytes. They considered the possibility that DCT may result in a dysregulation of $Ca_V1.2$ gene expression. I could assess the cardiac function for HR, EF%, FS% as in Houser's paper [121]

Finally, another interesting aspect of the Cav1.2-DCT is the undefined role of Ser1928, a PKA phosphorylation site (ref first description). Ganesan reported a Ser1928A expression in CM that shows ineffective alteration in ISO response [65]. I have taken this one step further in the preliminary results in Ca imaging using a Ser1928E to mimic phosphorylation status of DCT with an opposite than expected result. Interestingly, Youn has proposed that Ser1928 is required for CDI regulation by AKAP15 and CaN [122].

5.2.2 DCT over-expression is required for ISO response in cardiomyocytes.

In order to understand the effects of the previous data using phospho-deficient DCT, I compared cardiomyocytes with and without DCT over-expressed with the addition of isoproterenol. Figure 5.2 shows Raw Ca^{2+} transients using cardiomyocytes paces at 1Hz for 1 min, then expose to 2uM ISO, paced for 2 min, then $0Ca^{2+}$ + Caffeine after 20 seconds. Means represent average steady state of

more than 40 points, or transients. It is notable that twitch amplitudes do not change except when DCT is over-expressed. This DCT diastolic baseline is reduced in cardiomyocytes vs. control with pre-post ISO, which is consistent with my global hypothesis of DCT acting as a RUDI. The complementary direction proposed to continue the evaluation of DCT on β-AR response in cardiomyocytes , 1) evaluate the current amplitudes using electrophysiology DCT over-expression in the presence of ISO, 2) examine the steady-state inactivation of DCT over-expressed cardiomyocytes in the presence of ISO. One limitation to the whole cell electrophysiology is the increase in background currents when stimulating cardiomyocytes using ISO may mask the increase in $I_{Ca,L}$.

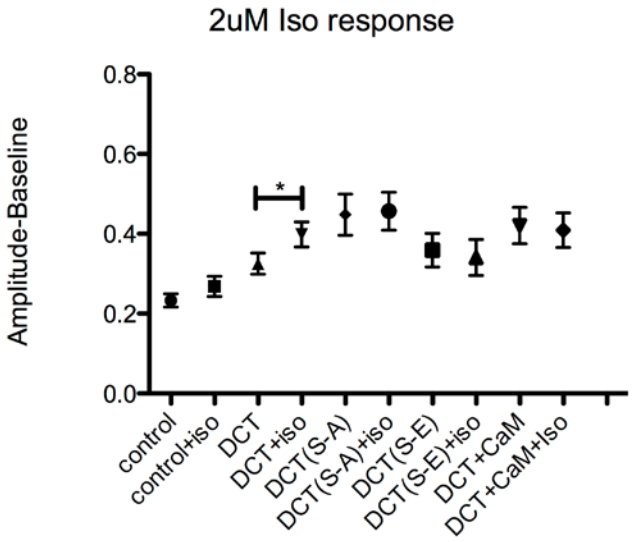

control	control+iso		DCT	DCT+iso		DCT(S-A)	DCT(S-A)+iso		DCT(S-E)	DCT(S-E)+iso		DCT+CaM	DCT+CaM+Iso
13	13		18	18		6	6		8	8		9	9

*	
Paired t test	
P value	0.0056

Figure 5.1 Cardiomyocytes respond to ISO when co-expressed with DCT. No change was observed with the addition of ISO in cardiomyocytes in the absence of DCT or with DCT-S1928A and DCT-S1928E phospho-deficient and phospho-mimetic mutants. Cardiomyocytes were loaded with Fura-2 am, 2uM for 8 min then paces at 1Hz for 1 min, then expose to 2uM ISO, paced for 2 min. Means represent average steady state of more than 40

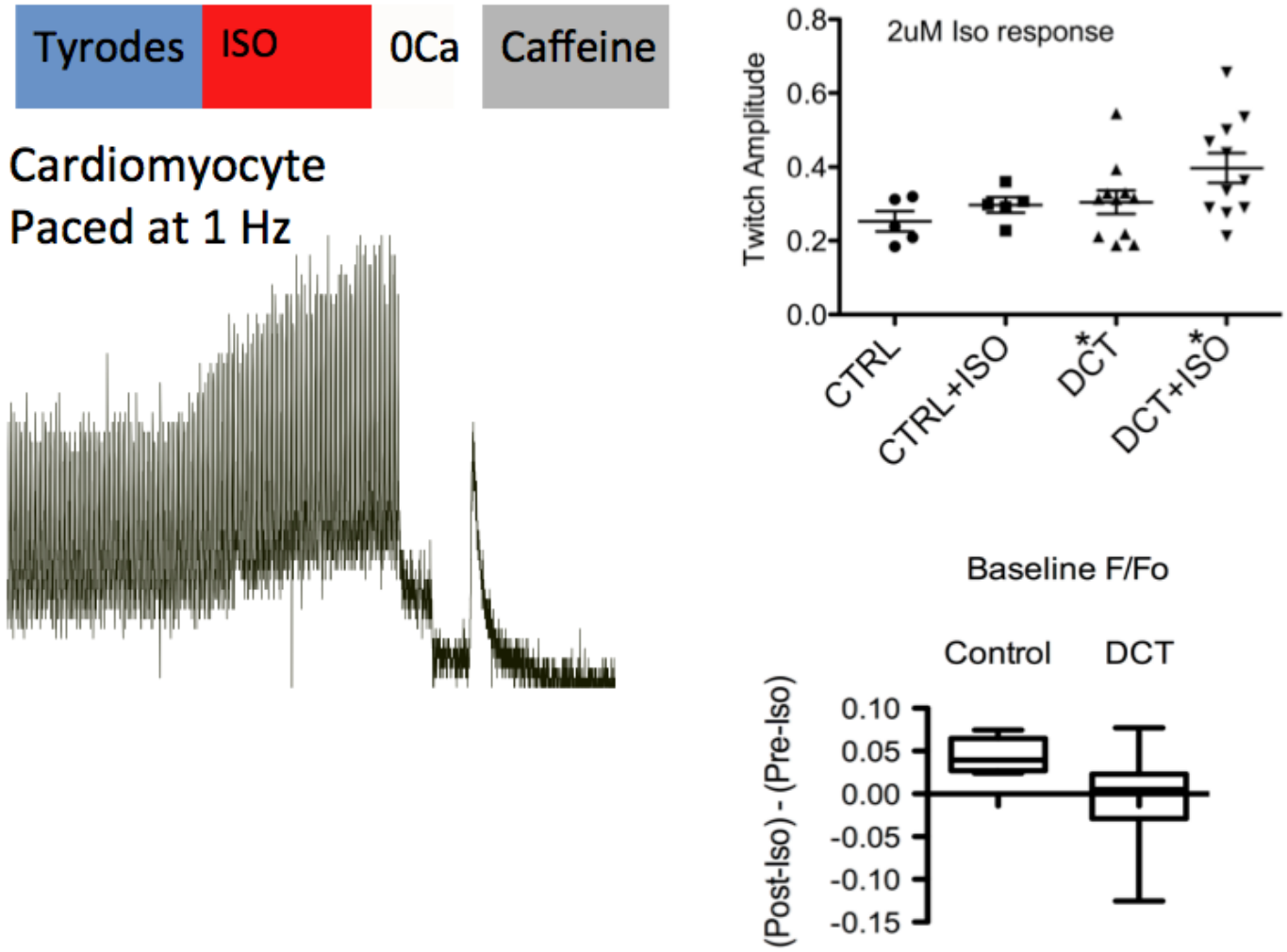

Figure 5.2. Raw Ca^{2+}-transients using Cardiomyocytes paces at 1Hz. Cardiomyocytes were paced for 1 min, then expose to 2uM isoproterenol (ISO), paced for 2 min, followed by 0Ca + Caffeine after 20 seconds. Means represent average steady state of more than 40 points, or transients. Twitch amplitudes do not change except when DCT is over-expressed. DCT diastolic baseline trends lower in cardiomyocytes versus control with pre-post ISO. Students t-test *p=0.022.

Copyright © Shawn M. Crump 2012

Reference:

1. Hulme, J.T., et al., *Autoinhibitory control of the CaV1.2 channel by its proteolytically processed distal C-terminal domain.* J Physiol, 2006. **576**(Pt 1): p. 87-102.
2. Catterall, W.A., et al., *International Union of Pharmacology. XLVIII. Nomenclature and structure-function relationships of voltage-gated calcium channels.* Pharmacol Rev, 2005. **57**(4): p. 411-25.
3. Miller, D.J., *Sydney Ringer; physiological saline, calcium and the contraction of the heart.* The Journal of Physiology, 2004. **555**(3): p. 585-587.
4. Ringer, S., *A further contribution regarding the influence of the different constituents of the blood on the contraction of the heart.* The Journal of Physiology, 1883. **4**(1): p. 29-42.
5. Bers, D.M., *Cardiac excitation-contraction coupling.* Nature, 2002. **415**(6868): p. 198-205.
6. Bers, D.M., *Calcium Cycling and Signaling in Cardiac Myocytes.* Annual Review of Physiology, 2008. **70**(1): p. 23-49.
7. Curtis, B.M. and W.A. Catterall, *Purification of the calcium antagonist receptor of the voltage-sensitive calcium channel from skeletal muscle transverse tubules.* Biochemistry, 1984. **23**(10): p. 2113-2118.
8. Hille, B., *Ion channels of excitable membranes*. 3rd ed2001, Sunderland, Mass.: Sinauer. xviii, 814 p.
9. Catterall, W.A., *STRUCTURE AND REGULATION OF VOLTAGE-GATED Ca2+ CHANNELS.* Annual Review of Cell and Developmental Biology, 2000. **16**(1): p. 521-555.
10. Perez-Reyes, E., et al., *Cloning and expression of a cardiac/brain beta subunit of the L-type calcium channel.* J. Biol. Chem., 1992. **267**(3): p. 1792-1797.
11. Pitt, G.S., W. Dun, and P.A. Boyden, *Remodeled cardiac calcium channels.* Journal of Molecular and Cellular Cardiology, 2006. **41**(3): p. 373-388.
12. Foell, J.D., et al., *Molecular heterogeneity of calcium channel β-subunits in canine and human heart: evidence for differential subcellular localization.* Physiological genomics, 2004. **17**(2): p. 183-200.
13. Bunemann, M., et al., *Functional Regulation of L-type Calcium Channels via Protein Kinase A-mediated Phosphorylation of the beta 2 Subunit.* J. Biol. Chem., 1999. **274**(48): p. 33851-33854.
14. Roden, D.M., et al., *CARDIAC ION CHANNELS.* Annual Review of Physiology, 2002. **64**(1): p. 431-475.
15. Crump, S.M., et al., *The L-type Calcium Channel Alpha-Subunit and Protein Kinase Inhibitors Modulate the Rem - Mediated Regulation of Current.* Am J Physiol Heart Circ Physiol, 2006: p. 00956.2005.

16. Richards, M.W., A.J. Butcher, and A.C. Dolphin, *Ca< sup> 2+</sup> channel β-subunits: structural insights AID our understanding.* Trends in Pharmacological Sciences, 2004. **25**(12): p. 626-632.
17. Walker, D. and M. De Waard, *Subunit interaction sites in voltage-dependent Ca2+ channels: role in channel function.* Trends Neurosci, 1998. **21**(4): p. 148-54.
18. Altier, C., et al., *Trafficking of L-type Calcium Channels Mediated by the Postsynaptic Scaffolding Protein AKAP79.* Journal of Biological Chemistry, 2002. **277**(37): p. 33598-33603.
19. Davies, A., et al., *Functional biology of the α2δ subunits of voltage-gated calcium channels.* Trends in Pharmacological Sciences, 2007. **28**(5): p. 220-228.
20. Gerhardstein, B.L., et al., *Proteolytic Processing of the C Terminus of the alpha 1C Subunit of L-type Calcium Channels and the Role of a Proline-rich Domain in Membrane Tethering of Proteolytic Fragments.* J. Biol. Chem., 2000. **275**(12): p. 8556-8563.
21. Catterall, W.A., *Structure and regulation of voltage-gated Ca2+ channels.* Annu Rev Cell Dev Biol, 2000. **16**: p. 521-55.
22. Birnbaumer, L., et al., *The naming of voltage-gated calcium channels.* Neuron, 1994. **13**(3): p. 505-6.
23. Satin, J. and E.A. Schroder, *Autoregulation of cardiac l-type calcium channels.* Trends Cardiovasc Med, 2009. **19**(8): p. 268-71.
24. Schroder, E., M. Byse, and J. Satin, *L-type calcium channel C terminus autoregulates transcription.* Circ Res, 2009. **104**(12): p. 1373-81.
25. Bers, D.M. and E. Perez-Reyes, *Ca channels in cardiac myocytes: structure and function in Ca influx and intracellular Ca release.* Cardiovascular Research, 1999. **42**(2): p. 339-360.
26. Reuter, H., *The dependence of slow inward current in Purkinje fibres on the extracellular calcium-concentration.* J Physiol, 1967. **192**(2): p. 479-92.
27. Hamill, O.P., et al., *Improved patch-clamp techniques for high-resolution current recording from cells and cell-free membrane patches.* Pflügers Archiv European Journal of Physiology, 1981. **391**(2): p. 85-100.
28. Reuter, H., *The dependence of slow inward current in Purkinje fibres on the extracellular calcium-concentration.* The Journal of Physiology, 1967. **192**(2): p. 479-492.
29. Tsien, R.W., et al., *Mechanisms of Selectivity, Permeation, and Block.* Annual review of biophysics and biophysical chemistry, 1987. **16**(1): p. 265-290.
30. Gao, T., et al., *C-terminal Fragments of the alpha 1C (CaV1.2) Subunit Associate with and Regulate L-type Calcium Channels Containing C-terminal-truncated alpha 1C Subunits.* J. Biol. Chem., 2001. **276**(24): p. 21089-21097.
31. Bers, D.M. and T.A.O. Guo, *Calcium Signaling in Cardiac Ventricular Myocytes.* Annals of the New York Academy of Sciences, 2005. **1047**(1): p. 86-98.

32. Xu, X., S.O. Marx, and H.M. Colecraft, *Molecular Mechanisms, and Selective Pharmacological Rescue, of Rem-Inhibited CaV1.2 Channels in Heart / Novelty and Significance.* Circulation Research, 2010. **107**(5): p. 620-630.
33. Bers, D.M. and V.M. Stiffel, *Ratio of ryanodine to dihydropyridine receptors in cardiac and skeletal muscle and implications for EC coupling.* American Journal of Physiology-Cell Physiology, 1993. **264**(6): p. C1587-C1593.
34. Cannell, M.B., H. Cheng, and W.J. Lederer, *The Control of Calcium Release in Heart Muscle.* Science, 1995. **268**(5213): p. 1045-1049.
35. Lopez-Lopez, J.R., et al., *Local Calcium Transients Triggered by Single L-Type Calcium Channel Currents in Cardiac Cells.* Science, 1995. **268**(5213): p. 1042-1045.
36. Rose, W.C., et al., *Macroscopic and unitary properties of physiological ion flux through L-type Ca2+ channels in guinea-pig heart cells.* The Journal of Physiology, 1992. **456**(1): p. 267-284.
37. Altamirano, J. and D.M. Bers, *Voltage Dependence of Cardiac Excitation–Contraction Coupling.* Circulation Research, 2007. **101**(6): p. 590-597.
38. Fabiato, A., *Calcium-induced release of calcium from the cardiac sarcoplasmic reticulum.* American Journal of Physiology-Cell Physiology, 1983. **245**(1): p. C1-C14.
39. Beuckelmann, D. and W. Wier, *Mechanism of release of calcium from sarcoplasmic reticulum of guinea-pig cardiac cells.* The Journal of Physiology, 1988. **405**(1): p. 233-255.
40. Franzini-Armstrong, C., F. Protasi, and V. Ramesh, *Shape, size, and distribution of Ca2+ release units and couplons in skeletal and cardiac muscles.* Biophysical journal, 1999. **77**(3): p. 1528-1539.
41. Findlay, I., et al., *Physiological modulation of voltage-dependent inactivation in the cardiac muscle L-type calcium channel: A modelling study.* Progress in Biophysics and Molecular Biology, 2008. **96**(1–3): p. 482-498.
42. An MT, Z.G. *Voltage-Dependent Inactivation of Voltage Gated Calcium Channels.* Madame Curie Bioscience Database [Internet]. 2000; Available from: http://www.ncbi.nlm.nih.gov/books/NBK6559/.
43. Splawski, I., et al., *Inaugural Article: Severe arrhythmia disorder caused by cardiac L-type calcium channel mutations.* PNAS, 2005. **102**(23): p. 8089-8096.
44. Findlay, I., *Physiological modulation of inactivation in L-type Ca2+ channels: one switch.* The Journal of Physiology, 2004. **554**(2): p. 275-283.
45. Cens, T., et al., *Voltage- and calcium-dependent inactivation in high voltage-gated Ca2+ channels.* Progress in Biophysics and Molecular Biology, 2006. **90**(1–3): p. 104-117.
46. Shi, C. and N.M. Soldatov, *Molecular determinants of voltage-dependent slow inactivation of the Ca2+ channel.* Journal of Biological Chemistry, 2002. **277**(9): p. 6813-6821.

47. Findeisen, F., et al., *Calmodulin overexpression does not alter Ca_v1.2 function or oligomerization state.* Channels, 2011. **5**(4): p. 320-324.
48. Erickson, M.G., et al., *Preassociation of calmodulin with voltage-gated Ca(2+) channels revealed by FRET in single living cells.* Neuron, 2001. **31**(6): p. 973-85.
49. Erickson, M.G., et al., *FRET two-hybrid mapping reveals function and location of L-type Ca2+ channel CaM preassociation.* Neuron, 2003. **39**(1): p. 97-107.
50. Pitt, G.S., et al., *Molecular basis of calmodulin tethering and Ca2+-dependent inactivation of L-type Ca2+ channels.* J Biol Chem, 2001. **276**(33): p. 30794-802.
51. Alseikhan, B.A., et al., *Engineered calmodulins reveal the unexpected eminence of Ca2+ channel inactivation in controlling heart excitation.* Proc Natl Acad Sci U S A, 2002. **99**(26): p. 17185-90.
52. Ravindran, A., et al., *Calmodulin-dependent gating of Ca(v)1.2 calcium channels in the absence of Ca(v)beta subunits.* Proc Natl Acad Sci U S A, 2008. **105**(23): p. 8154-9.
53. Peterson, B.Z., C.D. DeMaria, and D.T. Yue, *Calmodulin Is the Ca< sup> 2+</sup> Sensor for Ca< sup> 2+</sup>-Dependent Inactivation of L-Type Calcium Channels.* Neuron, 1999. **22**(3): p. 549-558.
54. Peterson, B.Z., et al., *Critical determinants of Ca2+-dependent inactivation within an EF-hand motif of L-type Ca2+ channels.* Biophysical journal, 2000. **78**(4): p. 1906-1920.
55. Halling, D.B., P. Aracena-Parks, and S.L. Hamilton, *Regulation of Voltage-Gated Ca2+ Channels by Calmodulin.* Sci. STKE, 2005. **2005**(315): p. re15-.
56. Mikami, A., et al., *Primary structure and functional expression of the cardiac dihydropyridine-sensitive calcium channel.* 1989.
57. Peterson, B.Z., et al., *Calmodulin is the Ca2+ sensor for Ca2+ -dependent inactivation of L-type calcium channels.* Neuron, 1999. **22**(3): p. 549-58.
58. Peterson, B.Z., et al., *Critical determinants of Ca(2+)-dependent inactivation within an EF-hand motif of L-type Ca(2+) channels.* Biophys J, 2000. **78**(4): p. 1906-20.
59. De Jongh, K.S., et al., *Differential proteolysis of the full-length form of the L-type calcium channel alpha 1 subunit by calpain.* J Neurochem, 1994. **63**(4): p. 1558-64.
60. Pang, C., et al., *Rem GTPase interacts with the proximal CaV1.2 C-terminus and modulates calcium-dependent channel inactivation.* Channels (Austin), 2010. **4**(3): p. 192-202.
61. Wu, Y., et al., *Calmodulin kinase and a calmodulin-binding 'IQ' domain facilitate L-type Ca2+ current in rabbit ventricular myocytes by a common mechanism.* The Journal of Physiology, 2001. **535**(3): p. 679-687.

62. Hudmon, A., et al., *CaMKII tethers to L-type Ca2+ channels, establishing a local and dedicated integrator of Ca2+ signals for facilitation.* J Cell Biol, 2005. **171**(3): p. 537-47.
63. Aita, Y., et al., *Protein kinase D regulates the human cardiac L-type voltage-gated calcium channel through serine 1884.* FEBS letters, 2011.
64. Fuller, M.D., et al., *Molecular Mechanism of Calcium Channel Regulation in the Fight-or-Flight Response.* Sci. Signal., 2010. **3**(141): p. ra70-.
65. Ganesan, A.N., et al., *{beta}-Adrenergic Stimulation of L-type Ca2+ Channels in Cardiac Myocytes Requires the Distal Carboxyl Terminus of {alpha}1C but Not Serine 1928.* Circ Res, 2006. **98**(2): p. e11-18.
66. Hulme, J.T., et al., *Phosphorylation of serine 1928 in the distal C-terminal domain of cardiac CaV1.2 channels during beta1-adrenergic regulation.* Proc Natl Acad Sci U S A, 2006. **103**(44): p. 16574-9.
67. Hulme, J.T., et al., *Beta-adrenergic regulation requires direct anchoring of PKA to cardiac CaV1.2 channels via a leucine zipper interaction with A kinase-anchoring protein 15.* Proc Natl Acad Sci U S A, 2003. **100**(22): p. 13093-8.
68. Yang, L., et al., *Ser1928 Is a Common Site for Cav1.2 Phosphorylation by Protein Kinase C Isoforms.* J. Biol. Chem., 2005. **280**(1): p. 207-214.
69. De Jongh, K.S., D.K. Merrick, and W.A. Catterall, *Subunits of purified calcium channels: a 212-kDa form of alpha 1 and partial amino acid sequence of a phosphorylation site of an independent beta subunit.* Proc Natl Acad Sci U S A, 1989. **86**(21): p. 8585-9.
70. Biel, M., et al., *Primary structure and functional expression of a high voltage activated calcium channel from rabbit lung.* FEBS Lett, 1990. **269**(2): p. 409-12.
71. Mikami, A., et al., *Primary structure and functional expression of the cardiac dihydropyridine-sensitive calcium channel.* Nature, 1989. **340**(6230): p. 230-233.
72. Tang, Z.Z., et al., *Transcript Scanning Reveals Novel and Extensive Splice Variations in Human L-type Voltage-gated Calcium Channel, Cav1.2 Œ±1 Subunit.* Journal of Biological Chemistry, 2004. **279**(43): p. 44335-44343.
73. Liao, P., et al., *Splicing for alternative structures of Cav1.2 Ca2+ channels in cardiac and smooth muscles.* Cardiovascular Research, 2005. **68**(2): p. 197-203.
74. Hulme, J.T., et al., *Sites of proteolytic processing and noncovalent association of the distal C-terminal domain of CaV1.1 channels in skeletal muscle.* Proc Natl Acad Sci U S A, 2005. **102**(14): p. 5274-9.
75. Gomez-Ospina, N., et al., *The C Terminus of the L-Type Voltage-Gated Calcium Channel CaV1.2 Encodes a Transcription Factor.* Cell, 2006. **127**(3): p. 591-606.
76. Wei, X., et al., *Modification of Ca2+ channel activity by deletions at the carboxyl terminus of the cardiac alpha 1 subunit.* J. Biol. Chem., 1994. **269**(3): p. 1635-1640.

77. Gao, T., et al., *Role of the C terminus of the alpha 1C (CaV1.2) Subunit in Membrane Targeting of Cardiac L-type Calcium Channels.* J. Biol. Chem., 2000. **275**(33): p. 25436-25444.
78. Dubuis, E., et al., *Evidence for multiple Src binding sites on the a1c L-type Ca2+ channel and their roles in activity regulation.* Cardiovascular Research, 2006. **69**(2): p. 391-401.
79. Wei, S., et al., *Ca2+ Channel Modulation by Recombinant Auxiliary ß Subunits Expressed in Young Adult Heart Cells.* Circulation Research, 2000. **86**(2): p. 175-184.
80. Seisenberger, C., et al., *Functional embryonic cardiomyocytes after disruption of the L-type α1C (Ca v 1.2) calcium channel gene in the mouse.* Journal of Biological Chemistry, 2000. **275**(50): p. 39193-39199.
81. Xu, M., et al., *Enhanced Expression of L-type Cav1.3 Calcium Channels in Murine Embryonic Hearts from Cav1.2-deficient Mice.* J. Biol. Chem., 2003. **278**(42): p. 40837-40841.
82. Muth, J.N., et al., *Cardiac-specific Overexpression of the alpha 1 Subunit of the L-type Voltage-dependent Ca2+ Channel in Transgenic Mice. LOSS OF ISOPROTERENOL-INDUCED CONTRACTION.* J. Biol. Chem., 1999. **274**(31): p. 21503-21506.
83. Song, L.S., et al., *Ca2+ Signaling in Cardiac Myocytes Overexpressing the a1 Subunit of L-Type Ca2+ Channel*, 2002, Am Heart Assoc. p. 174-181.
84. Moosmang, S., et al., *Analysis of calcium channels by conditional mutagenesis.* Handb Exp Pharmacol, 2007(178): p. 469-90.
85. Fan, I.Q., B. Chen, and J.D. Marsh, *Transcriptional Regulation of L-type Calcium Channel Expression in Cardiac Myocytes.* Journal of Molecular and Cellular Cardiology, 2000. **32**(10): p. 1841-1849.
86. Kobrinsky, E., et al., *Voltage-gated Mobility of the Ca2+ Channel Cytoplasmic Tails and Its Regulatory Role.* J. Biol. Chem., 2003. **278**(7): p. 5021-5028.
87. Splawski, I., et al., *CaV1.2 Calcium Channel Dysfunction Causes a Multisystem Disorder Including Arrhythmia and Autism.* Cell, 2004. **119**(1): p. 19-31.
88. Splawski, I., et al., *CACNA1H Mutations in Autism Spectrum Disorders.* J. Biol. Chem., 2006. **281**(31): p. 22085-22091.
89. Catterall, W.A., *Structure and function of voltage-gated ion channels.* Trends Neurosci, 1993. **16**(12): p. 500-6.
90. De Jongh, K.S., C. Warner, and W.A. Catterall, *Subunits of purified calcium channels. Alpha 2 and delta are encoded by the same gene.* J Biol Chem, 1990. **265**(25): p. 14738-41.
91. Bezanilla, F., *The Voltage Sensor in Voltage-Dependent Ion Channels.* Physiological Reviews, 2000. **80**(2): p. 555-592.
92. Gao, T., et al., *C-terminal fragments of the alpha 1C (CaV1.2) subunit associate with and regulate L-type calcium channels containing C-terminal-truncated alpha 1C subunits.* J Biol Chem, 2001. **276**(24): p. 21089-97.

93. Van Petegem, F., F.C. Chatelain, and D.L. Minor, Jr., *Insights into voltage-gated calcium channel regulation from the structure of the CaV1.2 IQ domain-Ca2+/calmodulin complex.* Nat Struct Mol Biol, 2005. **12**(12): p. 1108-15.
94. Fu, Y., et al., *Deletion of the Distal C Terminus of CaV1.2 Channels Leads to Loss of Œ≤-Adrenergic Regulation and Heart Failure in Vivo.* Journal of Biological Chemistry, 2011. **286**(14): p. 12617-12626.
95. Satin, J., E.A. Schroder, and S.M. Crump, *L-type calcium channel auto-regulation of transcription.* Cell Calcium, 2011. **49**(5): p. 306-13.
96. Balijepalli, R.C., et al., *From the Cover: Localization of cardiac L-type Ca2+ channels to a caveolar macromolecular signaling complex is required for beta2-adrenergic regulation.* PNAS, 2006. **103**(19): p. 7500-7505.
97. Hullin, R., et al., *Increased Expression of the Auxiliary β2-subunit of Ventricular L-type Ca2+ Channels Leads to Single-Channel Activity Characteristic of Heart Failure.* PLoS One, 2007. **2**(3): p. e292.
98. Kim, E.Y., et al., *Multiple C-terminal tail Ca2+/CaMs regulate CaV1.2 function but do not mediate channel dimerization.* EMBO J, 2010. **29**(23): p. 3924-3938.
99. Lester, W.C., et al., *Steady-state coupling of plasma membrane calcium entry to extrusion revealed by novel L-type calcium channel block.* Cell Calcium, 2008. **44**(4): p. 353-362.
100. Mikami, A., et al., *Primary structure and functional expression of the cardiac dihydropyridine-sensitive calcium channel.* Nature, 1989. **340**(6230): p. 230-3.
101. Slish, D.F., et al., *Evidence for the existence of a cardiac specific isoform of the alpha 1 subunit of the voltage dependent calcium channel.* FEBS letters, 1989. **250**(2): p. 509-14.
102. Crump, S.M., et al., *L-type calcium channel alpha-subunit and protein kinase inhibitors modulate Rem-mediated regulation of current.* Am J Physiol Heart Circ Physiol, 2006. **291**(4): p. H1959-71.
103. Frampton, J.E., C.H. Orchard, and M.R. Boyett, *Diastolic, systolic and sarcoplasmic reticulum [Ca2+] during inotropic interventions in isolated rat myocytes.* J Physiol, 1991. **437**: p. 351-75.
104. Hondeghem, L.M. and D.J. Snyders, *Class III antiarrhythmic agents have a lot of potential but a long way to go. Reduced effectiveness and dangers of reverse use dependence.* Circulation, 1990. **81**(2): p. 686-90.
105. Campbell, D.L., et al., *The calcium-independent transient outward potassium current in isolated ferret right ventricular myocytes. II. Closed state reverse use-dependent block by 4-aminopyridine.* The Journal of General Physiology, 1993. **101**(4): p. 603-626.
106. Yang, T. and D.M. Roden, *Extracellular Potassium Modulation of Drug Block of IKr.* Circulation, 1996. **93**(3): p. 407-411.
107. Hohnloser, S.H. and R.L. Woosley, *Sotalol.* The New England journal of medicine, 1994. **331**(1): p. 31-8.

108. Grandi, E., F.S. Pasqualini, and D.M. Bers, *A novel computational model of the human ventricular action potential and Ca transient.* Journal of Molecular and Cellular Cardiology, 2010. **48**(1): p. 112-121.
109. Pang, C., et al., *Rem GTPase interacts with the proximal CaV1.2 C-terminus and modulates calcium-dependent channel inactivation.* Channels, 2010. **4**(3): p. 192-202.
110. Brunet, S., T. Scheuer, and W.A. Catterall, *Cooperative regulation of Ca(v)1.2 channels by intracellular Mg(2+), the proximal C-terminal EF-hand, and the distal C-terminal domain.* The Journal of general physiology, 2009. **134**(2): p. 81-94.
111. Pitt, G.S., et al., *Molecular basis of calmodulin tethering and Ca2+-dependent inactivation of L-type Ca2+ channels.* The Journal of biological chemistry, 2001. **276**(33): p. 30794-802.
112. Dzhura, I., et al., *C terminus L-type Ca2+ channel calmodulin-binding domains are 'auto-agonist' ligands in rabbit ventricular myocytes.* J Physiol, 2003. **550**(Pt 3): p. 731-8.
113. Cohen, N.M. and W.J. Lederer, *Changes in the calcium current of rat heart ventricular myocytes during development.* The Journal of Physiology, 1988. **406**(1): p. 115-146.
114. Fatkin, D., et al., *Neonatal cardiomyopathy in mice homozygous for the Arg403Gln mutation in the α cardiac myosin heavy chain gene.* The Journal of Clinical Investigation, 1999. **103**(1): p. 147-153.
115. Green, E.L., *Biology of the laboratory mouse.* Biology of the laboratory mouse, 1966(2nd ed).
116. Wahler, G.M., et al., *Time course of postnatal changes in rat heart action potential and in transient outward current is different.* American Journal of Physiology-Heart and Circulatory Physiology, 1994. **267**(3): p. H1157-H1166.
117. Wang, L.J. and E.A. Sobie, *Mathematical model of the neonatal mouse ventricular action potential.* American Journal of Physiology-Heart and Circulatory Physiology, 2008. **294**(6): p. H2565-H2575.
118. Schroder, E.A., Y. Wei, and J. Satin, *The developing cardiac myocyte: maturation of excitability and excitation-contraction coupling.* Ann N Y Acad Sci, 2006. **1080**: p. 63-75.
119. Fu, Y., et al., *Deletion of the Distal C Terminus of CaV1. 2 Channels Leads to Loss of β-Adrenergic Regulation and Heart Failure in Vivo.* Journal of Biological Chemistry, 2011. **286**(14): p. 12617.
120. Navedo, M.F., et al., *Increased coupled gating of L-type Ca 2+ channels during hypertension and timothy syndrome.* Circulation Research, 2010. **106**(4): p. 748-756.
121. Chen, X., et al., *Calcium influx through Cav1.2 is a proximal signal for pathological cardiomyocyte hypertrophy.* Journal of Molecular and Cellular Cardiology, 2011. **50**(3): p. 460-470.

122. Youn, D.-h., et al., *Ser1928 is Required for Regulation of Calcium-Dependent Inactivation of CaV1.2 L-Type Calcium Channels by AKAP79-Anchored PKA and Calcineurin.* Biophysical journal, 2012. **102**(3, Supplement 1): p. 128a.

Vita

Shawn M. Crump

University of Kentucky College of Medicine

Department of Physiology

EDUCATION

2005 B.A. in Chemistry

University of Kentucky, Lexington, KY

RESEARCH/WORK EXPERIENCE

2005 Principle Research Analyst

Department of Physiology

University of Kentucky College of Medicine, Lexington, KY

Mentor: Jonathan Satin, Ph.D.

2003-2004 Research Analyst

Department of Physiology

University of Kentucky College of Medicine, Lexington, KY

Mentor: Jonathan Satin, Ph.D.

2002	Senior Technician Department of Physiology University of Kentucky College of Medicine, Lexington, KY Mentor: Jonathan Satin, Ph.D.
1999-2000	Undergraduate Research Assistant Department of Anatomy and Neurobiology, Lexington, KY Sanders Brown Center of Aging Mentor: Mark P. Mattson, Ph.D.
1998-1999	Quality Control Lab Technician Mallinckrodt Pharmaceutical Raleigh, NC
1997-1998	Quality Control Lab Technician Mallinckrodt Baker Specialty Chemical Paris, KY
1997-1997	Teaching Assistant Department of Chemistry University of Kentucky College of Arts and Science, Lexington, KY
1994	Undergraduate Research Assistant Department of Chemistry University of Kentucky College of Arts and Science, Lexington, KY

Mentor: Robert Toreki, Ph.D.

RESEARCH/WORK EXPERIENCE (cont'd)

1992-1994	Undergraduate Research Assistant
	Department of Chemistry
	University of Kentucky College of Arts and Science, Lexington, KY
	Mentor: Thomas F. Guarr, Ph.D.

HONORS AND AWARDS

1994	Cook Summer Fellowship
1994	Undergraduate Research Grant
2008	Runner up Poster Award, Physiology Dept. Retreat
2009	NIH T32 Cardiovascular training Fellowship
2010	NIH T32 Cardiovascular training Fellowship
2011	Cardiac EP Society Basic Science Poster Finalist
	Delta Epsilon Iota Honor Society

PROFESSIONAL ACTIVITIES

2012	UC Davis Cardiovascular Symposium
2010	UC Davis Cardiovascular Symposium
2002- current	American Heart Association member
2003- current	Biophysical Society member
1998-1999	Lab team Safety training coordinator (Mallinckrodt Pharmaceutical)

University of Kentucky

1994	Students for the American Chemical Society, Treasurer

1992-1994 Students for the American Chemical Society, member

Teaching

1997 Gen. Chemistry 115 Lab, Teaching Assistant, 6 hrs Lab time/wk

Gen. Chemistry 104 Lab, Teaching Assistant, 2 hrs lectures and 12 hrs Lab time/wk

PEER REVIEWED PUBLICATIONS

1. FINLIN, B. S., **CRUMP, S. M.**, SATIN, J. & ANDRES, D. A. (2003) Regulation of voltage-gated calcium channel activity by the Rem and Rad GTPases. *PNAS*, 100, 14469-14474.

2. FINLIN, B. S., MOSLEY, A. L., **CRUMP, S. M.**, CORRELL, R. N., OZCAN, S., SATIN, J. & ANDRES, D. A. (2005) Regulation of L-type Ca2+ Channel Activity and Insulin Secretion by the Rem2 GTPase. *J. Biol. Chem*., 280, 41864-41871.

3. FINLIN, B. S., CORRELL, R. N., PANG, C., **CRUMP, S. M**., SATIN, J. & ANDRES, D. A. (2006) Analysis of the complex between Ca2+ channel beta -subunit and the rem GTPase. *J. Biol. Chem*., M604867200.

4. **CRUMP, S. M**., CORRELL, R. N., SCHRODER, E. A., LESTER, W. C., FINLIN, B. S., ANDRES, D. A. & SATIN, J. (2006) The L-type Calcium Channel Alpha-Subunit and Protein Kinase Inhibitors Modulate the Rem - Mediated Regulation of Current. *Am J Physiol Heart Circ Physiol*, 00956.2005.

5. Pang, C., **S. M. Crump**, L. Jin, R. N. Correll, B. S. Finlin, J. Satin and D. A. Andres. (2010). "Rem GTPase interacts with the proximal $Ca_V1.2$ C-terminus and modulates calcium-dependent channel inactivation." Channels (Austin) 4(3): 192-202.

6. Magyar, J.,. Kiper, C. E., Sievert, G., Cai, W., Shi, G., **Crump, S.M.**, Li, L., Niederer,, S., Smith, N., Andres,D. A., & Satin, J. (2012) "Rem-GTPase Regulates Cardiac Myocyte L-type Calcium Current." Channels (Austin)

Accepted March 28th 2012, in press

7. **CRUMP, S. M**., SIEVERT, G., ANDRES, D. A. & SATIN, J. (2012) The cardiac L-type calcium channel (LTCC) distal carboxyl-terminus (DCT) is a reverse- use dependent inhibitor of Ca-current in cardiomyocytes. *In revision AJP Heart July 2012*.

INVITED REVIEWS AND CHAPTERS

8. ANDRES, D. A., **CRUMP, S. M.**, CORRELL, R. N., SATIN, J., FINLIN, B. S. & WILLIAM E. BALCH, C. J. D. A. A. H. (2006) Analyses of Rem/RGK Signaling and Biological Activity. *Methods in Enzymology. Academic Press*.

9. Satin, J., E. A. Schroder, **Crump, SM**. (2011). "L-type calcium channel auto-regulation of transcription." Cell Calcium 49(5): 306-313.

REFEREED ABSTRACTS-NATIONAL MEETINGS

Crump, SM, Correll, RN, Finlin, Schroder, EA, Andres, DA, J, Satin. Calcium Channel Phosphorylation status Contributes to Auxiliary Subunit/RGK- Regulation of Current.

Presented to the Annual Meeting of the American Heart Conference, New Orleans, LA, 2004.

Crump, SM, Correll, RN, Finlin, Schroder, EA, Andres, DA, J, Satin. Calcium channel alpha-subunit phosphorylation site modulates the RGK-calcium channel beta-subunit regulation of current. Platform Presentation to the American Heart Scientific Sessions, Orlando, FL, 2003.

Satin, J, **Crump, SM**, Yidong, W, Fox, L, Finlin, Andres, DA. Monomeric G-Proteins Chronically Regulate Cardiac Calcium Current Expression. American Heart Scientific Sessions, Chicago, IL, 2002.

Crump, SM, Schroder, EA, Yozwiak, D, J, Satin. Sustained L-type Calcium Channel Block Elicits Multiple Transcriptional Changes Converging on L-type Channel Function. St. Jude Children's Research Hospital National Graduate Student Symposium, Memphis, TN, 2009.

Crump, SM, Schroder, EA, Andres, DA, Satin, J. The L-type Calcium C-terminus is a mobile domain that competes with calmodulin modulation of Calcium Currents. Gordon Research Conference: Cardiac Regulatory Mechanisms. New London, NH 2010

Crump, SM, Siever, G, Andres, DA, Satin, J. The Cardiac L-type calcium channel distal carboxyl-terminus (DCT) is a reverse-use dependent inhibitor (RUDI) of Ca-current. Cardiac Electrophysiology Society Annual meeting, Orlando, FL 2011.

ABSTRACTS

Crump, SM, Siever, G, Andres, DA, Satin, J. The Cardiac L-type calcium channel distal carboxyl-terminus (DCT) is a reverse-use dependent inhibitor (RUDI) of Ca-current. 55th Biophysical Society Annual meeting, San Diego, CA 2012.

Crump, SM, Siever, G, Andres, DA, Satin, J. The Cardiac L-type calcium channel distal carboxyl-terminus (DCT) is a reverse-use dependent inhibitor (RUDI) of Ca-current. Gill Heart Institute Cardiovascular Research Day, Lexington, KY, 2011.

Crump, SM, Schroder, EA, Andres, DA, Satin, J. CALMODULIN INTERFERES WITH $Ca_V1.2$ C-TERMINAL REGULATION OF L-Type CALCIUM CHANNEL CURRENT. 54th Annual Meeting of the Biophysical Society Platform Talk, Baltimore, MD 2011

Crump, SM, Schroder, EA, Yozwiak, D, J, Satin. The L-type Calcium C-terminus is a mobile domain that competes with calmodulin modulation of Calcium Currents. 54th Annual Meeting of the Biophysical Society, San Francisco, CA 2010

Crump, SM, Schroder, EA, Yozwiak, D, J, Satin. Sustained L-type Calcium Channel Block Elicits Multiple Transcriptional Changes Converging on L-type Channel Function. 53rd Annual Meeting of the Biophysical Society, Boston, MA 2009

Crump, SM, Correll, RN, Finlin, Lester, W, Schroder, EA, Andres, DA, J, Satin. The L-type Calcium Channel Alpha-Subunit Phosphorylation Site Modulates the Rem - Calcium Channel Beta-subunit Regulation of Current. 50th Annual Meeting of the Biophysical Society, Salt Lake City, UT, 2006.

Crump, SM, Correll, RN, Finlin, Lester, W, Schroder, EA, Andres, DA, J, Satin. Calcium Channel Phosphorylation status Contributes to Auxiliary Subunit/RGK- Regulation of Current. Gill Heart Institute Cardiovascular Research Day, Lexington, KY, 2005.

Crump, SM, Correll, RN, Finlin, Schroder, EA, Andres, DA, J, Satin. Calcium channel alpha-subunit phosphorylation site modulates the RGK-calcium channel beta-subunit regulation of current. 49th Annual Meeting of the Biophysical Society, Long Beach, CA, 2005.

Crump, SM, Correll, RN, Finlin, Schroder, EA, Andres, DA, J, Satin. $Ca_V\beta$ and Rem-GTPase Regulation of $Ca_V1.2$ (L-type Calcium Channel) in mouse heart. 48th Annual Meeting of the Biophysical Society, Baltimore, MD, 2004.

Crump, SM, Correll, RN, Finlin, Schroder, EA, Andres, DA, J, Satin. Calcium Channel Phosphorylation status Contributes to Auxiliary Subunit/RGK- Regulation of Current. Gill Heart Institute Cardiovascular Research Day, Lexington, KY, 2004.

Crump, SM, Finlin, Schroder, EA, Andres, DA, J, Satin. Ca_V-beta and Rem-GTPase Regulation of Cav1.2 (L-type Calcium Channel) in mouse heart. Gill Heart Institute Cardiovascular Research Day, Lexington, KY, 2003.

Crump, SM, Finlin, BF, Andres, DA, J, Satin. Cardiac Ca2+ Channel Functional Expression is Regulated by Monomeric G-proteins and Protein Kinase A (PKA). Gill Heart Institute Cardiovascular Research Day, Lexington, KY, 2002.